Determination and quantification of surface lipid metabolites in maize silks: A pathway model for surface lipid biosynthesis based on simultaneous profiling of polar and non-polar metabolites

by

Layton Andrew Peddicord

A thesis submitted to the graduate faculty

in partial fulfillment of the requirements for the degree of

MASTER OF SCIENCE

Major: Genetics

Program of Study Committee:
Nick Lauter, Co-Major Professor
Marna Yandeau-Nelson, Co-Major Professor
Basil J. Nikolau, Co-Major Professor
Drena Dobbs
Peng Liu

Iowa State University

Ames, Iowa

2013

DEDICATION

I'd like to dedicate this research to my family, Layton, Judy and Rebecca, who have been supportive throughout my research and educational experience.

TABLE OF CONTENTS

LIST OF FIGURES

LIST OF TABLES

NOMENCLATURE

SL	Surface Lipid
FA	Fatty Acid
HC	Hydrocarbon
DMDS	Dimethyl Disulfide
VLC	Very Long Chain
SHCs	Surface Hydrocarbons
AMDIS	Automated Mass Spectral Deconvolution and Identification System
GC-MS	Gas Chromatography Mass Spectrometry
TLC	Thin Layer Chromatography
ANOVA	Analysis Of Variance
ADO	Aldehyde-Deformylating Oxygenase
M^+	Molecular Ion
VLCFA	Very Long Chain Fatty Acid
IBM	Intermated B73xMo17
IBMDHLs	Intermated B73xMo17 Doubled Haploid Lines
IBMRILs	Intermated B73xMo17 Recombinant Inbred Lines
RI	Retention Index

ACKNOWLEDGEMENTS

I would like to thank professors Lauter, Yandeau-Nelson and Nikolau for guidance and support throughout the course of my MSc dissertation research. The work herein is part of a large interdisciplinary project spearheaded by these investigators, requiring significant management, personnel, physical and financial resources that were collaboratively provided by them. Many individuals contributed to this work. Specifically, I thank the maize genetics and field team (Dr. Lauter, Dr. Yandeau-Nelson, Miriam Lopez, Hannah Cox, Grace Kuehne, David Hessel, Adam Bossard) for assistance in generating genetic stocks, growing plant materials, and collecting and processing silk samples. I also thank the metabolomics team (Dr. Yandeau-Nelson, Dr. Nikolau, Sam Condon, Dr. Lauter, Dr. Zhihong Song and Dr. Ann Perera) for sharing expertise in experimental design, chemical extraction, GC-MS methods, and biochemical interpretation. I am also grateful to my Program of Study Committee members which include Dr. Peng Liu and Dr. Drena Dobbs for their guidance and to Dr. Chris Tuggle and Ms. Linda Wild for administrative support during my degree program. Thanks also to my father Layton, mom Judy, and sister Rebecca for their encouragement and financial support throughout my education and to my fiancée Sarah Cloud for her patience, respect and love. Finally, I wish to acknowledge the sources of funds that made this research possible: ISU Interdepartmental Genetics Graduate Program, USDA-NIFA, NSF-EFRI, and DOE.

ABSTRACT

The elongated stigmas in maize (i.e. silks) are a vital organ for the reproductive success of a major U.S. agricultural crop. These silks possess an extractible coat of surface lipids that is predominantly composed of a complex array of hydrocarbons that function to protect the silks against abiotic and biotic stresses. While hydrocarbons are most likely produced from the conversion of fatty acids, the exact biochemical mechanisms for their synthesis remain unknown. Our team is leveraging genetic variation and morphological gradients during silk development to dissect the metabolic network responsible for surface lipid accumulation.

These metabolomic efforts require a series of large-scale parallel investigations that rely on metabolite extraction and gas chromatography mass spectrometry (GC-MS) for metabolite identification and quantification. To extract and quantify the intermediate- (e.g. fatty acids and aldehydes) and end-point (e.g. hydrocarbons) surface lipid metabolites in a single extraction procedure, we have undertaken a methods development study to identify the best extraction solvent, the best incubation time, the consequences of filtering through silica, and the best GC-MS protocol. We found that a 9:1 mixture of hexanes to diethyl ether, a long incubation time, and the omission of silica performed best as judged by 1) throughput efficiency, 2) the breadth of identified metabolites, 3) the degree to which the quantifications of subsets of

metabolites matched results from our previous best methods, and 4) the efficacy and efficiency of the GC-MS protocol required to differentiate the metabolites.

From this study alone, new insights into maize hydrocarbon biosynthesis have already been gained. For example, we have identified homologous series of saturated and unsaturated fatty acids, aldehydes and hydrocarbons, which suggest a decarbonylation mechanism that produces even- and odd-chain hydrocarbons from odd- and even-chain fatty acids, respectively. Moreover, we have demonstrated that a homologous series of alkenes with double bonds situated at the 7^{th} and 9^{th} positions are most abundant, and we have identified a corresponding series of unsaturated fatty acids with double bonds positioned at ω—7 and ω—9. Together, these data suggest that the reduction of even- and odd-numbered fatty acids (saturated or unsaturated) followed by the decarbonylation of their corresponding aldehydes represent a key pathway for hydrocarbon synthesis on maize silks.

CHAPTER 1. INTRODUCTION

Rationale: The cuticular surface lipids (SLs) that coat maize silks consist of a wide array of saturated and unsaturated hydrocarbon (HC), aldehyde and fatty acid (FA) constituents, with minor contributions from alcohols and ketones in certain maize lines [1,2,3,4]. The SLs on silks are primarily (>90%) non-isoprenoid hydrocarbons, including alkanes and alkenes (monoenes and dienes). By contrast, juvenile and adult maize leaves have been shown to have far lower levels of HCs and are mostly made up of fatty alcohols, esters and aldehydes [5,6].

The protective properties inherent to the coating on the silk are often underappreciated, despite their importance in successfully receiving pollen for reproduction [7]. SLs have been found to provide protection against abiotic stresses such as dessication [8,9] and UV radiation [10], and biotic stresses, such as insect feeding by moths and beetles [2,11,12] and pathogen invasion [13].

After pollen grains are deposited on the silk epidermis they germinate and the pollen tubes elongate via tip growth to enter the silk channel through the thin walls of small trichomes, or hairlike cells [14,15]. These trichomes can be prone to osmotic stress which can hinder silk receptivity to pollen entry by causing cell wall and subsequent densification of cuticular components [16]. The SLs on maize silks are rich in very long chain (VLC) alkanes. Similar highly non-polar metabolites found in the leaf cuticle in Arabidopsis have been found to limit water diffusion [17] on the cuticle. We

hypothesize that specific compositions of the silk SL metabolome confer protection of this vital organ against drought and other environmental stresses.

Maize silks are an excellent model system for dissecting the SL metabolome because, 1) silk development is rapid 3-12 grams of fresh silk biomass per ear are typically generated in the first three days following emergence of silks from the encasing husk leaves and, 2) SLs (primarily alkanes, alkenes and dienes) comprise nearly 2% of the dry weight of silks.

Knowing and understanding how the SL metabolome is regulated and protects against specific environmental stresses will allow for applied breeding to achieve "designer" SL compositions to improve resistance for stresses such as drought. The ability to breed agronomically important maize lines would not only provide an opportunity to increase productivity (yield), but it could lead to a decrease in agricultural inputs (e.g. chemical treatments, irrigation).

Since similar SL chemistries also exist in other U.S. crops (e.g. rice, soybean and cotton), this work presents many important downstream applications to other reproductive organs, and aerial organs [18,19,20,21] not including maize. Seeing that surface HC content increases in both soybean and cotton in drought stressed plants [18,20], as well as in the anthers and leaves of rice [19,21], suggests that HC content is negatively correlated with water loss and cuticular permeability, indicating a role in tolerance to drought [21].

While the main goal of the larger project, as a whole, is to provide an insight into HC biosynthesis in corn and to find genetic elements that catalyze or regulate HC production, we feel this research could also have a downstream impact in the realm of engineering advanced biofuels. Most of the surface metabolites found on maize silks consist of alkane and alkene constituents which are nearly identical to the components found in fossil fuels. Elucidating the biochemical origins of these hydrocarbons and how they are biosynthesized could also be used in engineering target crops to produce novel waxes with specific chain-length distributions in oilseeds [22] which produce these highly advanced fuels.

Knowledge of how HCs are produced could be utilized in the biofuel sector, since gasoline and diesel fuel are currently made by crude fossil fuel consisting mixtures of diverse chain-length HCs [23]. Since silk SLs are mostly comprised of non-isoprenoid VLC HCs, knowledge of this HC synthesis pathway could be exploited in producing short, medium-chain and branched-chain HCs for renewable high-energy applications. It is our hypothesis that the cuticle ultrastructure and chemical composition (SLs) may have a major impact on conferring resistance to abiotic stresses. While little is known on what SL metabolites may confer this resistance, it is our understanding that these stress related conditions might induce changes upon the SL metabolome [3].

Development of a metabolomic method, herein, to simultaneously profile all SL metabolites including fatty acid, aldehyde and HC compounds would provide a gateway

to analyze these SL metabolome changes more directly from various stress related conditions.

LITERATURE REVIEW

While the biological production of HCs most likely occurs from the conversion of saturated and unsaturated FAs to alkanes and alkenes, respectively, the genetic triggers and exact biochemical mechanisms have not been well characterized in plants, except for recently in Arabidopsis [24] where new data suggests that CER1 [25] and CER3 [26] form an "alkane synthesis complex" suggesting the production of aldehyde intermediates from FA precursors. This was based on the cloning and characterization of *cer1* [27] as well as overexpressing CER1 [28] to see an increased accumulation of HCs on the cuticle suggesting a gene that encodes an aldehyde decarbonylase. Further evidence has shown that the cuticles of *cer1* and *cer22* mutants, recently found to be alleles of the same gene [29], have reduced levels of alkanes increased levels of aldehydes [17,30,31], which supports a decarbonylation mechanism from VLCFA precursors to alkanes.

While scientific approaches aimed at defining the pathway for HC biosynthesis have taken advantage of many mutants, such as in Arabidopsis [32], maize [33], rice [21,34,35] and tomato [36,37,38], our understanding of HC biosynthesis in maize (and other plants) still remains incomplete. GLOSSY1 in maize was considered to be a

homolog to CER1 in Arabidopsis, but recent characterization of the cuticular phenotype and sequence identity of *glossy1* mutants in maize [39,40] to *cer1* mutants in Arabidopsis has proven otherwise. From sequence comparisons at the protein level, glossy1 shared a 62% sequence identity to wax2, but only a 35% sequence identity to cer1 [40]. The Nikolau group has found glossy1 to be a functional homolog to CER3 in Arabidopsis, which in rice, has appeared to shown activity in the elongation of VLCFAs [35]. VLCFAs, which are the precursors for the synthesis of hydrocarbons, are synthesized by the fatty acid elongase system. This elongase system has been characterized and in maize corresponds to *glossy4* [33,41], *glossy8* [42,43,44] and *glossy26* (Nikolau group, unpublished data).

Over the past several decades, four main mechanisms for the biosynthesis of hydrocarbons have been proposed, but currently only one mechanism has been found to be active in plants [45]. These mechanisms are 1) a head-to-head condensation reaction between two fatty acids [46,47], 2) a decarboxylation reaction from a FA precursor [48], 3) a decarbonylation reaction, whereby a FA precursor is reduced to an aldehyde which is subsequently decarbonylated to the corresponding hydrocarbon [45] and 4) a dehydration mechanism, whereby a FA is first reduced to an aldehyde, which is further reduced to a primary alcohol intermediate, and the primary alcohol is dehydrated to a hydrocarbon of the same length as the VLCFA precursor [49].

Due to the high abundance of HCs, aldehydes and FAs in maize silks, alkanes and alkenes are thought to be biosynthesized by the decarbonylation of an aldehyde

intermediate, which have already been characterized in plants [45], insects [50], and algae [48]. Recent work in cyanobacterium has shown a decarbonylase-dependent alkane synthesis pathway in *Synechococcus elongatus* [51], but in subsequent research, in *Nostoc punctiforme* [52,53], a homologous enzyme revealed that the catalytic function actually acts as an aldehyde-deformylating oxygenase (ADO) to generate alkane and alkene end-point metabolites. While no known homolog in maize has been revealed, the ADO is thought to act on acyl-ACP substrates, which in advanced plants are limited to the mitochondria and plastids of 18-carbon chain lengths and shorter.

While a small subset of the odd-chained alkanes and alkenes found herein have been previously reported in *B73* [3], even-chained alkanes and alkenes had not, which points to a more complex pathway of possible odd-chained FA precursors. In select maize genotypes, even-chain HCs and odd-chain FAs and aldehydes have been detected in great abundancy [2]. Too add to these unique metabolites, in the maize inbred CO272, highly abundant methyl alkanes have been detected in the surface lipid fraction of maize silks [1]. These rare metabolites contained a methyl group attached to the second carbon and were seen to be as abundant as the saturated odd-alkanes at C27, C29 and C31.

For alkene biosynthesis, parallel pathways have been proposed, which consists of either elongation-desaturation or desaturation-elongation of the FA precursor, followed by direct decarbonylation [3]. While these proposed pathways were based on the detection of unsaturated fatty acids at C18, no other unsaturated fatty acids were

detected for chain lengths greater than C18 [3]. The other hindrance to the above proposed pathways was the lack of detection for saturated and unsaturated aldehdyes shorter than 26 carbons and longer than 30 carbons in chain length. One other pathway was proposed which involved elongation then isomerization; this was postulated to explain the origin of unsaturated methylketones [3].

THESIS OUTLINE

Chapter 1 focuses on the importance of this research project to the environmental sustainability and productivity for a major seed crop that would allow for future protection by improving SL compositions to the SL metabolome. A literature review is provided that describes the current understanding in the field regarding the biochemical mechanisms for the biosynthesis of hydrocarbons across organisms.

Chapter 2 describes the development of a metabolomic method that not only efficiently extracts non-polar SL metabolites (HCs) but also simultaneously extracts more polar SLs such as aldehydes, ketones and FA constituents. The goal of this work was to identify a method to extract precursors (FAs), intermediates (aldehydes, alcohols, etc.) and end-point metabolites (HCs and ketones) in one extraction method.

Chapter 3 reports the application of the method developed in Chapter 2 to into the actual dissection of this metabolomic network for HC biosynthesis by profiling saturated and unsaturated compounds by dimethyl disulfide derivitization. To view

precursors, intermediates and end-point metabolites in deciphering the metabolic network, lipid extractions from both ground and fresh silk materials were integrated. Compositionally, internal vs surface metabolites were also compared and quantified.

Chapter 4 provides a summary and conclusions for this body of work. Future experiments are proposed in which the methods developed in this thesis can be applied to further dissect the SL metabolic network.

REFERENCES

1. Miller SS, Reid LM, Butler G, Winter SP, McGoldrick NJ (2003) Long chain alkanes in silk extracts of maize genotypes with varying resistance to Fusarium graminearum. J Agric Food Chem 51: 6702-6708.

2. Yang G, Wiseman BR, Espelie KE (1992) Cuticular lipids from silks of seven corn genotypes and their effect on development of corn earworm larvae [Helicoverpa zea (Boddie)]. Journal of Agricultural and Food Chemistry 40: 1058-1061.

3. Perera MA, Qin W, Yandeau-Nelson M, Fan L, Dixon P, et al. (2010) Biological origins of normal-chain hydrocarbons: a pathway model based on cuticular wax analyses of maize silks. Plant Journal 64: 618-632.

4. Perera MAN, Nikolau B (2007) Metabolomics of Cuticular Waxes: A System for Metabolomics Analysis of a Single Tissue-Type in a Multicellular Organism. In: Nikolau

B, Wurtele E, editors. Concepts in Plant Metabolomics: Springer Netherlands. pp. 111-123.

5. Avato P, Bianchi G, Pogna N (1990) Chemosystematics of Surface-Lipids from Maize and Some Related Species. Phytochemistry 29: 1571-1576.

6. Bianchi G, Avato P, Salamini F (1978) Glossy mutants of maize. VIII. Accumulation of fatty aldehydes in surface waxes of gl5 maize seedlings. Biochem Genet 16: 1015-1021.

7. Bassetti P, Westgate ME (1993) Senescence and Receptivity of Maize Silks. Crop Sci 33: 275-278.

8. Jordan WR, Shouse PJ, Blum A, Miller FR, Monk RL (1984) Environmental Physiology of Sorghum. II. Epicuticular Wax Load and Cuticular Transpiration1. Crop Sci 24: 1168-1173.

9. Kosma D, Jenks M (2007) Eco-Physiological and Molecular-Genetic Determinants of Plant Cuticle Function in Drought and Salt Stress Tolerance. In: Jenks M, Hasegawa P, Jain SM, editors. Advances in Molecular Breeding Toward Drought and Salt Tolerant Crops: Springer Netherlands. pp. 91-120.

10. Long LM, Patel HP, Cory WC, Stapleton AE (2003) The maize epicuticular wax layer provides UV protection. Functional Plant Biology 30: 75-81.

11. Yang G, Isenhour DJ, Espelie KE (1991) Activity of Maize Leaf Cuticular Lipids in Resistance to Leaf-Feeding by the Fall Armyworm. The Florida Entomologist 74: 229-236.

12. Yang G, Wiseman BR, Isenhour DJ, Espelie KE (1993) Chemical and Ultrastructural Analysis of Corn Cuticular Lipids and Their Effect on Feeding by Fall Armyworm Larvae. Journal of Chemical Ecology 19: 2055-2074.

13. Javelle M, Vernoud V, Rogowsky PM, Ingram GC (2011) Epidermis: the formation and functions of a fundamental plant tissue. New Phytol 189: 17-39.

14. Miller EC (1919) Development of the pistillate spikelet and fertilization in Zea mays L. Journal of Agricultural Research 18: 0255-0265.

15. Heslopharrison Y, Reger BJ, Heslopharrison J (1984) The Pollen-Stigma Interaction in the Grasses .5. Tissue Organization and Cyto-Chemistry of the Stigma (Silk) of Zea-Mays-L. Acta Botanica Neerlandica 33: 81-99.

16. Heslopharrison J (1979) Pollen-Stigma Interaction in Grasses - a Brief Review. New Zealand Journal of Botany 17: 537-546.

17. Jenks MA, Tuttle HA, Eigenbrode SD, Feldmann KA (1995) Leaf Epicuticular Waxes of the Eceriferum Mutants in Arabidopsis. Plant Physiology 108: 369-377.

18. Bondada BR, Oosterhuis DM, Murphy JB, Kim KS (1996) Effect of water stress on the epicuticular wax composition and ultrastructure of cotton (Gossypium hirsutum L) leaf, bract, and boll. Environmental and Experimental Botany 36: 61-&.

19. Jung KH, Han MJ, Lee DY, Lee YS, Schreiber L, et al. (2006) Wax-deficient anther1 is involved in cuticle and wax production in rice anther walls and is required for pollen development. Plant Cell 18: 3015-3032.

20. Kim KS, Park SH, Kim DK, Jenks MA (2007) Influence of water deficit on leaf cuticular waxes of soybean (Glycine max [L.] Merr.). International Journal of Plant Sciences 168: 307-316.

21. Islam M, Du H, Ning J, Ye H, Xiong L (2009) Characterization of Glossy1-homologous genes in rice involved in leaf wax accumulation and drought resistance. Plant Molecular Biology 70: 443-456.

22. Jetter R, Kunst L (2008) Plant surface lipid biosynthetic pathways and their utility for metabolic engineering of waxes and hydrocarbon biofuels. Plant Journal 54: 670-683.

23. Nikolau BJ, Perera MA, Brachova L, Shanks B (2008) Platform biochemicals for a biorenewable chemical industry. Plant Journal 54: 536-545.

24. Bernard A, Domergue F, Pascal S, Jetter R, Renne C, et al. (2012) Reconstitution of plant alkane biosynthesis in yeast demonstrates that Arabidopsis ECERIFERUM1 and ECERIFERUM3 are core components of a very-long-chain alkane synthesis complex. Plant Cell 24: 3106-3118.

25. Chen X, Goodwin SM, Boroff VL, Liu X, Jenks MA (2003) Cloning and characterization of the WAX2 gene of Arabidopsis involved in cuticle membrane and wax production. Plant Cell 15: 1170-1185.

26. Rowland O, Lee R, Franke R, Schreiber L, Kunst L (2007) The CER3 wax biosynthetic gene from Arabidopsis thaliana is allelic to WAX2/YRE/FLP1. FEBS Lett 581: 3538-3544.

27. Aarts MG, Keijzer CJ, Stiekema WJ, Pereira A (1995) Molecular characterization of the CER1 gene of arabidopsis involved in epicuticular wax biosynthesis and pollen fertility. Plant Cell 7: 2115-2127.

28. Bourdenx B, Bernard A, Domergue F, Pascal S, Leger A, et al. (2011) Overexpression of Arabidopsis ECERIFERUM1 promotes wax very-long-chain alkane biosynthesis and influences plant response to biotic and abiotic stresses. Plant Physiology 156: 29-45.

29. Sakuradani E, Zhao L, Haslam TM, Kunst L (2013) The CER22 gene required for the synthesis of cuticular wax alkanes in Arabidopsis thaliana is allelic to CER1. Planta 237: 731-738.

30. Rashotte AM, Jenks MA, Ross AS, Feldmann KA (2004) Novel eceriferum mutants in Arabidopsis thaliana. Planta 219: 5-13.

31. Hannoufa A, McNevin J, Lemieux B (1993) Epicuticular waxes of eceriferum mutants of Arabidopsis thaliana. Phytochemistry 33: 851-855.

32. Koornneef M, Hanhart CJ, Thiel F (1989) A Genetic and Phenotypic Description of Eceriferum (cer) Mutants in Arabidopsis thaliana. Journal of Heredity 80: 118-122.

33. Schnable PS, Stinard PS, Wen TJ, Heinen S, Weber D, et al. (1994) The Genetics of Cuticular Wax Biosynthesis. Maydica 39: 279-287.

34. Mao B, Cheng Z, Lei C, Xu F, Gao S, et al. (2012) Wax crystal-sparse leaf2, a rice homologue of WAX2/GL1, is involved in synthesis of leaf cuticular wax. Planta 235: 39-52.

35. Yu D, Ranathunge K, Huang H, Pei Z, Franke R, et al. (2008) Wax Crystal-Sparse Leaf1 encodes a beta-ketoacyl CoA synthase involved in biosynthesis of cuticular waxes on rice leaf. Planta 228: 675-685.

36. Leide J, Hildebrandt U, Reussing K, Riederer M, Vogg G (2007) The developmental pattern of tomato fruit wax accumulation and its impact on cuticular transpiration barrier properties: effects of a deficiency in a beta-ketoacyl-coenzyme A synthase (LeCER6). Plant Physiology 144: 1667-1679.

37. Leide J, Hildebrandt U, Vogg G, Riederer M (2011) The positional sterile (ps) mutation affects cuticular transpiration and wax biosynthesis of tomato fruits. J Plant Physiol 168: 871-877.

38. Vogg G, Fischer S, Leide J, Emmanuel E, Jetter R, et al. (2004) Tomato fruit cuticular waxes and their effects on transpiration barrier properties: functional characterization of a mutant deficient in a very-long-chain fatty acid beta-ketoacyl-CoA synthase. J Exp Bot 55: 1401-1410.

39. Hansen JD, Pyee J, Xia Y, Wen TJ, Robertson DS, et al. (1997) The glossy1 locus of maize and an epidermis-specific cDNA from Kleinia odora define a class of receptor-like proteins required for the normal accumulation of cuticular waxes. Plant Physiology 113: 1091-1100.

40. Sturaro M, Hartings H, Schmelzer E, Velasco R, Salamini F, et al. (2005) Cloning and characterization of GLOSSY1, a maize gene involved in cuticle membrane and wax production. Plant Physiology 138: 478-489.

41. Liu S, Dietrich CR, Schnable PS (2009) DLA-based strategies for cloning insertion mutants: cloning the gl4 locus of maize using Mu transposon tagged alleles. Genetics 183: 1215-1225.

42. Dietrich CR, Perera MA, M DY-N, Meeley RB, Nikolau BJ, et al. (2005) Characterization of two GL8 paralogs reveals that the 3-ketoacyl reductase component of fatty acid elongase is essential for maize (Zea mays L.) development. Plant Journal 42: 844-861.

43. Xu X, Dietrich CR, Delledonne M, Xia Y, Wen TJ, et al. (1997) Sequence analysis of the cloned glossy8 gene of maize suggests that it may code for a beta-ketoacyl reductase required for the biosynthesis of cuticular waxes. Plant Physiology 115: 501-510.

44. Xu X, Dietrich CR, Lessire R, Nikolau BJ, Schnable PS (2002) The Endoplasmic reticulum-associated maize GL8 protein is a component of the acyl-coenzyme A elongase ivolved in the production of cuticular waxes. Plant Physiology 128: 924-934.

45. Cheesbrough TM, Kolattukudy PE (1984) Alkane biosynthesis by decarbonylation of aldehydes catalyzed by a particulate preparation from Pisum sativum. Proc Natl Acad Sci U S A 81: 6613-6617.

46. Sukovich DJ, Seffernick JL, Richman JE, Gralnick JA, Wackett LP (2010) Widespread Head-to-Head Hydrocarbon Biosynthesis in Bacteria and Role of OleA. Applied and Environmental Microbiology 76: 3850-3862.

47. Sukovich DJ, Seffernick JL, Richman JE, Hunt KA, Gralnick JA, et al. (2010) Structure, Function, and Insights into the Biosynthesis of a Head-to-Head Hydrocarbon in Shewanella oneidensis Strain MR-1. Applied and Environmental Microbiology 76: 3842-3849.

48. Reed JR, Quilici DR, Blomquist GJ, Reitz RC (1995) Proposed mechanism for the cytochrome P450-catalyzed conversion of aldehydes to hydrocarbons in the house fly, Musca domestica. Biochemistry 34: 16221-16227.

49. Park MO (2005) New pathway for long-chain n-alkane synthesis via 1-alcohol in Vibrio furnissii M1. J Bacteriol 187: 1426-1429.

50. Dennis M, Kolattukudy PE (1992) A cobalt-porphyrin enzyme converts a fatty aldehyde to a hydrocarbon and CO. Proc Natl Acad Sci U S A 89: 5306-5310.

51. Schirmer A, Rude MA, Li X, Popova E, del Cardayre SB (2010) Microbial biosynthesis of alkanes. Science 329: 559-562.

52. Li N, Norgaard H, Warui DM, Booker SJ, Krebs C, et al. (2011) Conversion of fatty aldehydes to alka(e)nes and formate by a cyanobacterial aldehyde decarbonylase: cryptic redox by an unusual dimetal oxygenase. J Am Chem Soc 133: 6158-6161.

53. Li N, Chang WC, Warui DM, Booker SJ, Krebs C, et al. (2012) Evidence for only oxygenative cleavage of aldehydes to alk(a/e)nes and formate by cyanobacterial aldehyde decarbonylases. Biochemistry 51: 7908-7916.

CHAPTER 2. METHODOLOGICAL IMPROVEMENTS FOR IDENTIFYING AND QUANTIFYING POLAR AND NON-POLAR SURFACE LIPID METABOLITES ON MAIZE SILKS

Not published

Authors and roles:

Conceived the experiments: LP, BJN, NL, MYN

Designed the experiments: LP, MYN

Executed the experiments: LP

Performed data analyses: LP, MYN, NL

Prepared the manuscript: LP, MYN, NL

ABSTRACT

Maize silks possess a unique and diverse array of complex surface lipid metabolites, including large quantities of both non-polar (hydrocarbons) and slightly more polar (fatty acids, aldehydes and ketones) constituents on the silk surface. Silk surface lipids are composed of mostly unbranched, linear hydrocarbons, including

alkanes, alkenes or dienes that are 14 to 35 carbons in length. The remaining SLs comprise fatty acid precursors and aldehyde/ketone intermediates of the hydrocarbon biosynthesis pathways, which remain enzymatically undefined. To extract and analyze this diversity of polar and non-polar lipids simultaneously, experiments to develop efficient metabolomic methods were undertaken. Five solvents with increasing levels of polarity, two treatments (with and without silica) and varied solvent incubation times were tested. As revealed by GC-MS metabolite profiling, silica removed virtually all moderately polar compounds (e.g. fatty acids) from the extracts, regardless of solvent choice. Overall, the hexanes: diethyl ether (90:10) solvent most efficiently extracted both fatty acids and hydrocarbons from the silk surface. Relative composition of extracted surface lipid metabolites was also affected by solvent; for example, alkenes were more readily extracted with the less polar solvent, hexanes: diethyl ether (95:5) as compared to the hexanes: diethyl ether (90:10) solvent. Solvent incubation time also affected the relative composition (alkenes, dienes and fatty acids) as well as the compound abundance of both non-polar and more polar silk lipids. Finally, analyses of intact vs. powderized silks have been executed to determine surface vs. internal metabolite abundances and compositional differences.

INTRODUCTION

The importance of maize silk cuticular lipids for protection against pathogen invasions [1], dessication [2,3], UV radiation [4], and pest feeding (moths, beetles and insects) [5,6,7] is often overlooked. Not only are silks a first point of contact for entry into the ear for pests and fungi from the outside environment, but they also serve as conduits for pollen to enable fertilization. The SLs that coat these silks have been found to have defense against abiotic and biotic stresses; during the critical time in pollen reception, this defense is essential for the reproductive success of a major seed crop [8].

Silk development is very fast; 3 to 12 grams (fresh weight) of biomass can be produced per ear in a short interval of time (< 7 days). Not only is this tissue easy to collect and process, but metabolomic studies have shown that surface lipids (SLs) comprise 2% of the dry weight of silks [9]. Of these SLs, 90% are non-isoprenoid hydrocarbons (e.g. alkanes, alkenes and dienes) while the remaining 10% is made up of fatty acids, ketones and aldehydes, which are presumed to be intermediates in the biosynthesis of these hydrocarbons [10]. While most maize lines contain high levels of odd alkanes and alkenes on their silk surfaces, the relative composition and array of metabolites is rather diverse and genotype specific [6]. Even though these hydrocarbons are prevalent on the silk cuticle, they are far less abundant on the cuticles of juvenile [11] and adult [12] maize leaves, which comprise mostly of fatty alcohols, esters, aldehydes with few amounts of alkanes.

Given that biological unsaturated (alkenes and dienes) and saturated (alkanes) hydrocarbons are rare in biological systems [13,14,15,16], maize silk provides a unique opportunity to explore and quantify a rich display of long and VLC hydrocarbons (C14-C35). However, the methods for extraction of this complex mixture of surface lipid metabolites may need further development.

Recently, the fatty acid content in lipid extracts have been detected, analyzed, and quantified by gas chromatography mass spectrometry (GC-MS). To improve recovery and volatility during gas chromatography, many free fatty acids are transformed into FA methyl esters (FAMEs) [17,18] via direct methylation or through transmethylation after lipid extraction. Direct methylation has been applied to a diverse range of tissues [19,20,21,22,23,24] and used as a cost-efficient strategy on relatively small samples of tissue, resulting in low solvent consumption [25]. It has also been shown to extract highly polar lipids with an astounding success rate compared to a normal extraction [23].

Traditionally, lipids have been extracted using three methods: the Bligh and Dyer (B&D) [26], Soxhlet [27] and acid hydrolysis [28]. While scientists have refined these basic procedures, little documentation of improvements and thorough evaluations is available in the present literature [29]. While the danger of the toxicity of chloroform is reduced in the B&D method (1:2 chloroform/methanol) from the original Folch (2:1 chloroform/methanol) [30], no significant difference was detected in

fatty acid composition [29], though the B&D is thought to increase recovery to >95% of the total lipids [31]. An alternative to the Folch method was developed in which a dry-column was used to extract lipids with anhydrous sodium sulfate and dichloromethane [32]; this method did however get tailored in respect to incubation time in experiments with liver and muscle tissues [33]. The most popular method to date for lipid extractions, the B&D, has been shown to yield high recovery in lipids across many diverse sets of tissues. While numerous modifications have been made in this technique with additions of 1M NaCl [34], acetic acid (0.5% v/v) [35], and acidification with HCl [36] to improve extraction efficiency, quantification and effectiveness of these modifications have not been reported extensively in respect to metabolite recovery.

While Franz Soxhlet first examined milk lipids with the extraction solvent diethyl ether [37], many scientists improved upon this method by using the solvent mixture ethanol: diethyl ether [38,39] for total lipid extractions. Concurrently, other specialized procedures were developed involving low-toxicity blends involving hexanes [40], hexanes/isopropanol [41,42,43], and a modified hexanes/isopropanol protocol to extract plant sphingolipids [44]. Other lipid extraction methods have used methyl-tert-butyl ether (MTBE) in conjunction with methanol and water [45] to extract lipids from blood [46] and from human brain tissue [47]. The accurate measurement of total lipid content is important for many tissue studies [29]. In the current study, a series of extraction methods were applied to silks harvested from the inbred line B73 with the

goal of developing an efficient method to simultaneously profile non-polar and polar cuticular wax metabolites.

The purpose of this work was to find a solvent mixture that maximized the capture of non-polar (hydrocarbons) and slightly polar (aldehydes, ketones and fatty acids) lipid metabolites simultaneously while allowing accurate quantification of metabolites. Using solvents varying in polarity, fatty acid content was also analyzed and quantified using transmethylation after the lipids were extracted from the silk tissue. Solvent incubation time was tested for recovery and abundance of metabolites within a set sensitivity threshold (medium) in AMDIS. Experimentally, lipid extracts were then subjected to silica purification to assess if the metabolite array and relative abundance differed upon application. While many method studies have looked at total lipid extractions, with various solvent mixtures, in specific tissue types, no reported literature in maize has examined, quantified and tested metabolite recovery and abundance with hexanes, chloroform and diethyl ether mixtures at various solvent incubation times.

RESULTS AND DISCUSSION

Methods development

To develop an efficient extraction method to extract and quantify the diverse range of slightly polar and non-polar metabolites from silks, solvent choice, purification treatment, and incubation time combinations were all integrated into a series of tests. A flowchart of the experimental scheme is presented in Figure 1.

Various solvents, with increasing polarity, have been tested including: hexanes, hexanes: diethyl ether (95:5), hexanes: diethyl ether (90:10), hexanes: chloroform (1:1) and chloroform. The dielectric constants range from 1.88 (hexanes) to 4.81 (chloroform). Within each solvent, a purification treatment of silica was applied or not applied to samples to assess whether the metabolite array stayed consistent or not. In addition, time length of extraction was also tested. Incubation times for different solvents ranged from 1 minute to 30 minutes of vortexing (Fig.1). The 1, 2, 5 and 10 minute vortexed extractions were based on a single extraction with 2ml of solvent, whereas the 20 minute and 30 minute extraction times were based on 2 and 3 10-min vortex extractions, respectively. Each sample contained a pinch of glass wool; this served two purposes: (1) as a filter for drawing up solvent in the silica samples, and as a (2) trap, after vortex and centrifugation, to separate silk debris from the extract. After samples had been vortexed (2min) and centrifuged (1min), the extracts were placed into a new clean glass tube upon drying and concentration, prior to the GC-MS run.

Figure 1

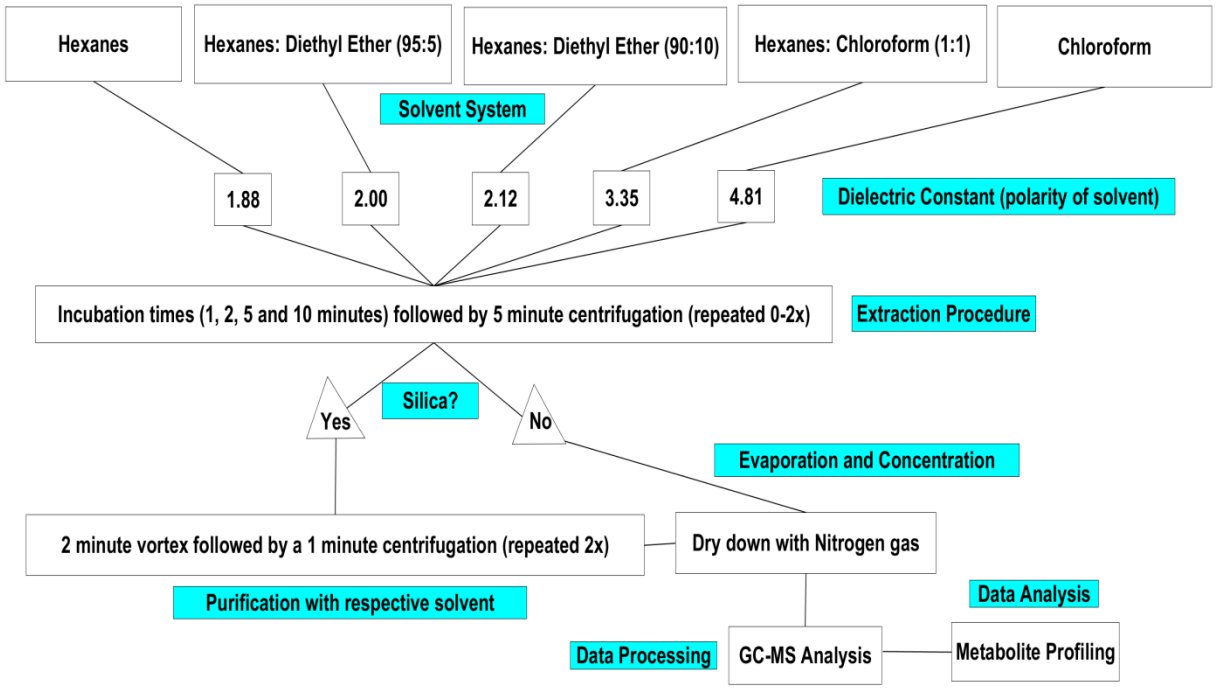

Figure 1 Metabolomic method testing scheme

Solvents tested are listed atop the scheme based on increasing polarity from left to right as inferred from their dielectric constants. As each solvent was used to extract SLs, multiple incubation times and repetitions were tested. After the extraction, the extracts were placed into tubes that either contained silica and glass wool or tubes that only contained glass wool. These samples were then vortexed for 2 minutes followed by a 1-minute centrifugation, which was repeated two times. After the samples had been purified, the extracts were then drawn up and placed into a new glass tube that was subjected to evaporation via N_2 gas. After the samples were concentrated, they were analyzed by GC-MS.

Silk lipid composition in powderized silk

Metabolite analyses from a 3 x 10 minute extraction of powderized silk with the solvent hexanes: diethyl ether (90:10), indicate that they consist of a homologous series of alkanes, alkenes or dienes that range from 14 to 33 carbon atoms (Table 1). Many compounds, such as the even saturated and unsaturated hydrocarbons, have not yet been previously reported in maize. Even without derivatization, many fatty acids were still evident, including constituents that range from 9 to 18 carbon atoms (C9-C18). For two different chain length fatty acids, unsaturated compounds were found and identified through DMDS adducts. These include one mono-unsaturated fatty acid (9-hexadecanoic) and one di-unsaturated fatty acid (9, 12-octadecadienoic). Both of these unsaturated compounds are also ones that were found when silks were immersed in chloroform for 60 seconds that were found on the silk cuticle alone [10]. The even and odd-chain hydrocarbon, fatty acid, and aldehyde constituents (Table 1) were identified and determined first before the solvent tests were conducted. This was to analyze and compare compositionally what metabolites would be recovered in greater abundance or lost in respect to different incubation times, solvent mixtures and through silica filtration.

The most predominant hydrocarbons that were recovered were the straight-chain alkanes, C27 and C29. Alkenes were also very prevalent in the GC-MS analyses, including a homologous series that ranged from C22 to C33 consecutively. Although a

diverse range of alkenes was seen in the GC-MS analysis of the DMDS adducts, only a few defined unsaturated alkyl chains were most prominent. For C22, an unsaturated hydrocarbon was found that was seen to have a double bond position located between the 6^{th} and 7^{th} carbon. For carbon chain lengths from 23 to 33, two discrete alkenes were identified that contained a double bond between the 7^{th} and 8^{th} carbon as well as the 9^{th} and 10^{th} carbon atoms. These two unsaturated alkenes (delta 7 and delta 9) were the most prominent in our analyses. In carbon chain lengths 29, 31 and 33, three alkenes were evident. Besides the delta 7 and 9 alkenes, a C29 alkene contained a double bond between the 14^{th} and 15^{th} carbon, while C31 and C33 contained an alkene with a double bond positioned between the 15^{th} and 16^{th} carbon atoms. These were the only carbon chain lengths that were found to contain measureable levels of more than two alkene isoforms. Also, many other less abundant alkenes were observed in the DMDS results that co-eluted with some of the discrete delta 6, 7, 9, 14 and 15 alkene isoforms. These delta values ranged from 4 to half of the length of the molecule rounded down. Many of these distinct alkenes have not yet been reported in maize, but were far less abundant than the ones mentioned already in this paper.

Mass-spectral analyses of dimethyl disulfide adducts of dienes identified the positions of the two double bonds. Since fragmentation was more difficult to decipher with these, many dienes have been labeled as such in the table (x,y). Analysis did identify one series of homologous dienes with double bond positions located between the 6^{th} and 7^{th} carbons as well as between the 9^{th} and 10^{th} carbons. This 6, 9 series of

odd-chain dienes were found for carbon length molecules of 25 through 31. Reported already from argentation TLC in B73 silk tissue, all the alkene metabolites found are of the *cis* configuration [10].

Other metabolites discovered in the 30 minute extraction were two aldehydes (tetracosanal and hexacosanal) and one methyl ketone (heptadecane-2-one). These three metabolites were very low in abundance, but detectable in AMDIS. Since these lipids were derived from powderized silks instead of surface lipids alone, composition as well as abundance may differ for hydrocarbons, aldehydes and fatty acid constituents. It has been shown that many aldehydes are displayed along the cuticle that we did not see in our powderized silk in GC-MS [6].

Table 1 Lipid composition from powderized B73 silks extracted in hexanes: diethyl ether (90:10)

Metabolite	nmole/g dry weight [a]	Metabolite	nmole/g dry weight [a]
9-carbon metabolites		**26-carbon metabolites**	
nonanoic acid	7.01 ± 13.33	hexacosane	61.27 ± 5.51
12-carbon metabolites		9-hexacosene	3.63 ± 7.17
dodecanoic acid	2.81 ± 5.73	7-hexacosene	tr
14-carbon metabolites		x,y-hexacosadiene	1.35 ± 3.56
tetradecane	tr	hexacosanal	tr
tetradecanoic acid	1.95 ± 3.56	**27-carbon metabolites**	
15-carbon metabolites		heptacosane	1,435.80 ± 37.25
pentadecane	tr	9-heptacosene	63.59 ± 6.98
pentadecanoic acid	0.37 ± 0.97	7-heptacosene	57.85 ± 9.95
16-carbon metabolites		6,9-heptacosadiene	39.03 ± 4.69
hexadecane	2.99 ± 3.78	**28-carbon metabolites**	
hexadecanoic acid	1,152.69 ± 25.48	octacosane	131.49 ± 12.56
9-hexadecenoic acid	tr	9-octacosane	tr
17-carbon metabolites		7-octacosane	20.20 ± 15.90
heptadecane	2.46 ± 2.38	x,y-octacosadiene	tr
heptadecanoic acid	1.75 ± 4.64	**29-carbon metabolites**	
heptadecane-2-one	0.06 ± 0.15	nonacosane	2,443.61 ± 43.30
18-carbon metabolites		14-nonacosene	108.14 ± 11.25
octadecane	1.52 ± 2.76	9-nonacosene	311 ± 23.29
octadecanoic acid	155.15 ± 107.51	7-nonacosene	566.27 ± 48.32
9,12-octadecadienoic acid	1,484.07 ± 35.25	6,9-nonacosadiene	268.93 ± 10.48
19-carbon metabolites		x,y-nonacosadiene	1.53 ± 3.18
nonadecane	0.42 ± 1.10	**30-carbon metabolites**	
21-carbon metabolites		triacontane	105.53 ± 12.51
heneicosane	tr	9-triacontene	tr
22-carbon metabolites		7-triacontene	10.11 ± 8.70
docosane	21.28 ± 27.01	x,y-triacontadiene	tr
6-docosene	11.14 ± 29.48	**31-carbon metabolites**	
x,y-docosadiene	1.60 ± 4.24	hentriacontane	751 ± 24.97
23-carbon metabolites		15-hentriacontene	182.73 ± 13.39
tricosane	35.76 ± 9.69	9-hentriacontene	749.34 ± 26.89
9-tricosene	tr	7-hentriacontene	347.68 ± 22.57
7-tricosene	tr	6,9-hentriacontadiene	107.57 ± 75.52
24-carbon metabolites		**32-carbon metabolites**	
tetracosane	60.84 ± 35.97	doctriacontane	0.54 ± 1.43
7-tetracosane	2.47 ± 4.25	**33-carbon metabolites**	
tetracosanal	7.21 ± 9.18	tritriacontane	53.31 ± 4.90
25-carbon metabolites		15-tritriacontene	54.51 ± 12.78
pentacosane	312.56 ± 41.32	9-tritriacontene	105.78 ± 8.97
9-pentacosene	82.58 ± 11.80	7-tritriacontene	31.83 ± 4.69
7-pentacosene	72.52 ± 9.73		
6,9-pentacosadiene	35.73 ± 11.74		

[a] Average value of seven independent analyses ± 1 standard deviation

tr, trace, < 10 pmol per g dry silk weight

Solvent impacts recovery of metabolites

In all the solvents tested on powderized silk samples, metabolite recoveries (i.e. the array of observed constituents) as well as metabolite abundances (i.e. the amount of each observed constituent) were clearly significant in the timed 30 minute extraction method. Hydrocarbon class traits seem to be highly correlated in both silica and non-silica treated samples among all six solvents tested (Fig. 2). The fact that all correlation coefficients are highly positive among the silica extracted samples (Fig. 2a) indicates that solvent choice has only a minimal impact on hydrocarbon class traits behavior in respect to one another ($p < 0.0001$). Within the samples not subjected to silica purification (Fig. 2b), in our timed 30 minute extraction, hydrocarbon class traits still seem to be highly correlated.

Figure 2

(a)

Correlations

	Total HC's	Odd Alkanes	Even Alkanes	Odd Alkenes	Even Alkenes
Total HC's	1.0000	0.9104	0.8349	0.8677	0.5963
Odd Alkanes	0.9104	1.0000	0.8855	0.5908	0.4535
Even Alkanes	0.8349	0.8855	1.0000	0.5224	0.6699
Odd Alkenes	0.8677	0.5908	0.5224	1.0000	0.5465
Even Alkenes	0.5963	0.4535	0.6699	0.5465	1.0000

(b)

Correlations

	Total	Odd Alkanes	Even Alkanes	Odd Alkenes	Even Alkenes
Total HC's	1.0000	0.7141	0.4161	0.7979	0.2782
Odd Alkanes	0.7141	1.0000	-0.0177	0.1709	0.0905
Even Alkanes	0.4161	-0.0177	1.0000	0.4604	0.2834
Odd Alkenes	0.7979	0.1709	0.4604	1.0000	0.1846
Even Alkenes	0.2782	0.0905	0.2834	0.1846	1.0000

Figure 2 Correlation among hydrocarbon class traits

Correlation coefficients are shown among four trait groups of SHC constituents. Coefficients in blue and gray denote strong and weak correlations, respectively. Coefficients are based on a 3 x 10 minute extraction time with 6 different solvents. Coefficients are shown for silica treated samples (a) and non-silica treated samples (b).

The solvent choice significantly impacted total recoveries of partial polar and non-polar metabolites ($R^2 = 0.94$, $p < 0.0001$), in the absence of silica (Fig. 3a). Recovery of total hydrocarbons using the hexanes: diethyl ether (90:10) solvent showed slightly higher recovery (~5%) than from the most non-polar solvent, hexanes ($p < 0.0001$). It was interesting to see that polarity also had a significant effect in class trait recoveries. Recovery of odd-numbered alkenes increased roughly ~10% in the hexanes: diethyl ether (95:5) solvent compared to the hexanes: diethyl ether (90:10) solvent ($p <$

0.0001). While in odd alkanes, hexanes: diethyl ether (90:10) out-performed the hexanes: diethyl ether (95:5) solvent (p< 0.0001). The highest abundance of hydrocarbons was recovered using hexanes: diethyl ether (90:10) (p< 0.0001).

Figure 3

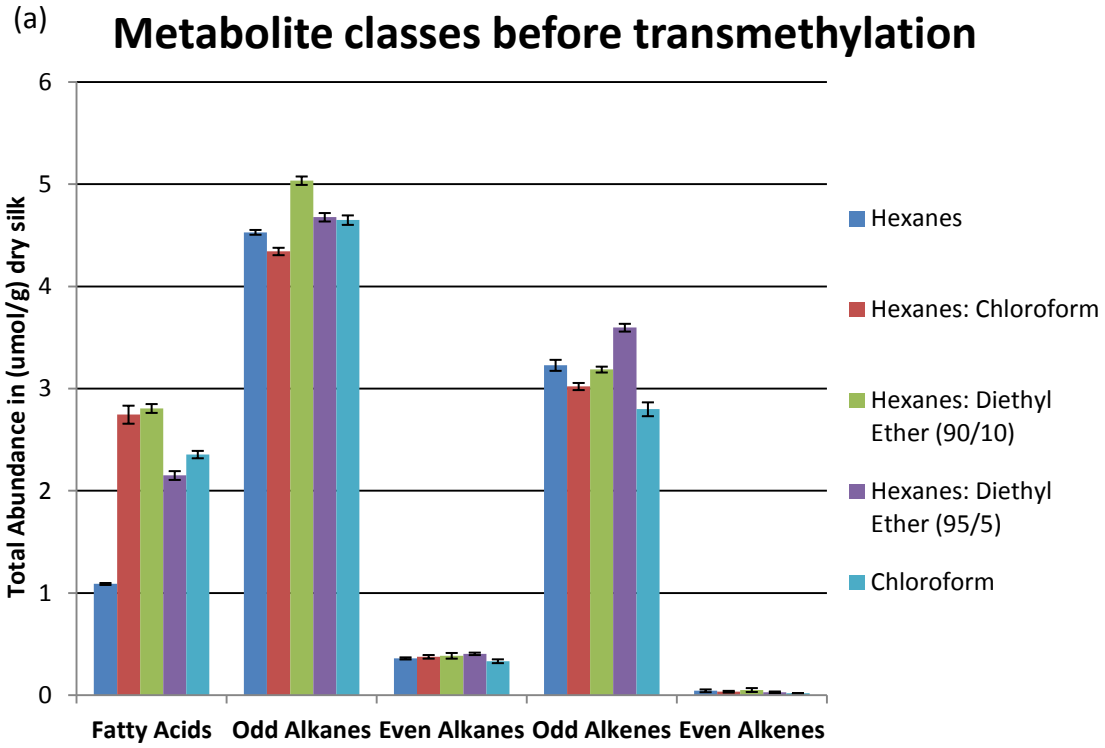

(b)

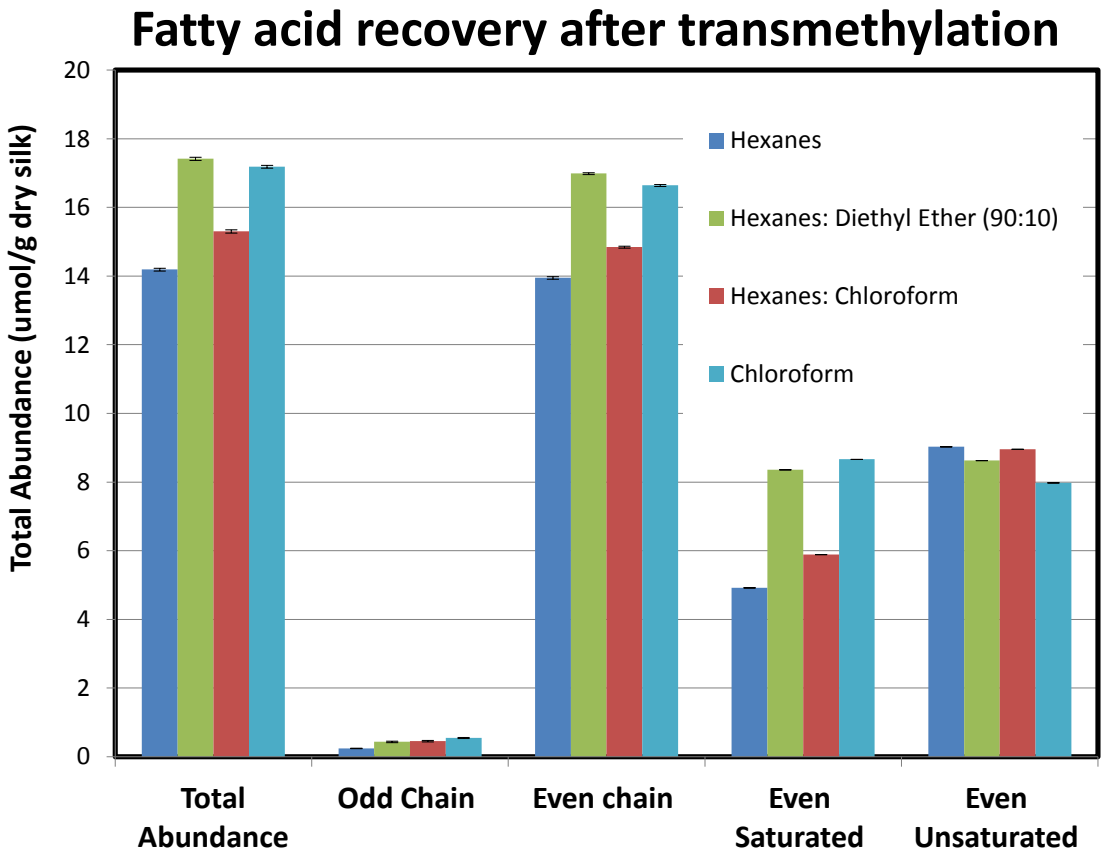

Figure 3 Solvent impact on recovery

(a) Metabolite class traits are compared among non-silica extracted samples with five solvents of differing polarities. Extraction shown is before derivatization via transmethylation. Error bars shown designate standard error among > 4 replicates for a 30 minute extraction time.
(b) Fatty acid class traits are broken down between unsaturated and saturated compositions based on even and odd-chain lengths. Error bars designate standard error among 3 replicates for a 30-minute extraction time with derivatized samples.

FA recovery drastically increased upon conversion to fatty-acid methyl esters via transmethylation prior to GC-MS (Fig. 3b). Total recovery increased > 5-fold with 21 FA constituents being identified. Solvent choice significantly impacted fatty acid recovery across all solvents ($p < 0.05$). Recovery of total FA's using hexanes: diethyl ether (90:10) is 20% higher than from extractions using hexanes ($p < 0.0001$). Not only did the hexanes: diethyl ether (90:10) solvent out-perform hexanes, but it also surpassed chloroform and hexanes: chloroform (1:1), the two solvents having the highest polarities tested. The three highest polarity solvents showed an increased abundance in fatty acid content compared to the most non-polar solvent (hexanes).

The solvent used to extract lipids explains most of the variance in silk metabolite group and relative composition traits, where $p < 0.0001$ in most cases (Table 2). The JMP fit "Y by X" analyses showed that solvent by trait variance in respect to the presence or absence of silica was very significant. In the silica column, all p-values were significant except for two relative composition traits (% even alkenes and % total HCs). The samples that were not treated with silica showed slightly lower R^2 and p-values, but most traits were conserved in significance compared to its counterpart (silica) treatment. Even numbered hydrocarbon class traits were the least significant among the class traits examined. This is most likely due to the low abundance of even hydrocarbons in our chromatograms as well as the threshold sensitivity (medium) set in AMDIS for detection. Nearly every hydrocarbon class trait was more significant in silica subjected samples compared to non-silica samples. In samples not filtered with silica,

sterols and other plant steroid derivatives (stigmastan dienes) are present and co-elute with the C31 and C33 alkenes and dienes. These co-eluting metabolites interfere with the deconvolution spectra within AMDIS for accurate detection and quantification.

Table 2 Solvent impact on silk lipid traits

(Extraction Solvent) by (Trait) ANOVAs				
SL group and relative composition traits				
	With Silica		**Without Silica**	
N=56	**R^2**	**P-value**	**R^2**	**P-value**
Odd Alkanes	0.971	<0.0001*	0.885	<0.0001*
Even Alkanes	0.829	<0.0001*	0.204	0.2042
Odd Alkenes	0.970	<0.0001*	0.870	<0.0001*
Even Alkenes	0.406	0.0222*	0.117	0.5222
Even HCs	0.794	<0.0001*	0.176	0.2831
Odd HCs	0.986	<0.0001*	0.928	<0.0001*
Total HCs	0.982	<0.0001*	0.911	<0.0001*
Short Alkanes (C<26)	0.953	<0.0001*	0.957	<0.0001*
Long Alkanes (C≥26)	0.969	<0.0001*	0.947	<0.0001*
Short Alkenes (C<26)	0.875	<0.0001*	0.614	<0.0001*
Long Alkenes (C≥26)	0.967	<0.0001*	0.854	<0.0001*
FAs	0.447	0.0113*	0.962	<0.0001*
Total SLs	0.976	<0.0001*	0.942	<0.0001*
% Odd Alkanes	0.848	<0.0001*	0.853	<0.0001*
% Even Alkanes	0.675	<0.0001*	0.263	0.0939
% Odd Alkenes	0.920	<0.0001*	0.939	<0.0001*
% Even Alkenes	0.289	0.1124	0.116	0.5266
% Even HCs	0.611	.0004*	0.108	0.5644
% Total HCs	0.225	0.2307	0.965	<0.0001*

* designates significance at the 0.05 level.
N=56 samples (5 solvents by 2 treatments) > 4 replicates of each

Silica does not permit fatty acid recovery

After the powderized silk samples had been extracted at various incubation times, half of the extracted replicates were subjected to a purification treatment using silica. In this treatment, 2 small scoops of silica were deposited in each clean test tube with a pinch of glass wool; this was used as a filter for purifying the solvent extract. After vortexing and centrifugation, the extracts were placed into a clean tube for concentrating under N_2 gas. This process was repeated twice more to recover as many lipids as possible from the silica purification tube. Samples were then analyzed via GC-MS.

Across all solvents, purification of extracts with silica removed virtually all moderate polar compounds (e.g. 9 fatty acid constituents). Figure 4 presents two chromatograms resulting from GC-MS analysis of extractions that either included (top panel) or removed silica from the procedure. Metabolite analyses showed that 85% of the variation in total fatty acid recovery, among the six extraction times between the five respective solvents, could be attributed to the silica purification step of the extraction method ($p < 0.0001$). Removal of the silica purification step proved to be significant in not only fatty acid recovery, but in recovery for all slightly polar metabolites in the silk metabolite array. Silica also contributed 91% to the overall variation seen in total hydrocarbon content among the five solvents used at the 30 minute extraction incubation time ($p < 0.0001$). Major differences were seen among

particular solvents in total hydrocarbon content. In chloroform extracted samples, hydrocarbon content was 26% higher in sample extracts that weren't subjected to silica, while hexanes: chloroform (1:1) extracted samples had an 8% higher hydrocarbon content in extracts subjected to silica ($p < 0.0001$). To extract both polar and non-polar metabolites from silks, silica purification must be removed from the extraction method.

Figure 4

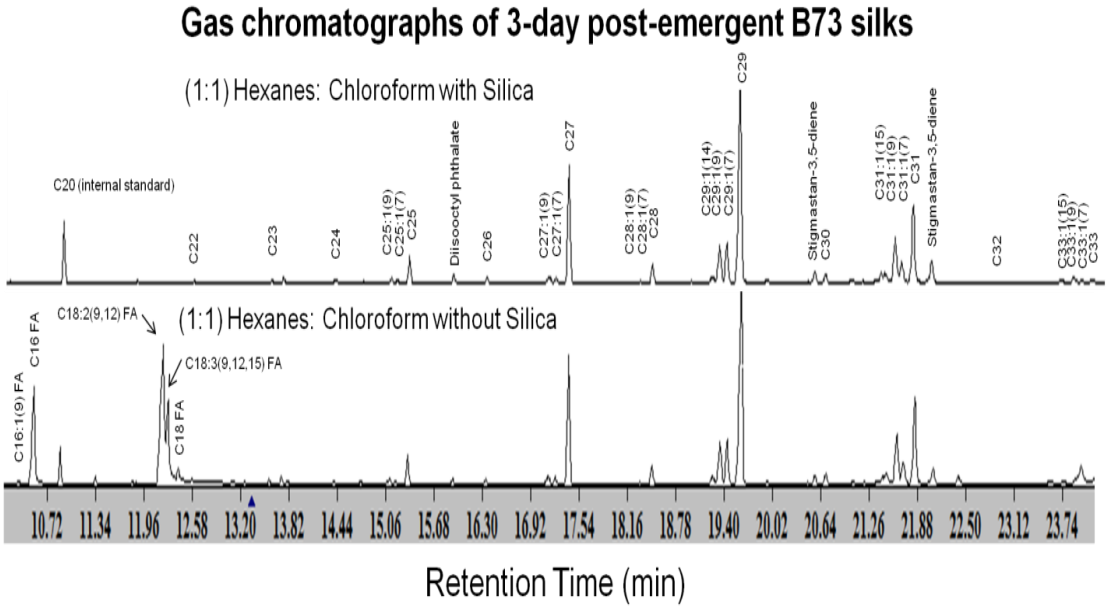

Figure 4 GC-MS chromatograms of metabolites derived from extractions performed with or without silica

Half of each solvent extract was subjected to silica treatment. Hydrocarbon metabolites are labeled in the silica chromatogram while fatty acids are labeled in the chromatogram without silica. Chromatograms are displayed in the same time scale of retention time. Five fatty acid constituents are displayed in the chromatogram without silica in between the retention times of 10 and 13 minutes. These polar metabolites are: hexadecanoic acid, (9)-hexadecenoic acid, octadecanoic acid, (9,12,15)-octadecatrienoic acid and (9,12)-octadecadienoic acid.

Among the polar and non-polar lipid fractions in maize silks, the use of silica dramatically changed the overall composition as well as percentages in the hydrocarbon class traits. When sample extracts were treated with silica, fatty acids were almost undetectable in extracts from all solvents (Fig. 5a). In contrast, fatty acids contributed roughly 21% of total metabolites in samples extracted without the use of silica (Fig. 5b). Among the six solvents, odd- numbered hydrocarbons consisted of ~94% of the total lipid composition, with the remaining ~6% coming from mostly even alkanes and alkenes. Odd-numbered hydrocarbons in extracts without silica contributed a far lesser portion (~75%), with the other ~25% coming from mostly even-numbered fatty acids as well as some even alkanes.

Figure 5

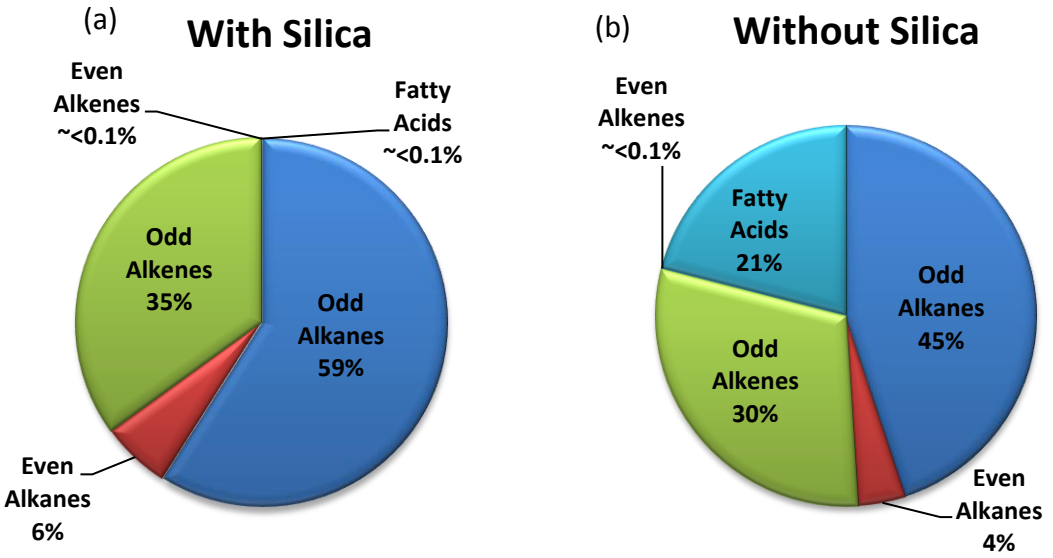

Figure 5 Lipid compositions derived from extractions performed with or without silica

Two treatments were applied to powderized silk tissue after samples were extracted with various solvents. Percentages are based from > 4 replicates of 5 solvents, taken from the 30 minute extraction time, out of the total abundance. Metabolite data is combined across solvent types.
(a) The left pie chart shows the relative abundance composition of metabolite class traits after samples were subjected to silica treatment.

Solvent incubation time affects metabolite abundance and recovery

Extraction incubation time was tested to see if it had an effect on metabolite recovery and abundance. Two different solvents hexanes: diethyl ether (90:10) and hexanes: chloroform (1:1), were subjected to different timed solvent incubations. To

tackle this, we used different timed vortexes along with different numbers of extractions on powderized B73 silk tissue. Some samples were subjected to one extraction at different vortex incubation times while others were extracted to two and three times at various vortex intervals. Among the samples that were extracted once, four different time points were used (1, 2, 5 and 10 minutes). The other samples were subjected to a 10 minute vortex extracted two and three times. This gave us a range of extraction incubation times at 30 minutes, 20 minutes, 10 minutes, 5 minutes, 2 minutes and 1 minute.

Extraction incubation time (Table 3), when evaluated across the two solvents, explained most of the variance in silk lipid traits. Among silica treated samples, solvent incubation effects on silk lipid traits ranged from explaining 19-89% of the observed variance with an average of 65% (not shown). Although the explanatory effect on non-silica treated samples was less, solvent incubation time effects on metabolite traits averaged 41%, which is still very significant. Taken together, hydrocarbon and fatty acid class trait abundances seem to be highly governed by the length of the incubation time, whether or not silica is used.

Table 3 Incubation time impact on silk lipid class traits

(Solvent incubation time) by (Trait) ANOVAs				
Class and relative composition traits	**With Silica**		**Without Silica**	
	R^2	**P-value**	**R^2**	**P-value**
Odd Alkanes	0.623	<0.0001*	0.356	0.0039*
Even Alkanes	0.765	<0.0001*	0.224	0.0750
Odd Alkenes	0.852	<0.0001*	0.780	<0.0001*
Even Alkenes	0.553	<0.0001*	0.186	0.1509
Even HCs	0.784	<0.0001*	0.245	0.0495*
Odd HCs	0.781	<0.0001*	0.400	0.0012*
Total HCs	0.790	<0.0001*	0.397	0.0013*
Short Alkanes (C<26)	0.892	<0.0001*	0.627	<0.0001*
Long Alkanes (C≥26)	0.578	<0.0001*	0.373	0.0025*
Short Alkenes (C<26)	0.754	<0.0001*	0.788	<0.0001*
Long Alkenes (C≥26)	0.852	<0.0001*	0.767	<0.0001*
Fatty Acids	0.286	0.0272*	0.208	0.1016
Total SLs	0.792	<0.0001*	0.252	0.0432*
% Odd Alkanes	0.761	<0.0001*	0.598	<0.0001*
% Even Alkanes	0.507	<0.0001*	0.107	0.4822
% Odd Alkenes	0.679	<0.0001*	0.905	<0.0001*
% Even Alkenes	0.199	0.1396	0.172	0.1899
% Even HCs	0.519	<0.0001*	0.152	0.2604
% Total HCs	0.309	0.0166*	0.405	0.0010*

* designates significance at the 0.05 level.
N=86 samples (2 solvents with 2 treatments by 6 incubation times) >3 replicates of each

In the heat map displayed (Fig. 6) metabolite abundances were looked at for 63 constituent metabolites among different extraction times. For samples with and without silica, a 30 minute incubation time (3 extractions at 10 minutes) showed the

highest abundance overall for the majority of the 63 constituent metabolites among the six different solvent incubation times tested ($p < 0.0001$). Among silica treated samples, solvent incubation time for the two solvents tested, accounted for 79% of the variance seen in total silk lipid abundance ($p < 0.0001$). With samples not subjected to silica, 25% of the variance in total abundance was accounted for by solvent incubation time ($p = 0.0432$). For the samples that weren't subjected to silica, a gradual decrease in the heat map array was seen from a 30 minute extraction to a 1 minute extraction in most of the metabolite constituent abundances.

The analyses demonstrate that the vortex time and the number of extractions are significant in relation to metabolite abundances. It is interesting to note that since the metabolites are listed based on their retention time through the GC-MS column, the first third of the metabolites in each panel consists of fatty acids and short chain hydrocarbons, while the last two thirds is representative of the long chain hydrocarbons. This represents a visual for long vs. short chain hydrocarbons as well as the abundances of the 9 fatty acid constituents located within the first third of the columns of each panel in Fig. 6.

After looking at the relative abundances of metabolite constituents, the metabolites were then grouped into class traits based on their composition. Hydrocarbon and fatty acid metabolite compounds were broken down into saturated and unsaturated class traits (Fig. 7). Within the hydrocarbon composition classes,

alkanes and alkenes were separated and compared among even and odd-numbered chain lengths. HC classes were further categorized them as long ≥C26 in length or short <C26 in length. Altogether, 35 diverse class traits were examined from the original 65 constituent metabolites. Among the various extraction times, the 30 minute extraction procedure resulted in the highest abundance of most all of the metabolite class traits examined.

Figure 6

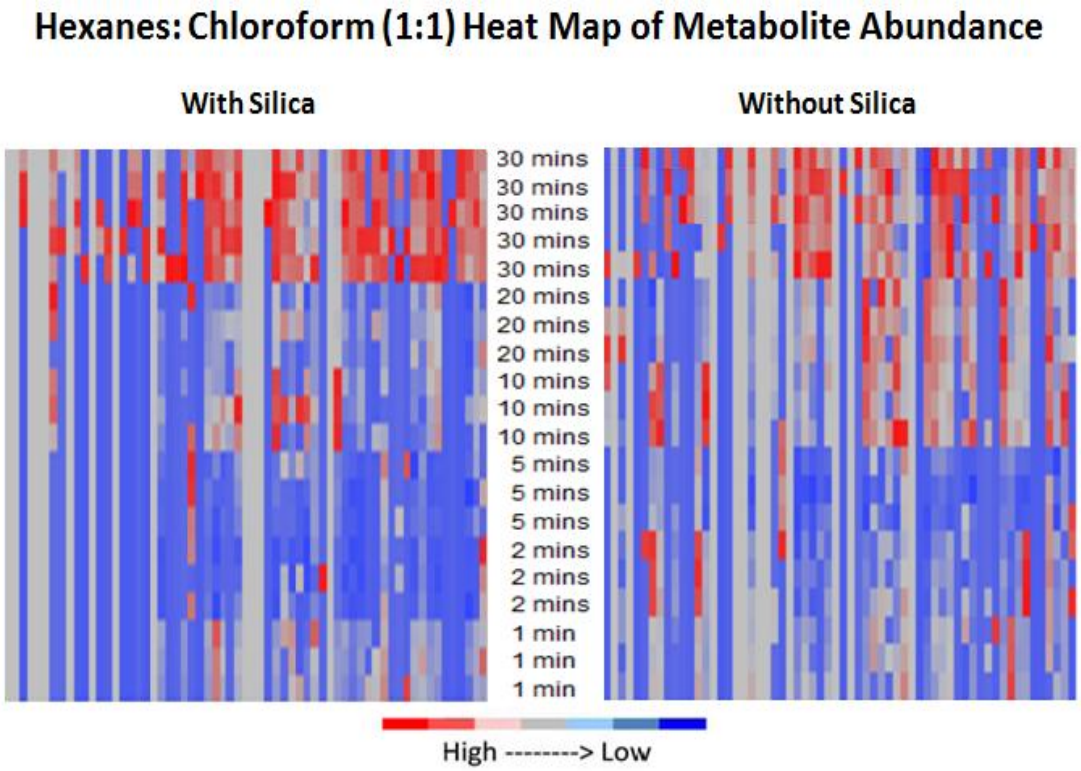

Figure 6 Abundance expressions at different solvent incubation times

The heat map displays a side by side visual of relative abundance expression across 63 different non-polar and polar constituent metabolites. The metabolites are displayed in each column (x-axis) for both the left and right heat panels, while at two different extraction treatments (with silica and without silica). From left to right, metabolites are ordered by their retention time through the GC-MS column. The first third of the metabolites in each panel consists of FAs and short chin HCs, while the last two thirds is representative of the long chain HCs. The middle panel denotes the total extraction incubation time for >3 replicates for each given treatment (y-axis).

Figure 7

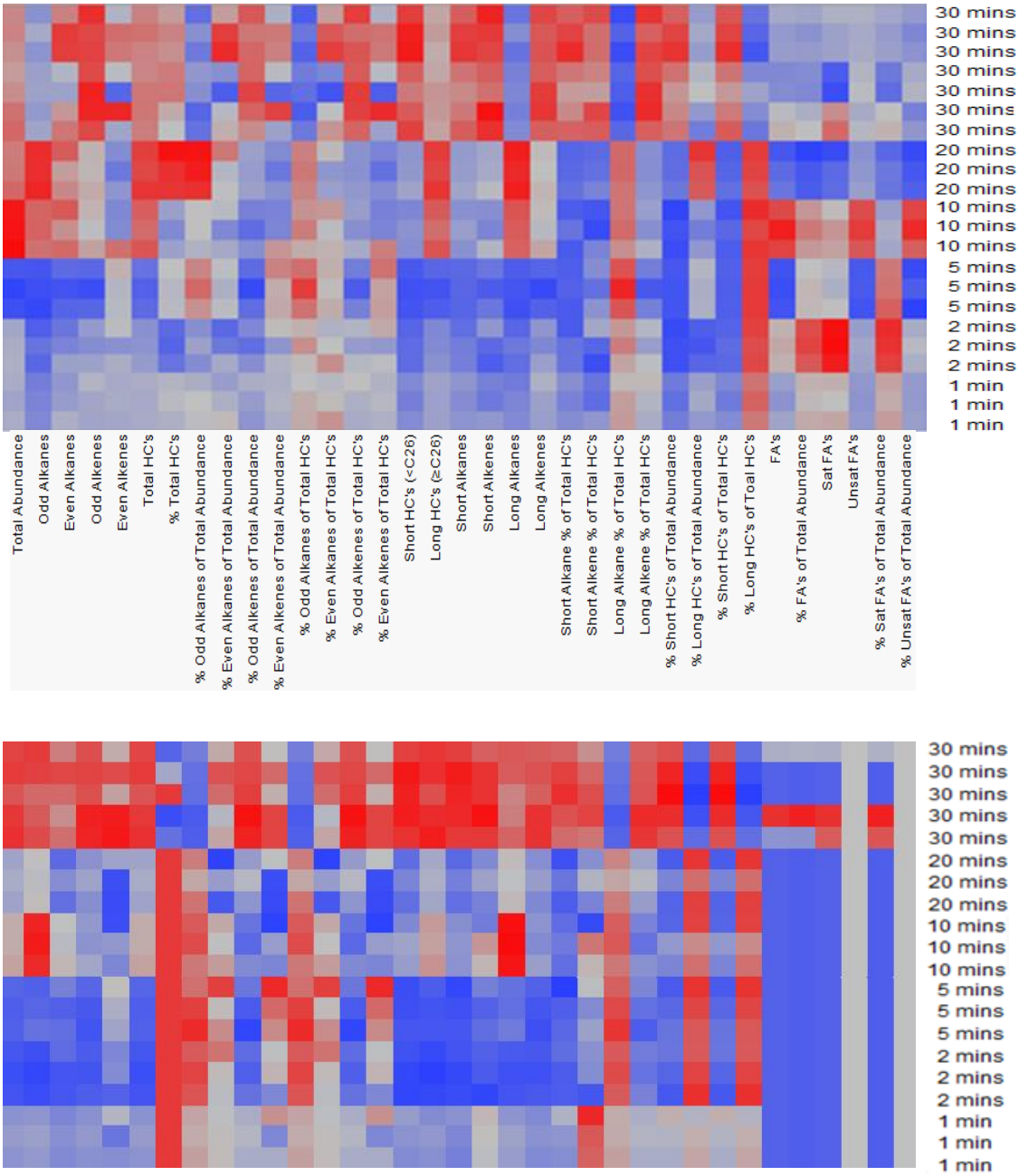
30 mins
30 mins
30 mins
30 mins
30 mins
30 mins
30 mins
20 mins
20 mins
20 mins
10 mins
10 mins
10 mins
5 mins
5 mins
5 mins
2 mins
2 mins
2 mins
1 min
1 min
1 min
Total Abundance
Odd Alkanes
Even Alkanes
Odd Alkenes
Even Alkenes
Total HC's
% Total HC's
% Odd Alkanes of Total Abundance
% Even Alkanes of Total Abundance
% Odd Alkenes of Total Abundance
% Even Alkenes of Total Abundance
% Odd Alkanes of Total HC's
% Even Alkanes of Total HC's
% Odd Alkenes of Total HC's
% Even Alkenes of Total HC's
Short HC's (<C26)
Long HC's (≥C26)
Short Alkanes
Short Alkenes
Long Alkanes
Long Alkenes
Short Alkane % of Total HC's
Short Alkene % of Total HC's
Long Alkane % of Total HC's
Long Alkene % of Total HC's
% Short HC's of Total Abundance
% Long HC's of Total Abundance
% Short HC's of Total HC's
% Long HC's of Toal HC's
FA's
% FA's of Total Abundance
Sat FA's
Unsat FA's
% Sat FA's of Total Abundance
% Unsat FA's of Total Abundance

30 mins
30 mins
30 mins
30 mins
30 mins
20 mins
20 mins
20 mins
10 mins
10 mins
10 mins
5 mins
5 mins
5 mins
2 mins
2 mins
2 mins
1 min
1 min
1 min

Figure 7 Abundance expression among surface lipid class traits

These two heat maps display relative abundances in hydrocarbon and fatty acid class traits for non-silica treated samples (top panel) and silica-treated samples (bottom panel). For each given treatment and extraction time, >3 replicates are shown.

As abundance expression decreased with respect to extraction time, the breadth of the array of constituent metabolites also lessened. The relative composition of even alkenes diminished drastically as extraction time went from 30 minutes to 20 minutes, a loss of 6 metabolites. This trend also stayed consistent down to a 1 minute extraction, a final detection loss of 7 even unsaturated hydrocarbons as compared to the 30 minute extraction time. Not only was there a reduction in the recovery of even alkenes, but all odd and even hydrocarbon and fatty acid class traits were affected by solvent incubation time, whether or not silica was used ($p < 0.0001$). In metabolite recovery across the two solvents hexane: diethyl ether (90:10) and hexanes: chloroform (1:1), solvent incubation time contributed to 82% of the variance seen among silica purified samples (Fig. 8). This percentage was lessened for samples not subjected to silica (57%) but still very significant in respect to recovery ($p < 0.0001$).

When comparing a 30 minute solvent incubation extraction to a 1 minute, recovery of the total composition was significantly lost. Recovery loss on average, from a 30-minute incubation compared to a 1 minute, for the two solvents, went from 36 to 23 metabolites in silica samples and 36 to 28 metabolites in non- silica samples ($p < 0.0001$). Even though fatty acids are recovered in the samples without silica, a

detection loss of 6 fatty acid constituents on average was still evident when a 1-minute incubation was used as a comparison to a 30-minute incubation. The recovery of three fatty acid constituents was seen in non-silica purified samples whether or not the number of extractions or incubation time varied; these were hexadecanoic acid, 9, 12-octadecenoic acid and octadecanoic acid.

Figure 8

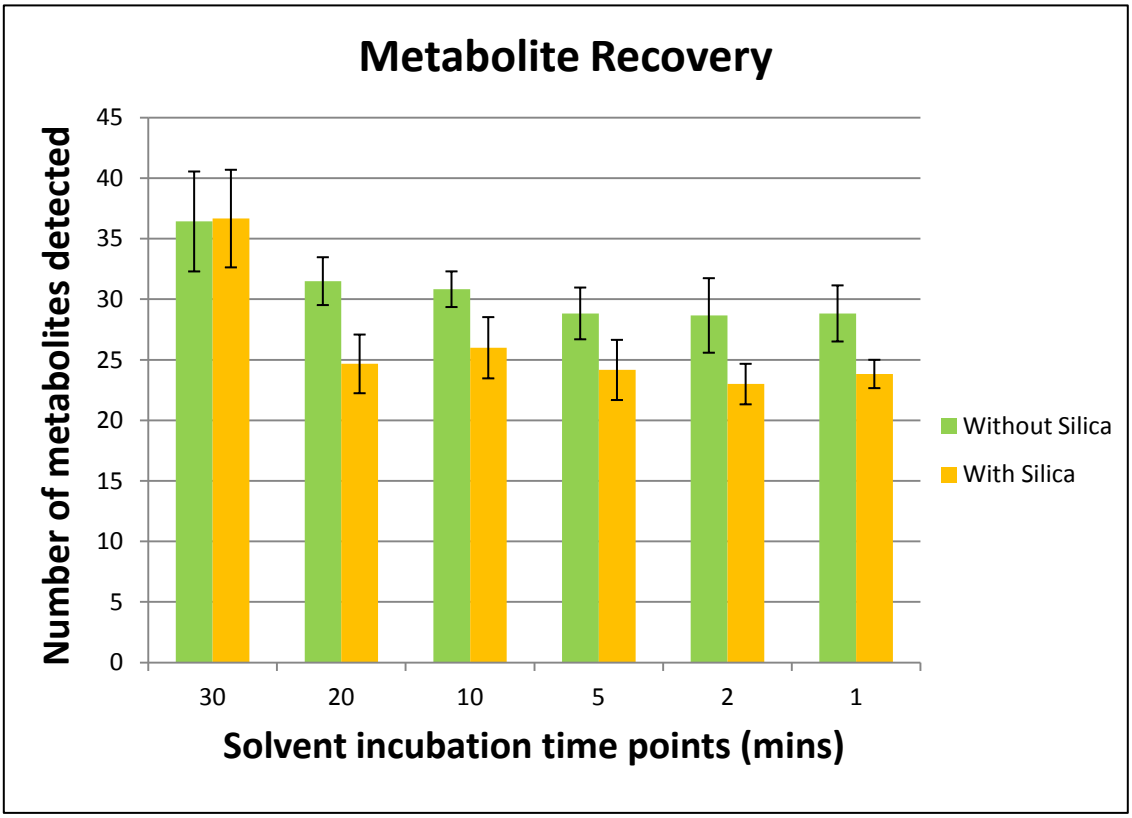

Figure 8 Metabolite recovery for different solvent incubation times

Shown in the bar graph are two treatments applied to two sets of different solvent extracts (hexanes: diethyl ether (90:10) and hexanes: chloroform (1:1)) in respect to various solvent incubation times. Three replicates were performed at each incubation time point. Error bars shown depict one standard deviation from the mean among the 6 total replicates from the two solvents.

Surface lipid composition from extracts of whole silks immersed in solvent

Since our analyses clearly showed that the hexanes: diethyl ether (90:10) solvent out- performed the other 4 solvents with respect to hydrocarbon and fatty acid abundances, we chose to use this solvent for analyzing silk surface lipids extracted from whole silks by dipping the fresh tissue into the solvent, rather than extracting lipids from dry powderized silks. Table 4 shows results from three replicates from an extraction of whole silks, immersed for 60 seconds in hexanes: diethyl ether (90:10) solvent. Table 4 displays the abundance data of constituent metabolites of a moderately concentrated SL extract with GC-MS. While only surface hydrocarbons are present from these extractions, we can see striking differences in the constituent metabolite abundances compared to the metabolite arrays recovered from powderized silks (Table 1). Although fatty acids were not seen in the extracts from whole silks, they were observed in powderized silks (Fig. 9), which suggests that fatty acids are found within the cell and not on the silk surface. It is important to note that although aldehydes were not observed in these specific extracts, they are present in extracts that are highly concentrated (data not shown).

Table 4 B73 silk surface lipid composition

Metabolite	nmole/g dry weight [a]	Metabolite	nmole/g dry weight [a]
21-carbon metabolites		**28-carbon metabolites**	
heneicosane	45.72 ± 3.03	octacosane	153.28 ± 11.19
22-carbon metabolites		7-octacosene	26.33 ± 2.18
docosane	65.86 ± 3.16	9-octacosene	3.96 ± 0.50
23-carbon metabolites		**29-carbon metabolites**	
tricosane	632.342 ± 19.06	nonacosane	2413.84 ± 6.80
7-tricosene	23.24 ± 2.01	7-nonacosene	1173.32 ± 14.61
24-carbon metabolites		9-nonacosene	719.65 ± 17.38
tetracosane	135.14 ± 11.57	14-nonacosene	258.13 ± 17.52
6-tetracosene	2.38 ± 0.65	6,9-nonacosadiene	301.61 ± 20.96
7-tetracosene	0.29 ± 0.05	**30-carbon metabolites**	
9-tetracosene	3.64 ± 0.51	triacontane	63.30 ± 7.14
25-carbon metabolites		7-triacontene	7.25 ± 0.99
pentacosane	688.76 ± 18	9-triacontene	7.79 ± 1.14
7-pentacosene	221.36 ± 1.14	**31-carbon metabolites**	
9-pentacosene	346.41 ± 9.02	hentriacontane	648.48 ± 8.08
6,9-pentacosadiene	55.66 ± 1	7-hentriacontene	318.85 ± 6.71
26-carbon metabolites		9-hentriacontene	758.13 ± 13.86
hexacosane	47.94 ± 2.39	15-hentriacontene	185.66 ± 9.30
7-hexacosene	0.97 ± 0.07	6,9-hentriacontadiene	106.28 ± 5.63
27-carbon metabolites		**33-carbon metabolites**	
heptacosane	1358.50 ± 3.88	tritriacontane	20.78 ± 2.09
7-heptacosene	292.01 ± 9.35	7-tritriacontene	20.45 ± 4.58
9-heptacosene	429.34 ± 15.48	9-tritriacontene	60.23 ± 0.55
6,9-heptacosadiene	150.30 ± 4.09	15-tritriacontene	35.20 ± 1.23

[a] Average value of three independent analyses ± 1 standard deviation

The effect of solvent incubation time on surface lipid abundance

To look at the variation in metabolite arrays and abundances in relation to incubation time, five different time points were tested on whole silks immersed in solvent: 60 seconds, 90 seconds, 2 minutes, 3 minutes and 5 minutes. While only surface hydrocarbons were detected in a 60 second non-concentrated sample, the metabolite composition changed drastically, within the same dissolved concentration, in respect to incubation time. Fatty acids as well as saturated even-chain aldehydes became more evident as the incubation time increased (Fig. 9a). While SHCs comprise >90% of the surface lipids, the composition changed drastically as the silks were immersed for longer periods of time. Aldehydes ranging from 20 to 32 carbons were evident as well as fatty acids ranging from 16 to 24 carbons. Not only were free fatty acids evident as immersion time increased, but also naturally occurring fatty acid methyl ester derivatives. These ranged from 16 to 24 carbons in length and seemed to be most abundant when extracted for 2 minutes compared to a 60 second or 5 minute incubation. For SHCs, abundance increased for most of the metabolites analyzed as incubation time increased. Clearly, in Fig. 9b, all SHC class traits were more abundant as the fresh silks soaked for longer periods of time in the solvent. On average, 87% of the abundance variance seen across all 70 metabolites could be attributed to the solvent incubation time. Table 5 shows the effect of incubation time on SL traits upon silk emergence. For all the class traits examined, incubation time greatly contributed to the abundance variation that was seen.

Figure 9

(a)

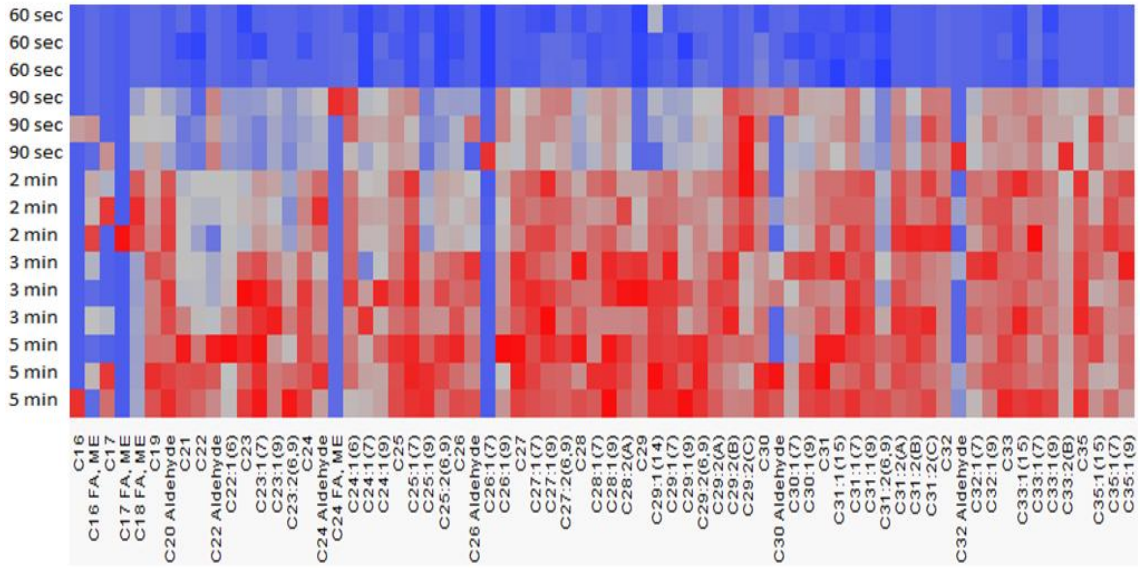
60 sec
60 sec
60 sec
90 sec
90 sec
90 sec
2 min
2 min
2 min
3 min
3 min
3 min
5 min
5 min
5 min
C16
C16 FA, ME
C17
C17 FA, ME
C18 FA, ME
C19
C20 Aldehyde
C21
C22
C22 Aldehyde
C22:1(6)
C23
C23:1(7)
C23:1(9)
C23:2(6,9)
C24
C24 Aldehyde
C24 FA, ME
C24:1(6)
C24:1(7)
C24:1(9)
C25
C25:1(7)
C25:1(9)
C25:2(6,9)
C26
C26 Aldehyde
C26:1(7)
C26:1(9)
C27
C27:1(7)
C27:1(9)
C27:2(6,9)
C28
C28:1(7)
C28:1(9)
C28:2(A)
C29
C29:1(14)
C29:1(7)
C29:1(9)
C29:2(6,9)
C29:2(A)
C29:2(B)
C29:2(C)
C30
C30 Aldehyde
C30:1(7)
C30:1(9)
C31
C31:1(15)
C31:1(7)
C31:1(9)
C31:2(6,9)
C31:2(A)
C31:2(B)
C31:2(C)
C32
C32 Aldehyde
C32:1(7)
C32:1(9)
C33
C33:1(15)
C33:1(7)
C33:1(9)
C33:2(B)
C35
C35:1(15)
C35:1(7)
C35:1(9)

(b)

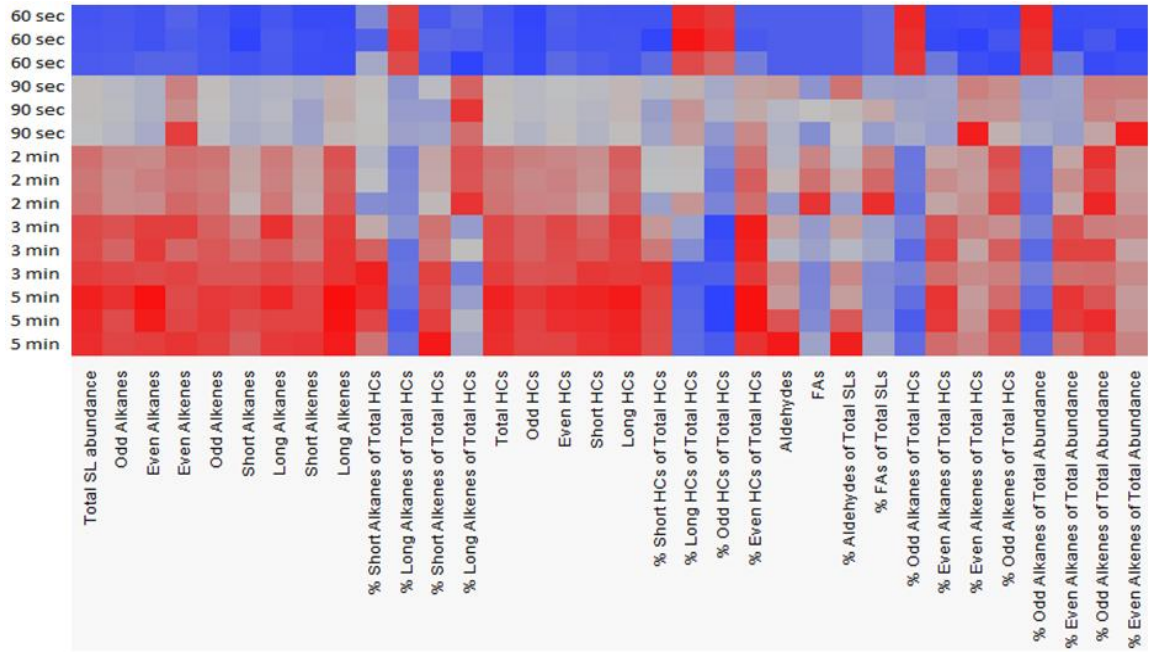
60 sec
60 sec
60 sec
90 sec
90 sec
90 sec
2 min
2 min
2 min
3 min
3 min
3 min
5 min
5 min
5 min
Total SL abundance
Odd Alkanes
Even Alkanes
Even Alkenes
Odd Alkenes
Short Alkanes
Long Alkanes
Short Alkenes
Long Alkenes
% Short Alkanes of Total HCs
% Long Alkanes of Total HCs
% Short Alkenes of Total HCs
% Long Alkenes of Total HCs
Total HCs
Odd HCs
Even HCs
Short HCs
Long HCs
% Short HCs of Total HCs
% Long HCs of Total HCs
% Odd HCs of Total HCs
% Even HCs of Total HCs
Aldehydes
FAs
% Aldehydes of Total SLs
% FAs of Total SLs
% Odd Alkanes of Total HCs
% Even Alkanes of Total HCs
% Even Alkenes of Total HCs
% Odd Alkenes of Total HCs
% Odd Alkanes of Total Abundance
% Even Alkanes of Total Abundance
% Odd Alkenes of Total Abundance
% Even Alkenes of Total Abundance

Figure 9 SL relative composition varies according to incubation times

The heat maps display the relative abundances across 70 different constituent metabolites, including hydrocarbons, fatty acids and aldehydes of different chain lengths (A) and class traits for these metabolites (B). Lipids were extracted with hexanes: diethyl ether (90:10) from 3 replicates for each incubation time. Colors are based on metabolite abundances; blue-low, grey-moderate, red-high. Fatty acids are displayed as (FA) and natural occurring methyl esters are displayed as (ME).

Table 5 Analysis of Variance: The impact of incubation time on silk relative composition traits using hexanes: diethyl ether (90:10) (no silica was used)

N= 15 (3 replicates x 5 time points)	R^2	P-value
Odd Alkanes	0.996	<0.0001*
Even Alkanes	0.994	<0.0001*
Odd Alkenes	0.998	<0.0001*
Even Alkenes	0.973	<0.0001*
Even HCs	0.996	<0.0001*
Odd HCs	0.999	<0.0001*
Total HCs	0.949	<0.0001*
Short Alkanes (C<26)	0.990	<0.0001*
Long Alkanes (C≥26)	0.995	<0.0001*
Short Alkenes (C<26)	0.993	<0.0001*
Long Alkenes (C≥26)	0.999	<0.0001*
Fatty Acids	0.914	<0.0001*
Aldehydes	0.858	0.0003*
Total SLs	0.999	<0.0001*
% Odd Alkanes	0.993	<0.0001*
% Even Alkanes	0.971	<0.0001*
% Odd Alkenes	0.981	<0.0001*
% Even Alkenes	0.947	<0.0001*
% Even HCs	0.983	<0.0001*
% Total HCs	0.849	0.0004*

SUMMARY

By not using silica, more of the polar lipids, especially fatty acids, are recovered from the lipid fraction. The hydrocarbon and fatty acid composition changed dramatically when silica was not applied to the extracts. Across all solvents, the fatty acid composition, without the presence of silica and without transmethylation treatment, constituted ~21% of the lipids from powderized silks. With silica purification, the fatty acid composition was less than 1%. Averaged across 6 replicate samples for each of the 5 solvents with and without silica, metabolite analyses showed that presence versus absence of silica explained 91% of the overall variation that was seen in total hydrocarbon content and explained 85% of the variation seen in total fatty acid recovery. Silica also had a major impact on hydrocarbon content among all solvents; hexanes: chloroform (1:1) showed an 8% higher hydrocarbon content in extracts subjected to silica than non-silica extracts, while chloroform showed a 26% higher abundance of hydrocarbons when extracts weren't subjected to silica purification than extracts filtered by silica. By removing the silica purification step, the opportunity to extract and quantify polar and non-polar metabolites from the silks is achievable.

While the use of silica impacted the composition of the metabolite array, the solvent choice significantly impacted the recovery of metabolites detected as well as the abundance of constituent metabolites. The hexanes: diethyl ether (90:10) solvent showed the highest recovery for hydrocarbons among all solvents. Class trait

recoveries were dependent among the polarity of the solvent choice; the hexanes: diethyl ether (90:10) solvent outperformed the hexanes: diethyl ether (95:5) solvent in the abundance of odd alkanes, but was shown to be less efficient than the hexanes: diethyl ether (95:5) solvent in respect to recovery for odd alkenes. Upon transmethylation of free fatty acids, recovery increased nearly 5-fold; among all the solvents tested, 21 FA constituents were detected. Again, the hexanes: diethyl ether (90:10) solvent showed the highest recovery among all solvents in total fatty acids and proved to be 20% higher than hexane-extracted samples. The three polar solvents (chloroform, hexanes: chloroform (1:1) and hexanes: diethyl ether (90:10)) extracted fatty acids in greater abundance compared to the most non-polar solvent (hexanes). The fatty acid analysis clearly showed that the solvent polarity is important with respect to abundance and recovery of fatty acid constituents.

Both hydrocarbon and fatty acid class trait abundances seemed to be governed by the incubation time length whether or not silica was used. The 30 min incubation showed the highest abundance for both constituent metabolites as well as for class traits among the other incubation times examined. This showed that abundance is highly correlated with extraction incubation time as well as the number of extractions performed. For silica treated samples, for the two solvents tested, hexanes: diethyl ether (90:10) and hexanes: chloroform (1:1), solvent incubation time accounted for 79% of the variance seen in total silk lipid abundance, while for samples not subjected to silica, 25% of the variance seen could be attributed to incubation time.

While the abundance of constituent metabolites decreased in respect to extraction incubation time, the recovery of metabolite classes also tapered. While even-numbered alkenes drastically diminished as extraction time lessened, all hydrocarbon class traits as well as fatty acids were reduced upon a lowered incubation time whether or not silica was used. In metabolite recovery between the solvents, hexanes: diethyl ether (90:10) and hexanes: chloroform (1:1), solvent incubation time contributed to 82% of the variance in silica-purified samples and 57% in samples not subjected to silica. Overall, significant recovery loss was seen when a 30 min solvent incubation time was reduced to a 1 min incubation. Average detectable constituent metabolite recovery loss, from a 30 min extraction to a 1 min extraction, went from 36 to 23 metabolites in silica samples and 36 to 28 metabolites in non-silica samples.

For whole silk extractions, incubation time was tested to determine abundance differences as well as composition variation when silks were immersed into the selected solvent. Not only was composition shown to vary in respect to an increased solvent incubation time, but abundances increased as well. On average, 87% of the variation seen in the constituent SL abundances was due to the incubation time. Not only was recovery of specific constituents greater for aldehydes and fatty acids when immersion time increased, but abundance was also significantly greater for all constituents analyzed. Seen by the abundance deviations (Table 1 and Table 4) for HCs alone, great variation exists among lipids extracted from whole intact silks compared to lipids extracted from powderized silk.

While fatty acids were the predominant constituents extracted from powderized silks, aldehydes and HCs were the most abundant metabolites extracted from dipped whole silks. These differences were extensively characterized in Chapter 3. For extracting non-polar and polar metabolites from fresh whole silks, a longer incubation time proved to be best to capture aldehydes and fatty acid constituents which weren't detected at a 60 sec solvent immersion. For powderized silk, hexanes: diethyl ether (90:10) proved to be the best solvent in extracting fatty acids and hydrocarbons in the greatest abundance. Along with this solvent choice, a longer incubation time and the omission of silica lead to the broadest array of metabolites captured as well as abundance.

EXPERIMENTAL METHODS

Plant material

Experimental tests were conducted using the maize (*Zea mays L.*) inbred line B73. Developing ear shoots were covered with Lawson #217 shoot bags prior to silk emergence. Daily checking for silk emergence from the husk leaves allowed the silks of each of the ears to be collected at 3 days post silk emergence.

Silks used in the powderized silk experiments were collected from plants grown on the Iowa State University Agronomy Farm in 2012. Whole ears were carried back to the lab

on ice in coolers, where silks were cut free at the emergence point and placed into 50 ml conical tubes. Silk fresh weights were recorded for each sample. Samples were flash frozen with liquid nitrogen and stored at -80°C. Before SL extractions were performed, the silks were lyophilized, dry-weighed, then ground with six 5/32" stainless steel beads for 5 minutes using a Genogrinder2010.

The B73 silks used in the solvent immersion experiments were planted in the spring of 2013 in the Plant Pathology greenhouse at Iowa State University (Ames, IA). Silks were harvested as described above, and were then transported to the lab on ice for SL extractions. Silks were cut at the emergence point and fresh-weighed prior to extraction.

Extraction Method

Powderized silks: Lipid metabolites were extracted with five different solvents: hexanes, hexanes: diethyl ether (95:5), hexanes: diethyl ether (90:10), hexanes: chloroform (1:1) and chloroform. Each powderized sample was initially spiked with 5-10µl of the internal standard, eicosane (1mg/ml) depending on the mass of the sample (5 µl of standard for 0.04 to 0.06g of sample and 10 µl of standard for 0.09 to 0.11g of sample). Solvent (2ml) was added to each sample, vortexed for 10 min and centrifuged for 5 min at 3,250 rpm. Extracts were moved to fresh tubes and the extraction of the silk sample was repeated up to 3 times, depending on the time length of the extraction

(Fig. 1). Combined extracts for each sample were concentrated under N_2 gas and subjected to GC-MS analysis.

For samples that were incubated with silica, silk samples were extracted 1-3 times in solvent and the resulting extracts were transferred to a fresh tube containing 2 grams of silica (40-140 mesh; JT Baker, http://www.jtbaker.com). Samples were vortexed for 2 minutes and centrifuged. Extracts were removed using glass wool as a filter to prevent the transfer of silica. Combined extracts for each sample were concentrated under N_2 gas and subjected to GC-MS analysis.

Whole silks: Each fresh silk sample was extracted in 8ml of hexanes: diethyl ether (90:10) solvent that had been spiked with 5-10 µl of the internal standard, eicosane (1mg/ml). The silks were immersed into the solvent for 60 sec, and then the solvent was poured from the beaker into a clean glass tube and capped [10]. Extracts were concentrated under N_2 gas and analyzed via GC-MS.

Transmethylation and dimethyl disulfide derivatization

For fatty acid analysis, transmethylation derivatization was conducted. Metabolite extracts were derivatized via transmethylation by adding 2ml of 1N HCl in methanol [48]. Extracts were incubated at 80˚C for 1 hr. After incubation, 2 ml of 0.9% NaCl and 0.5 ml of hexanes were added to the extract. Extracts were vortexed and then centrifuged at 3,000 rpm for 5 min to separate the two fractions. The hexane layer was recovered and moved to a separate GC vial. To the original tube, another 1 ml of

hexanes was added to allow for full recovery of the lipid metabolites. To confirm carbon-carbon double bond positions for unsaturated metabolites (alkene, diene and unsaturated fatty acid), extracts were subjected to dimethyl disulfide derivatization [10]. After the organic phase (hexane layer) was recovered 3x with the addition of hexanes, dimethyl disulfide adducts were then concentrated and analyzed via GC-MS [49,50,51,52,53,54].

Analytical Instrumentation

Gas chromatography was performed with an HP-5MS cross-linked (5%) diphenyl (95%) dimethyl polysiloxane column (30m in length; 0.25-mm inner diameter) using helium as the carrier gas, and an Agilent Technologies series 6890 gas chromatograph, equipped with a model 5973 mass detector (Agilent Technologies, http://www.home.agilent.com). After a 1 µl sample injection (splitless), the initial temperature (120˚C) of the oven was raised to 260˚C, at a rate of 10˚C/min, and held for 1min. This was followed by an increase to 300˚C, at a ramp of 5˚C/min, and held for 1 min, then a subsequent ramp to 320˚C by 5˚C/min.

Lipid Analysis

For metabolite confirmation, the mass spectra as well as the retention times and retention indices for each compound were used. The retention indices of these metabolites were calculated based on a calibration file of straight chain hydrocarbons (C7-C40). Quantification analysis was performed with AMDIS

(http://chemdata.nist.gov/mass-spc/amdis/). The NIST Mass Spectral library (http://webbook.nist.gov/chemistry/) was used for identifying compounds by mass spec comparisons.

Statistical Methods

All metabolite abundances were quantified according to the initial amount of internal standard placed in each extraction tube. Data was generated from a minimum of triplicate biological replicates. The error bars shown in the bar graphs were calculated based on standard error between replicates of a similar solvent condition. The JMP software package from SAS was used for statistical analyses as well as for the generation of heat maps, bar and pie charts, correlation tables and fit model analyses. All p-value statistics shown are based on a 0.05 significance level, while if significant, an asterisk would appear next to it.

Acknowledgements

We thank members of the Lauter research group (David Hessel, Adam Bossard, Hannah Cox and Merriam Lopez) for assistance in sample collection, Sam Condon, Wenmin Qin (Nikolau group) and Zhihong Song and Ann Perera (W.M. Keck Metabolomics Research Laboratory) for technical assistance with GC-MS.

REFERENCES

1. Javelle M, Vernoud V, Rogowsky PM, Ingram GC (2011) Epidermis: the formation and functions of a fundamental plant tissue. New Phytol 189: 17-39.

2. Jordan WR, Shouse PJ, Blum A, Miller FR, Monk RL (1984) Environmental Physiology of Sorghum. II. Epicuticular Wax Load and Cuticular Transpiration1. Crop Sci 24: 1168-1173.

3. Kosma D, Jenks M (2007) Eco-Physiological and Molecular-Genetic Determinants of Plant Cuticle Function in Drought and Salt Stress Tolerance. In: Jenks M, Hasegawa P, Jain SM, editors. Advances in Molecular Breeding Toward Drought and Salt Tolerant Crops: Springer Netherlands. pp. 91-120.

4. Long LM, Patel HP, Cory WC, Stapleton AE (2003) The maize epicuticular wax layer provides UV protection. Functional Plant Biology 30: 75-81.

5. Yang G, Isenhour DJ, Espelie KE (1991) Activity of Maize Leaf Cuticular Lipids in Resistance to Leaf-Feeding by the Fall Armyworm. The Florida Entomologist 74: 229-236.

6. Yang G, Wiseman BR, Espelie KE (1992) Cuticular lipids from silks of seven corn genotypes and their effect on development of corn earworm larvae [Helicoverpa zea (Boddie)]. Journal of Agricultural and Food Chemistry 40: 1058-1061.

7. Yang G, Wiseman BR, Isenhour DJ, Espelie KE (1993) Chemical and Ultrastructural Analysis of Corn Cuticular Lipids and Their Effect on Feeding by Fall Armyworm Larvae. Journal of Chemical Ecology 19: 2055-2074.

8. Bassetti P, Westgate ME (1993) Senescence and Receptivity of Maize Silks. Crop Sci 33: 275-278.

9. Perera MAN, Nikolau B (2007) Metabolomics of Cuticular Waxes: A System for Metabolomics Analysis of a Single Tissue-Type in a Multicellular Organism. In: Nikolau B, Wurtele E, editors. Concepts in Plant Metabolomics: Springer Netherlands. pp. 111-123.

10. Perera MA, Qin W, Yandeau-Nelson M, Fan L, Dixon P, et al. (2010) Biological origins of normal-chain hydrocarbons: a pathway model based on cuticular wax analyses of maize silks. Plant Journal 64: 618-632.

11. Bianchi G, Avato P, Salamini F (1978) Glossy mutants of maize. VIII. Accumulation of fatty aldehydes in surface waxes of gl5 maize seedlings. Biochem Genet 16: 1015-1021.

12. Avato P, Bianchi G, Pogna N (1990) Chemosystematics of Surface-Lipids from Maize and Some Related Species. Phytochemistry 29: 1571-1576.

13. Prügel B, Lognay G (1996) Composition of the Cuticular Waxes of Picea abies and P. sitchensis. Phytochemical Analysis 7: 29-36.

14. Dallerac R, Labeur C, Jallon JM, Knipple DC, Roelofs WL, et al. (2000) A delta 9 desaturase gene with a different substrate specificity is responsible for the cuticular

diene hydrocarbon polymorphism in Drosophila melanogaster. Proc Natl Acad Sci U S A 97: 9449-9454.

15. Nelson DR, Tissot M, Nelson LJ, Fatland CL, Gordon DM (2001) Novel wax esters and hydrocarbons in the cuticular surface lipids of the red harvester ant, Pogonomyrmex barbatus. Comp Biochem Physiol B Biochem Mol Biol 128: 575-595.

16. Cameron KD, Teece MA, Bevilacqua E, Smart LB (2002) Diversity of cuticular wax among Salix species and Populus species hybrids. Phytochemistry 60: 715-725.

17. Sirot V, Oseredczuk M, Bemrah-Aouachria N, Volatier J-L, Leblanc J-C (2008) Lipid and fatty acid composition of fish and seafood consumed in France: CALIPSO study. Journal of Food Composition and Analysis 21: 8-16.

18. Kozlova TA, Khotimchenko SV (2000) Lipids and fatty acids of two pelagic cottoid fishes (Comephorus spp) endemic to Lake Baikal. Comp Biochem Physiol B Biochem Mol Biol 126: 477-485.

19. Lepage G, Roy CC (1986) Direct transesterification of all classes of lipids in a one-step reaction. Journal of Lipid Research 27: 114-120.

20. Ulberth F, Henninger M (1992) One-step extraction/methylation method for determining the fatty acid composition of processed foods. Journal of the American Oil Chemists' Society 69: 174-177.

21. Carrapiso AI, Luisa Timon MA, Jesus Petron MA, Tejeda JF, Garcia C (2000) In situ transesterification of fatty acids from Iberian pig subcutaneous adipose tissue. Meat Sci 56: 159-164.

22. Dickey LA, Teter BB, Sampugna J, Woods LC (2002) Comparison of a Direct Transesterification Method and the Bligh and Dyer Method to Determine Fatty Acid Content in Striped Bass Tissues and Diet. North American Journal of Aquaculture 64: 158-163.

23. Meier S, Mjos SA, Joensen H, Grahl-Nielsen O (2006) Validation of a one-step extraction/methylation method for determination of fatty acids and cholesterol in marine tissues. J Chromatogr A 1104: 291-298.

24. Araujo P, Nguyen TT, Froyland L, Wang J, Kang JX (2008) Evaluation of a rapid method for the quantitative analysis of fatty acids in various matrices. J Chromatogr A 1212: 106-113.

25. Xiao LP, Mjos SA, Haugsgjerd BO (2012) Efficiencies of three common lipid extraction methods evaluated by calculating mass balances of the fatty acids. Journal of Food Composition and Analysis 25: 198-207.

26. Bligh EG, Dyer WJ (1959) A rapid method of total lipid extraction and purification. Can J Biochem Physiol 37: 911-917.

27. Anonymous (1998) Official Methods and Recommended Practices of the American Oil Chemists' Society. American Oil Chemists' Society. Urbana, IL, USA.

28. Anonymous (1999) Animal Feeding Stuffs-determination of Fat Content. International Organization for Standardization.

29. Iverson SJ, Lang SL, Cooper MH (2001) Comparison of the Bligh and Dyer and Folch methods for total lipid determination in a broad range of marine tissue. Lipids 36: 1283-1287.

30. Folch J, Lees M, Sloane Stanley GH (1957) A simple method for the isolation and purification of total lipides from animal tissues. J Biol Chem 226: 497-509.

31. Christie WW (1982) *Lipid Analysis*. 2nd ed. New York: Pergamon Press.

32. Marmer WN, Maxwell RJ, Williams JE (1981) Effects of dietary regimen and tissue site on bovine fatty acid profiles. Lipids 16: 365-378.

33. Elmer-Frohlich K, Lachance P (1992) Faster and easier methods for quantitative lipid extraction and fractionation from miniature samples of animal tissues. Journal of the American Oil Chemists Society 69: 243-245.

34. Hajra A (1974) On extraction of acyl and alkyl dihydroxyacetone phosphate from incubation mixtures. Lipids 9: 502-505.

35. Weerheim AM, Kolb AM, Sturk A, Nieuwland R (2002) Phospholipid composition of cell-derived microparticles determined by one-dimensional high-performance thin-layer chromatography. Analytical Biochemistry 302: 191-198.

36. Jensen SK (2008) Improved Bligh and Dyer extraction procedure. Lipid Technology 20: 280-281.

37. Soxhlet F (1879) Die gewichtsanalytische Bestimmung des Milchfettes. Dingler's Polytechnisches 232: 461-465.

38. Bloor WR (1928) The determination of small amounts of lipid in blood plasma. Journal of Biological Chemistry 17: 53-73.

39. Sheppard AJ (1963) Suitability of lipid extraction procedures for gas-liquid chromatography. Journal of the American Oil Chemists' Society 40: 545-548.

40. Baümler E, Crapiste G, Carelli A (2010) Solvent Extraction: Kinetic Study of Major and Minor Compounds. Journal of the American Oil Chemists' Society 87: 1489-1495.

41. Hara A, Radin NS (1978) Lipid extraction of tissues with a low-toxicity solvent. Anal Biochem 90: 420-426.

42. Eder K, Reichlmayr-Lais AM, Kirchgessner M (1993) Studies on the extraction of phospholipids from erythrocyte membranes in the rat. Clin Chim Acta 219: 93-104.

43. Guckert JB, White DC (1988) Evaluation of a hexane/isopropanol lipid solvent system for analysis of bacterial phospholipids and application to chloroform-soluble Nuclepore (polycarbonate) membranes with retained bacteria. Journal of Microbiological Methods 8: 131-137.

44. Markham JE, Li J, Cahoon EB, Jaworski JG (2006) Separation and Identification of Major Plant Sphingolipid Classes from Leaves. Journal of Biological Chemistry 281: 22684-22694.

45. Matyash V, Liebisch G, Kurzchalia TV, Shevchenko A, Schwudke D (2008) Lipid extraction by methyl-tert-butyl ether for high-throughput lipidomics. J Lipid Res 49: 1137-1146.

46. Ichihara K, Yoneda K, Takahashi A, Hoshino N, Matsuda M (2011) Improved methods for the fatty acid analysis of blood lipid classes. Lipids 46: 297-306.

47. Abbott SK, Jenner AM, Mitchell TW, Brown SH, Halliday GM, et al. (2013) An improved high-throughput lipid extraction method for the analysis of human brain lipids. Lipids 48: 307-318.

48. Kates M (1986) Techniques of lipidology : isolation, analysis, and identification of lipids. Amsterdam ; New York, NY, U.S.A.: Elsevier ; Sole distributors for the U.S.A. and Canada, Elsevier Science Pub. Co. xx, p.p. 464.

49. Rieley G, Teece MA, Peakman TM, Raven AM, Greene KJ, et al. (1998) Long-chain alkenes of the haptophytes Isochrysis galbana and Emiliania huxleyi. Lipids 33: 617-625.

50. Buser HR, Arn H, Guerin P, Rauscher S (1983) Determination of double bond position in mono-unsaturated acetates by mass spectrometry of dimethyl disulfide adducts. Analytical Chemistry 55: 818-822.

51. Pepe C, Sayer H, Dagaut J, Couffignal R (1997) Determination of double bond positions in triunsaturated compounds by means of gas chromatography mass spectrometry of dimethyl disulfide derivatives. Rapid Communications in Mass Spectrometry 11: 919-921.

52. Scribe P, Guezennec J, Dagaut J, Pepe C, Saliot A (1988) Identification of the position and the stereochemistry of the double bond in monounsaturated fatty acid methyl esters by gas chromatography/mass spectrometry of dimethyl disulfide derivatives. Analytical Chemistry 60: 928-931.

53. Pepe C, Sayer H, Bacelon P (1999) Letter: Determination of positions of double bonds in conjugated alkadienes by means of gas chromatography/mass spectrometry of dimethyl disulfide derivatives. European Mass Spectrometry 5: 285-287.

54. Moss CW, Lambert-Fair MA (1989) Location of double bonds in monounsaturated fatty acids of Campylobacter cryaerophila with dimethyl disulfide derivatives and combined gas chromatography-mass spectrometry. J Clin Microbiol 27: 1467-1470.

CHAPTER 3. DETERMINATION AND QUANTIFICATION OF UNSATURATED METABOLITES IN MAIZE SILK: AN UPDATED PATHWAY MODEL FOR SURFACE LIPID BIOSYNTHESIS

Not published

Authors and roles:

Conceived the experiments: LP, BJN, NL, MYN

Designed the experiments: LP, MYN, NL

Executed the experiments: LP

Performed data analyses: LP, MYN, NL

Prepared the manuscript: LP, BJN, MYN, NL

ABSTRACT

A unique and diverse array of surface lipids is found on the silks of maize, including large quantities of non-isoprenoid hydrocarbons (alkanes, alkenes and dienes). In the maize inbred B73, we have identified both even- and odd-numbered hydrocarbons ranging in chain lengths from 14 to 37 carbons. The remaining

metabolites (fatty acids, aldehydes and ketones) are proposed to be the precursors in the biosynthesis of these hydrocarbons, and to date, the genetic elements and biochemical mechanisms for their synthesis remain unclear. Through GC-MS analysis of dimethyl disulfide adducts derived from lipid extracts from dry, powderized or fresh, whole silk samples, a homologous series of odd and even-chain length alkenes with double bonds at the 7^{th} and 9^{th} positions and monoenoic fatty acids (ω-7 and ω-9) have been identified. These findings suggest a pathway that involves sequential desaturation of the fatty acid, followed by elongation then decarbonylation via a fatty aldehyde intermediate to produce the respective alkenes. Also detected by mass-spectral identification was a homologous series of odd-chain dienes that ranged from 23 to 33 carbons in length. This series of dienes, with double bond positions situated at the 6^{th} and 9^{th} positions, are thought to be derived from the elongation of linoleic acid. Also found by mass-spectral fragmentation was the presence of odd and even-chain length saturated fatty aldehydes that range from 9 to 34 carbons in length. Based on these results, we propose that even-numbered alkanes and alkenes are derived from odd-chain saturated fatty acids and aldehydes. Finally, extractions have been performed and metabolites have been quantified that compare the composition differences between fresh dipped and dry powderized silk, which represent surface lipids and total silk lipids, respectively.

INTRODUCTION

The stigmatic silks in *Zea mays* L. (maize) are the conduits for fertilization and are therefore important for reproductive success (i.e. yield). The surface lipids (SLs) that coat these silks consist of a wide array of hydrocarbons (HCs), aldehydes and fatty acids (FAs) with minor amounts of ketones and alcohols in select genotypes [1,2,3]. While maize leaves tend to have high abundances in fatty alcohols, esters and aldehydes [4,5], maize silks consist mainly of linear HCs (alkanes, alkenes and dienes). For example, hydrocarbons comprise >90% of the surface lipids on maize silks and make up ~2% of silk dry weight, making silks the most abundant source of hydrocarbons in the plant. These SLs protect against abiotic stresses, including desiccation [6,7] and UV radiation [8], and biotic stresses, such as pathogen invasion [9] and insect feeding (moths, insects and beetles) [1,10,11], especially during the critical time for pollen reception, which exists for only a few short days [12].

Hydrocarbons are presumed to be synthesized from fatty acids, however the metabolic reactions and the enzymes involved in hydrocarbon biosynthesis are largely undefined. Over many decades, four mechanisms of synthesis have been proposed, each of which initiates from fatty acid precursors [13,14,15,16,17]: 1) head-to-head condensation of two fatty acids, 2) decarboxylation of a fatty acid, 3) reduction of a fatty acid to an aldehyde, followed by decarbonylation, and 4) sequential reduction of the fatty acid to an aldehyde and alcohol, followed by dehydration and reduction.

Head-to-head condensation has been shown to occur in the bacterium *Shewanella oneidensis* [18,19] and in the bacterium *Micrococcus luteus*, where it catalyzes the production of ketones and alkenes [20]. Evidence has shown that alkanes and alkenes in the house fly [21] are biosynthesized from a decarboxylation mechanism from a FA precursor. Evidence for a reduction-decarbonylation mechanism exists in several organisms [22,23,24,25] and recently has been more extensively characterized in the plant, Arabidopsis [21].

An elegant analysis of surface lipid metabolites on maize silks suggests that alkanes and alkenes are biosynthesized by three potential decarbonylation-based pathways. One of these, is an elongation-isomerization-decarbonylation pathway, while the other two consist of parallel pathways of either desaturation-elongation or elongation-desaturation of the FA followed by sequential reduction and decarbonylation [2].

Although far less abundant than HCs of odd-numbered chain lengths, a very complex array of hydrocarbons (Chapter 2) of even-numbered chain lengths (alkanes, alkenes and dienes) and odd-chained aldehydes and saturated and unsaturated fatty acids (Chapter 3) have been identified. This broad array of metabolites suggests a metabolic network for HC production that is more complex than originally predicted [2]. While these latter metabolites, which include even-chain HCs and odd-chain FAs,

are not new in select maize silk genotypes [1], they have not been shown to exist in B73 [2].

In this article, the surface lipids of the silk cuticle as well as the lipids from powderized silk were extracted and analyzed to provide insight and depth into plant HC biosynthesis, which remains largely undiscovered. Herein, unsaturated fatty acids, aldehydes and hydrocarbons were extracted, separated into different fractions and then assessed for positions of double bonds. While studies have indicated that alkenes could be biosynthesized by a pathway that involves the elongation of saturated FAs, which are desaturated followed by reduction to corresponding aldehydes and then decarbonylated to produce alkenes [2], data presented in this Chapter suggest that FAs first undergo desaturation followed by elongation, and then reduction to an aldehyde intermediate, which is decarbonylated to generate the defined alkenes. Likewise, for alkanes and alkenes of even-numbered chain lengths, we hypothesize that these hydrocarbons are likely derived from odd numbered fatty acids via a reduction-decarbonylation mechanism.

RESULTS & DISCUSSION

Surface lipid analyses

Silks from the maize inbred, B73 were harvested three days after silks first emerged. To extract the metabolites that accumulate on the silk surface, fresh silks were immediately immersed in the solvent, hexanes: diethyl ether (9:1), according to the protocol established in Chapter 2. This method ensures that only surface metabolites (and not intracellular metabolites) will be extracted, as compared to extracts prepared from powderized silks. The extracts were analyzed via GC-MS and the resulting total ion chromatograms revealed a range of fatty acid, aldehyde and hydrocarbon constituents (Fig. 10, Table 6). To confirm the identification of these constituents, deconvoluted mass spectra were analyzed using AMDIS and these spectra were also compared to co-elution commercial standards that consisted of alkanes ranging from 7 to 40 carbons. Surface hydrocarbon metabolites ranged from 14 to 37 carbons in length and as observed in previous reports [1,3], predominantly included odd–numbered alkanes and alkenes, which eluted very close to alkanes of the same chain lengths (Fig. 10b). In addition, even-numbered hydrocarbons (alkanes, alkenes and dienes) were also identified, albeit at lower levels than odd-numbered hydrocarbons (Fig. 10b).

In addition to hydrocarbons, a total of 24 aldehyde constituents ranging from 9- to 34-carbons (C9-C34) in length were identified; these included all odd- and even-chain lengths excluding C31 and C33. This suite of aldehydes was only identified in a very concentrated sample derived from an extract of 1.5 grams of fresh silk and then concentrated to 30 µL, under N_2 gas. However, many of the even-numbered saturated

aldehydes with chain lengths ranging from 20 to 28 carbons were observed in a more dilute sample (500 µl), and thus are more prevalent on the silk surface.

Figure 10

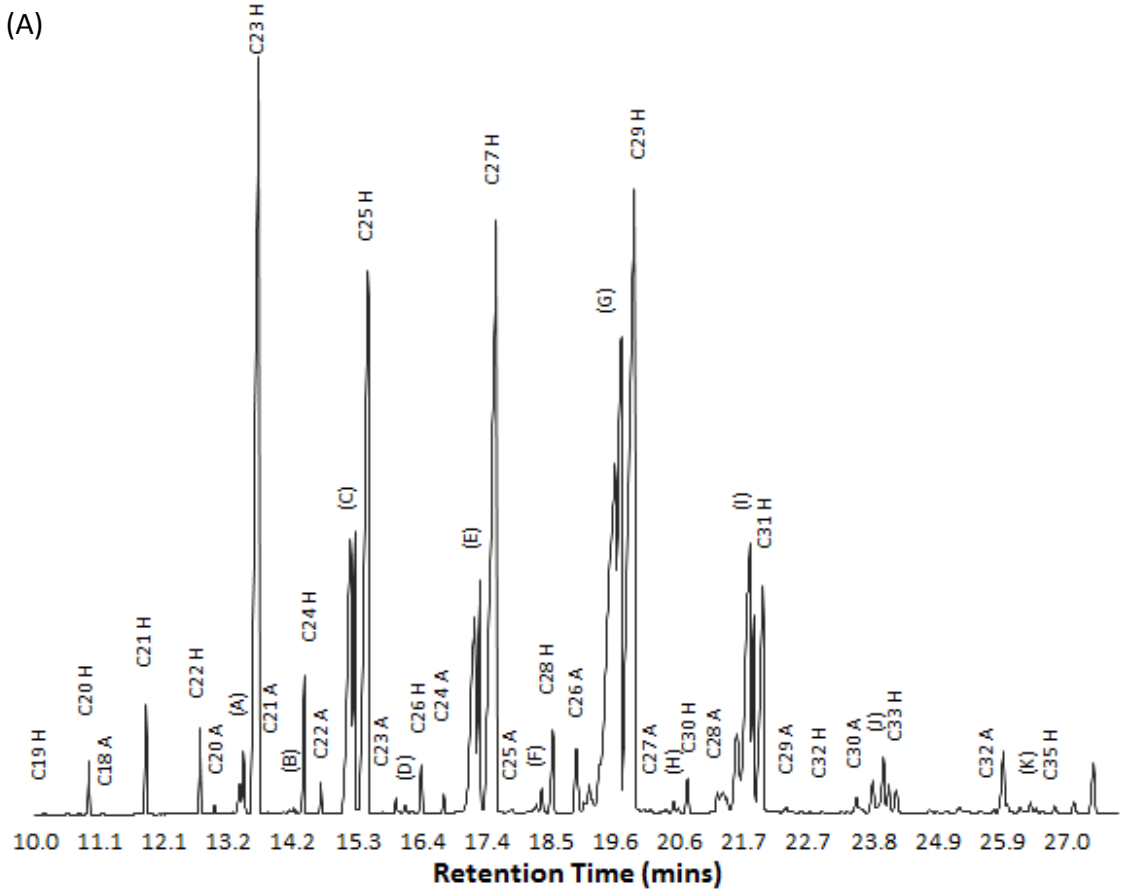

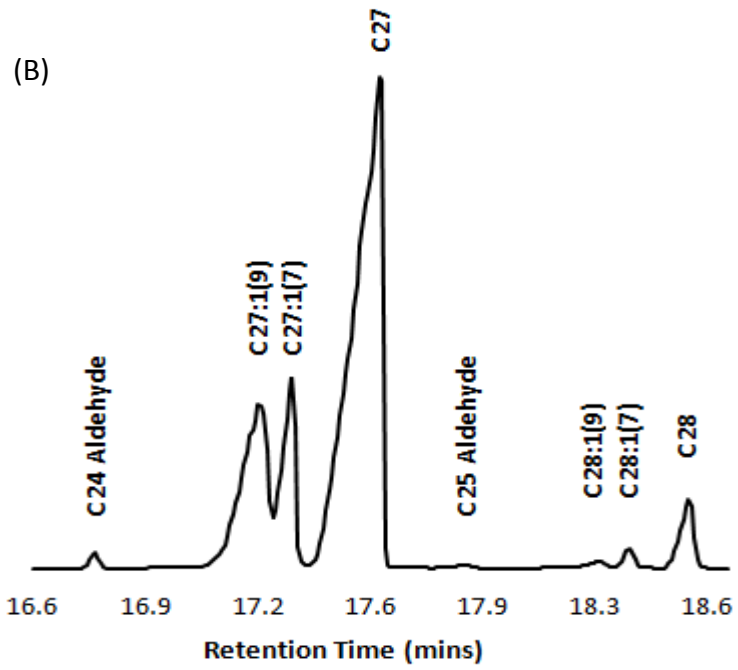

Figure 10 Gas chromatograph of the surface lipid fraction of B73 emerged silks

Shown in the figure is the total ion chromatogram of the surface lipid portion of 3-day post emergent silks (a), and the expanded view of a portion of the chromatograph in (a) between the retention times of 16.6 and 18.6 minutes (b). For the expanded chromatograph (b), metabolites are labeled. Compounds were verified by comparing with the NIST metabolite library and co-elution with authentic commercial standards (not shown).
(A),(B),(C),(D),(E),(F),(G),(H),(I),(J) and (K) represent alkenes and dienes associated with C23, C24, C25, C26, C27, C28, C29, C30, C31, C33 and C35, respectively. Letters listed next to metabolite names distinguish aldehydes from hydrocarbons (A, aldehydes and H, hydrocarbons).

To identify fatty acids that may be present in the surface lipid extracts, extracts were derivatized via transmethylation to convert fatty acids to fatty acid methyl esters

and then analyzed via GC-MS (Table 6). In addition to hydrocarbons, fatty acids and aldehydes were also observed in these derivatized extracts (Table 6). The arrays of these constituents suggest that the even-numbered hydrocarbons are synthesized via a reduction-decarbonylation pathway. For example, homologous series' of odd-numbered fatty acids and odd-numbered aldehydes, ranging from 9 to 31 carbons in length, were identified in these extracts and both metabolite classes are predicted to be intermediates in a decarbonylation-based pathway that produces even-numbered fatty acids. Likewise, odd-numbered HCs would be biosynthesized by even-chain FA and aldehyde precursors via reduction-decarbonylation. Moreover, the corresponding N-1 HCs, which refers to the loss of the carbonyl group from the FA after decarbonylation, were also present in these extracts. Together, these data suggest that even-numbered alkanes are derived from odd-numbered FA precursors, which after FA elongation, get reduced to corresponding aldehydes then decarbonylated to generate the even-numbered alkanes identified on the silk surface.

Table 6 Surface lipid composition of B73 maize silks determined from transmethylated extracts

Metabolite	nmole/g dry weight [a]	Metabolite	nmole/g dry weight [a]
13-carbon metabolites		**26-carbon metabolites**	
tridecanoic acid	0.04 ± 0.08	hexacosane	120.64 ± 9.63
14-carbon metabolites		7-hexacosene	2.92 ± 0.85
tetradecanoic acid	4.68 ± 0.29	9-hexacosene	4.34 ± 3.76
15-carbon metabolites		hexacosanoic acid	6.11 ± 0.77
pentadecanoic acid	2.20 ± 0.59	**27-carbon metabolites**	
16-carbon metabolites		heptacosane	3,186.40 ± 23.79
hexadecanoic acid	209 ± 7.39	7-heptacosene	802.08 ± 18.39
9-hexadecenoic acid	2.63 ± 0.05	9-heptacosene	1,130.76 ± 14.50
17-carbon metabolites		6,9-heptacosadiene	299.60 ± 14.91
heptadecanoic acid	4.93 ± 0.48	**28-carbon metabolites**	
18-carbon metabolites		octacosane	384.51 ± 7.77
octadecanoic acid	375.21 ± 22.73	7-octacosene	66.23 ± 0.76
9-octadecenoic acid	7.73 ± 0.55	9-octacosene	21.53 ± 2.75
11-octadecenoic acid	4.67 ± 0.70	octacosanoic acid	1.94 ± 1.84
19-carbon metabolites		**29-carbon metabolites**	
nonadecane	5.36 ± 0.51	nonacosane	4,958.77 ± 22.82
nonadecanoic acid	1.60 ± 0.18	7-nonacosene	3,027.30 ± 5.49
20-carbon metabolites		9-nonacosene	2,875.32 ± 20.02
eicosanoic acid	4.74 ± 0.72	14-nonacosene	806.90 ± 16.52
21-carbon metabolites		6,9-nonacosadiene	621.98 ± 4
heneicosane	176.08 ± 13.52	(a,b)-nonacosadiene	46.26 ± 5.35
heneicosanoic acid	0.06 ± 0.10	(c,d)-nonacosadiene	114.98 ± 12.99
22-carbon metabolites		(e,f)-nonacosadiene	12.24 ± 3.01
docosane	178.17 ± 8.36	**30-carbon metabolites**	
6-docosene	0.65 ± 0.12	triacontane	186.84 ± 8.62
docosanal	5.87 ± 0.64	7-triacontene	22.31 ± 1.05
docosanoic acid	27.59 ± 5.73	9-triacontene	33.59 ± 2.80
23-carbon metabolites		**31-carbon metabolites**	
tricosane	1,563.94 ± 34.52	hentriacontane	1,805.04 ± 11.16
7-tricosene	71.04 ± 7.54	7-hentriacontene	1,049.30 ± 16.91
9-tricosene	42.60 ± 3.41	9-hentriacontene	2,327.47 ± 23.11
6,9-tricosadiene	2.64 ± 2.32	15-hentriacontene	713.07 ± 12.55
tricosanoic acid	1.13 ± 0.15	(a,b)-hentriacontadiene	196.89 ± 10.31
24-carbon metabolites		(c,d)-hentriacontadiene	175.34 ± 3.89
tetracosane	329.50 ± 13.12	(e,f)-hentriacontadiene	106.80 ± 13.69
6-tetracosene	3.42 ± 0.62	**32-carbon metabolites**	
7-tetracosene	3.63 ± 0.36	doctriacontane	10.89 ± 1.04
9-tetracosene	2.56 ± 4.43	9-doctriacontene	4.86 ± 0.35
tetracosanal	3.19 ± 0.50	**33-carbon metabolites**	
tetracosanoic acid	28.17 ± 1.57	tritriacontane	147.40 ± 2.89
25-carbon metabolites		7-tritriacontene	139.57 ± 3.34
pentacosane	1,617.76 ± 15.46	9-tritriacontene	366.92 ± 5.38
7-pentacosene	565.99 ± 17.07	15-tritriacontene	188.42 ± 6.24
9-pentacosene	973.60 ± 19.05	**35-carbon metabolites**	
6,9-pentacosadiene	135.90 ± 4.42	pentatriacontane	11.84 ± 1.72
pentacosanoic acid	0.44 ± 0.14	7-pentatriacontene	12.67 ± 2.44
		9-pentatracontene	24.89 ± 2.30
		15-pentatriacontene	23.94 ± 4.70

[a] Average value of three biological replicates ± 1 standard deviation

Dimethyl disulfide confirmation of double bond positions in unsaturated alkyl chains

To identify the carbon-carbon double bond positions in unsaturated metabolites (Table 6), extracts were incubated with dimethyl disulfide (DMDS) [26], which reacts at the double bond and introduces methyl sulfide adducts. Resulting DMDS-surface lipid adducts were analyzed using electron ionization mass spectrometry, which induces cleavage of the carbon-carbon bond between the adjacent carbons carrying the methyl sulfide (CH_3S) group. This ionization generated fingerprint mass ions $(A)^+$ and $(B)^+$ for which double bond positions could be determined.

For alkenes of even and odd-numbered chain lengths, unsaturated positions at the 7^{th} and 9^{th} carbons were predominant. For chain lengths of 23 to 28 carbons, 2 alkene peaks prevailed at each chain length; the first peak, closest to the alkane, was the Δ7, while the 2^{nd} peak which eluted first, consisted of many alkenes. While Δ9 alkenes were the most prominent hydrocarbon represented in this 2^{nd} peak, the peak also contained a complex array of other alkenes that eluted in the same position in GC-MS. For example, the analysis of the 23-carbon alkene (Fig. 11a) showed fragmentation ions with mass/charge (m/z) values of $(A)^+$ 145 and $(B)^+$ 271, indicating the presence of a double bond between the 7^{th} and 8^{th} carbons (i.e. a Δ7-C23 alkene). For the second 23-carbon alkene (Fig. 11b), daughter ions with m/z values of $(A)^+$ 173 and $(B)^+$ 243 correspond to a double bond between the 9^{th} and 10^{th} carbons (i.e. a Δ9-C23 alkene). While these were the two most commonly seen double bond positions, comprising

>50% of the abundance for any given carbon chain length, alkenes with other, unique double bond positions were also present in lesser amounts (Table 7). These consisted of unsaturated positions at the 1^{st}, 4^{th} and 5^{th} carbons to half the length of the molecule.

GC-MS analysis of DMDS adducts also confirmed the presence of numerous dienes, including a 23-carbon diene with double bonds at the 6^{th} and 9^{th} carbons (Fig. 11c). Fragmentation of the cyclic DMDS adduct resulted in fragmentation ions with m/z values of 131 (A+; corresponding to the 6^{th} carbon), and 243 (D+; corresponding to the 9^{th} carbon). Since the double bonds are within 4 carbons apart, a thietane ring is formed based on the distance of the double bonds. Other characteristic ions were C^+ ($M^+ - A^+$), B^+ ($M^+ - D^+$), the molecular ion (M^+) and ($M^+ - 47$) and ($M^+ - 95$). Loss of the methylthio group from the larger fragment (D^+) resulted in the mass ion 155 ($B^+ - 48$), whereas the loss of the methylthio group from the smaller fragment (A^+) resulted in 267 ($C^+ - 48$). These fragmentations are all shown in Fig. 11c.

While the largest set of dienes had double bond positions at the 6^{th} and 9^{th} carbons for alkenes of odd-numbered chain lengths from 23 to 33, many other dienes, which formed non-cyclic adducts were also found. For (7,19)-heptacosadiene (Fig. 11d), we saw in the mass spec (A^+) 145, $(B)^+$ 419, $(C)^+$ 405, (D^+) 159, ($B^+ - 48$) 371, ($B^+ - 94$) 325, ($C^+ - 48$) 357, ($C^+ - 94$) 311, as well as other characteristic mass ions (M^+) 564, ($M^+ - 94$) 470, and ($M^+ - 141$) 423. These daughter ions are all displayed (Fig. 11d)

where the resulting fragmentation breaks were at. Since the mass ion 145 is a characteristic fragment of a double bond situated 7 carbons from the end of the molecule, we can conclude that one of our double bonds is situated on the 7^{th} carbon. Concurrently, we can also conclude that since we have a non-cyclic adduct molecular weight for this diene, the 159 daughter ion belongs to an unsaturated position occurring 8 carbons from the other end of the molecule. These two fragments show that there are double bonds situated at the 7^{th} and 19^{th} positions on the 27 carbon chain length compound. The 159 fragment is further confirmed by the mass ions (C^+ - 48) and (C^+ - 94), which prove that (C^+) was 405.

Many other dienes, which formed non-cyclic adducts from mass spec analysis, were also identified in low abundance for carbon chain lengths of 25, 27, 29 and 31. While many 29-carbon dienes were detected by DMDS, three compounds had significantly higher abundances than the rest, which may perhaps be the three C29 diene metabolites that we were unable to distinguish in Table 6. These three separate dienes had carbon-carbon double bonds situated at the 7^{th} and 19^{th}, 10^{th} and 16^{th}, and 8^{th} and 16^{th} positions. Other C29 dienes that were detectable in lesser amounts had double bonds positioned at the 9^{th} and 16^{th} carbons, 9^{th} and 15^{th}, 8^{th} and 21^{st}, 8^{th} and 14^{th}, 7^{th} and 17^{th} and 7^{th} and 15^{th} carbons. For C25, three non-cyclic dienes were identified; they were found to contain double bonds at the 7^{th} and 15^{th} carbons, 7^{th} and 16^{th}, as well as one other at the 7^{th} and 17^{th} positions. For C27, four dienes were identified which had double bonds at the 7^{th} and 17^{th} carbons, 7^{th} and 18^{th}, 7^{th} and 19^{th}

as well as one other at the 9th and 17th carbons. For C31, four were detected as well, which consisted of carbon-carbon double bonds at the 7th and 19th carbons, 9th and 17th, 9th and 19th, as well as one last one at the 10th and 18th positions. Three of these C31 dienes, while unsure of which, could represent the three dienes unidentified in Table 6. While they were detectable in very concentrated extracts, the dienes mentioned above, had relatively low abundances compared to the abundant 6,9-diene series. It has been already reported for alkenes in B73 silk that the double bonds exist in the *cis* configuration, as confirmed by co-migration of the alkenes with cis-alkene standards via argentation TLC [2].

Figure 11

(a)

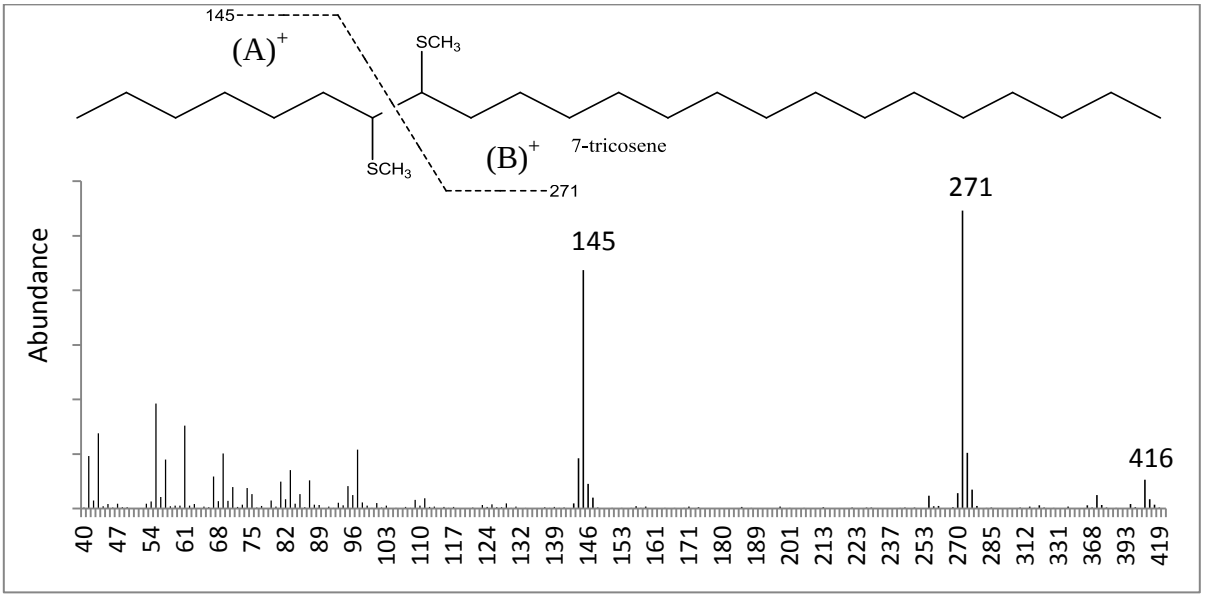

(b)

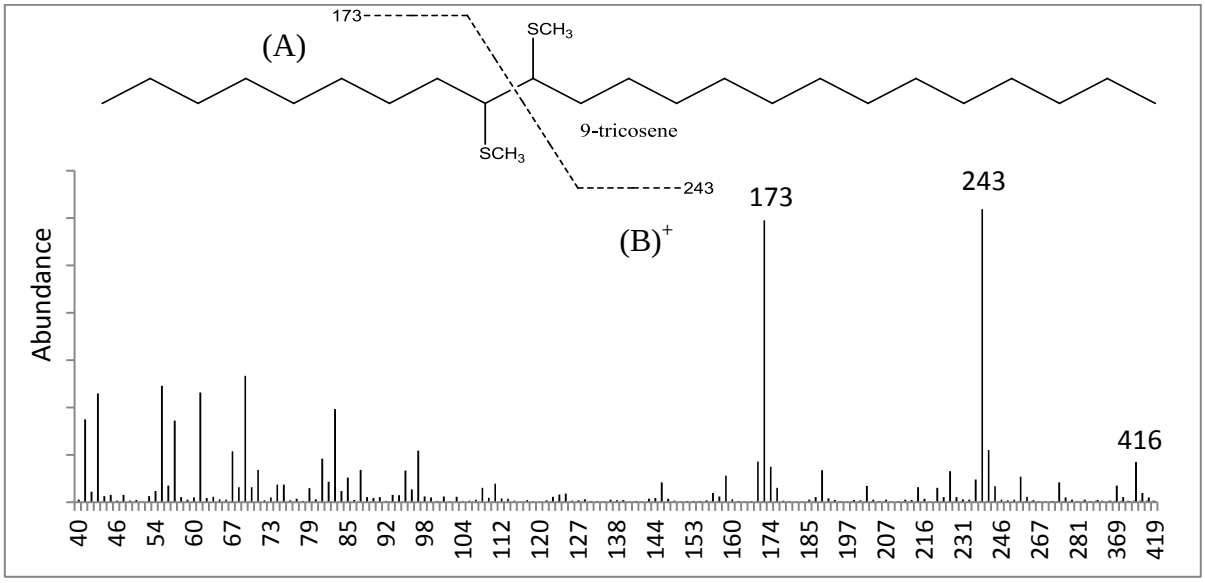
(A)
173
SCH3
SCH3
9-tricosene
243
(B)+
173
243
416
Abundance
40 46 54 60 67 73 79 85 92 98 104 112 120 127 138 144 153 160 174 185 197 207 216 231 246 267 281 369 419

(c)

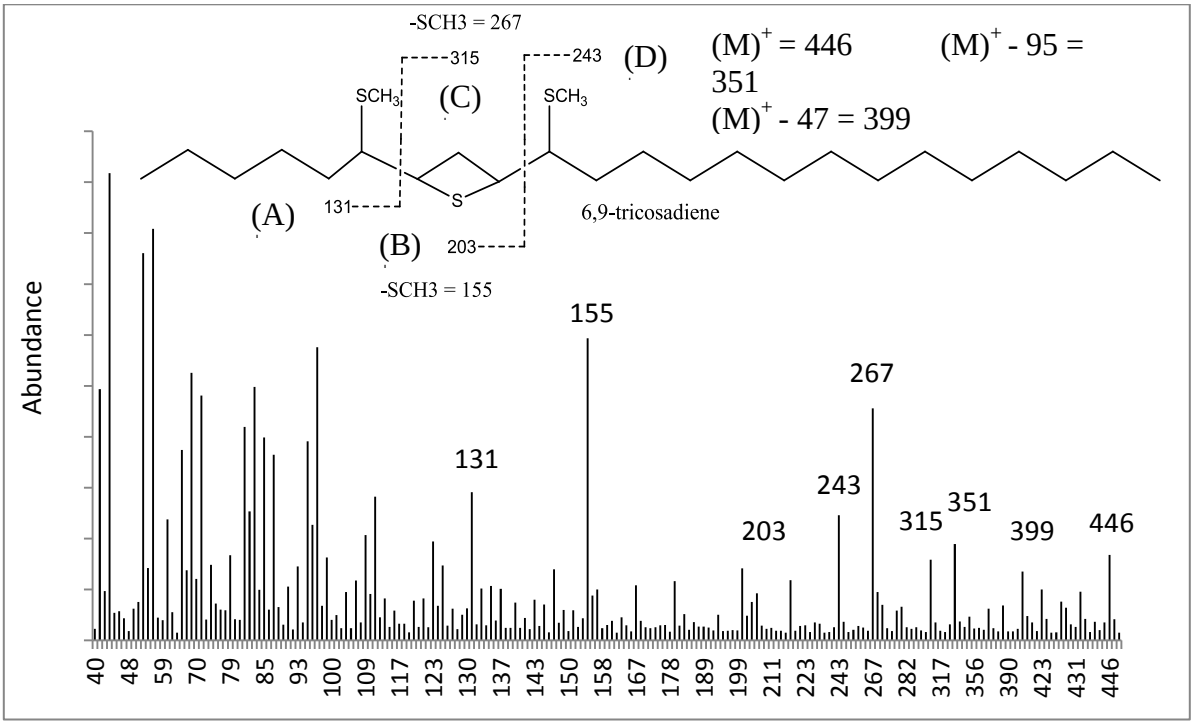
-SCH3 = 267
315
243
(D)
(M)+ = 446
(M)+ - 95 = 351
(M)+ - 47 = 399
SCH3
(C)
SCH3
(A)
131
S
6,9-tricosadiene
(B)
203
-SCH3 = 155
155
267
131
243
203
315
351
399
446
Abundance
40 48 59 70 79 85 93 100 109 117 123 130 137 143 150 158 167 178 189 199 211 223 243 267 282 317 356 390 423 431 446

(d)

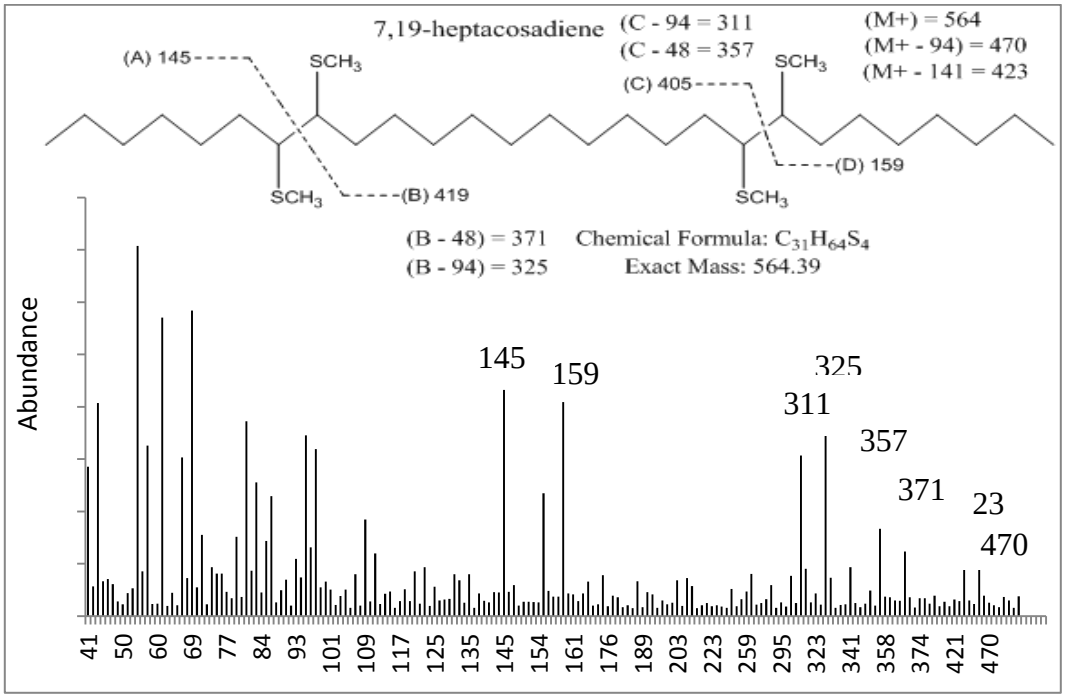

Figure 11 Determination of unsaturated metabolites with mass-spectral detection

(a-d) After lipids were extracted, extracts were then treated with dimethyl disulfide, to look at the resulting mass spectral adducts by GC-MS analysis. For 7-tricosene (a), fragmentation generated daughter ions of 145 [$C_8H_{17}S$] and 271 [$C_{17}H_{35}S$], which places the double bond between the 7th and 8th positions. For 9-tricosene (b), resulting adducts yielded two mass ions of 173 [$C_{10}H_{21}S$] and 243 [$C_{15}H_{31}S$], placing the double bond between the 9th and 10th carbons. For the di-unsaturated compound, (6,9)- tricosadiene (c), daughter ions of 131 [$C_7H_{15}S$], 315 [$C_{18}H_{35}S_2$], 203 [$C_{10}H_{19}S_2$] and 243 [$C_{15}H_{31}S$] were prominent. Other important ions for confirming the cyclic adduct at the 6th and 9th positions were the molecular ion (M^+), (M^+ - 47) and the (M^+ - 95) fragments. For 7,19-heptacosadiene (d) mass ions of 145 [$C_8H_{17}S$] and 159 [$C_9H_{19}S$] were prominent, indicating double bond positions at the 7th and 19th carbons. Dashed lines in the figures represent fragmentation breaks that result in the daughter mass ions shown. $(M)^+$ is an abbreviation for the molecular ion which is equivalent to the molecular weight of a molecule.

Composition comparisons between fresh, whole and dry, powderized silks

Since powderized silks contain a complex and broad array of unsaturated FAs (Table 8), we conducted experiments to see if the most abundant alkenes identified in powderized silks, were compositionally proportional to the alkenes extracted from whole silks. To propose our pathways for hydrocarbon biosynthesis, we would need to look at the unsaturated FA data profiled from powderized silk. We extracted lipids from intact vs. powderized silk tissue in hexanes: diethyl ether (9:1). Only hydrocarbons common between the two tissues were examined (Fig. 12). For the lipids extracted from both methods, the saturated and unsaturated HCs stayed consistent in terms of double bond position as well as in chain length, however relative abundances of these metabolites varied between the two methods (Fig. 12). The silk samples that were extracted from each method, for example, alkenes as well as alkanes ranging from 21 to 26 carbons were more abundant in extracts from the fresh dipped silks. For alkanes and alkenes ranging in chain length from 27 to 33 carbons, abundance variation was not as dynamic between the two extraction methods, even though fresh dipped silks did have a higher abundance in alkenes for C27 and C29.

According to the results shown in Fig. 12, some hydrocarbon metabolites are more prevalent on the cuticle alone compared to those extracted from powderized silk. Since the same even-chain and odd-chain HCs in powderized silks were also detected in whole silks, the HCs seem to be part of the silk cuticle alone. The abundances of nearly

every constituent extracted from whole silks, on a per gram dry weight basis, were higher than those for hydrocarbon metabolites derived from powderized silk. Dry weights were estimated from fresh silks, as described in the Methods.

Figure 12 Hydrocarbon composition comparison between extracts from dry, powderized silks vs. fresh silks immersed in solvent

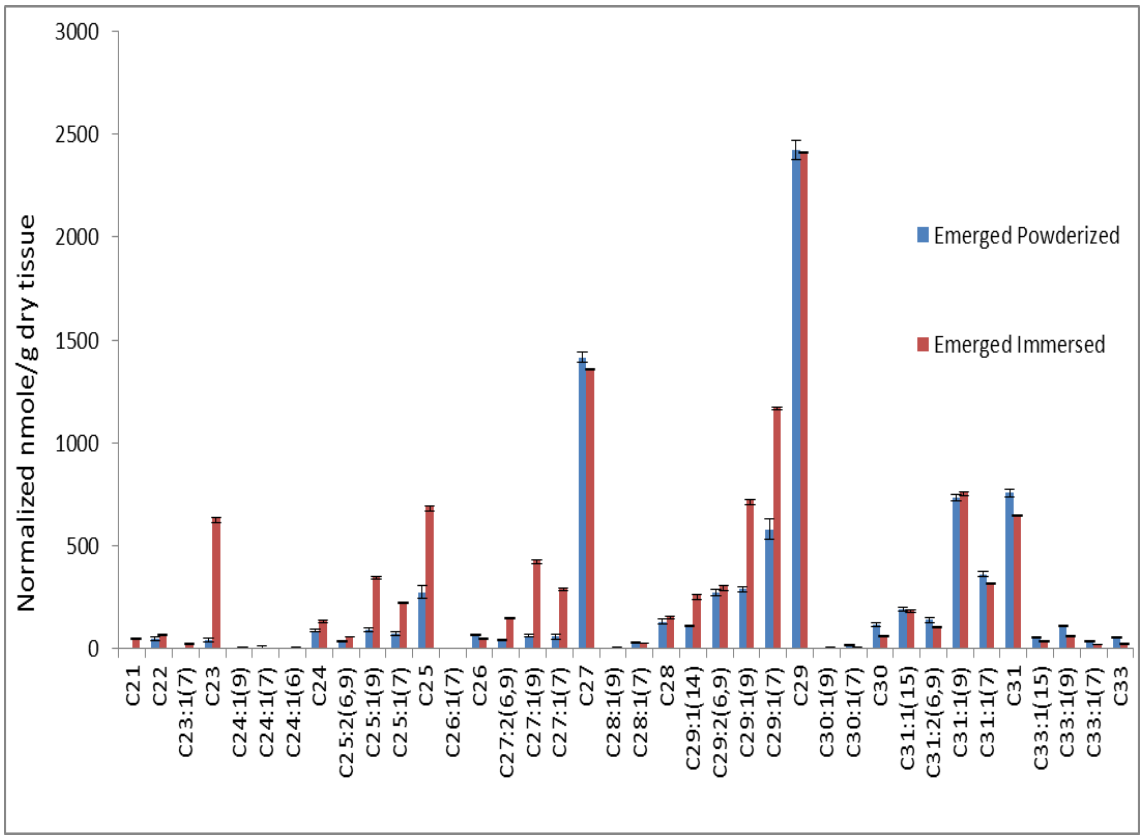

Fig. 12 Hydrocarbons extracted from the silk surface or powderized silks

Hydrocarbons that accumulate on emerged silk tissue (N=three biological replicates) were extracted either from fresh silks that were immersed in solvent (i.e. surface hydrocarbons) or from lyophilized and powderized silks (i.e. surface + internal hydrocarbons). While relative abundances differ between the two extraction methods, mostly the same metabolites are identified in both types of extracts. Error bars shown depict one standard deviation from the mean among 3 biological replicates.

Due to the complex array of HCs detected, a table was made to determine the relative abundance of each particular alkene that was detected by looking at their DMDS adducts. Chemstation was used to integrate the entire peak area under the curve as well as to analyze the average mass spectra for that retention time the peak encompassed. Through this process, double bond positions for all alkenes were identified in extracts derived from powderized silks and alkenes identified in extracts derived from immersed silks (Table 7). For odd-chain lengths ranging from 31 to 37 carbons, a third hydrocarbon peak was evident, which mainly consisted of strictly a carbon-carbon double bond situated at the 15th position. For C29, a third peak was identified as well, but it was mostly made up of two distinct alkenes, which consisted of double bonds situated at the 12^{th} and 14^{th} carbons, respectively.

The alkene composition from powderized silks differed slightly, but mostly in the percentages of the most dominant $\Delta 7$ and $\Delta 9$ alkenes per carbon chain length (Table 7). Interesting differences between the two extraction methods were observed for the C21 and C22 alkenes. For C21, a $\Delta 6$ alkene was detected when the silks were

immersed in the solvent, but not seen from powderized silk. For C22, no alkenes were detected from powderized silks, whereas three C21 alkenes (Δ6, Δ7 and Δ8 alkenes) were observed in extracts from fresh, immersed silks. Two other striking differences were the large abundances of Δ6 alkenes at carbon chain lengths of 24 and 26 in extracts from powderized silks. From the immersed silk analyses, these two alkenes contributed very little to the overall alkene composition at those carbon chain lengths. This perhaps suggests that some specific alkenes are actually intracellular and are not extractible from the silk surface. One other significant drop in abundance was with the Δ10 alkene at C32; while it represented nearly 19% of the alkene fraction at that chain length in the dip analysis, for extracts from powderized silks, it represented only 8% of the alkene composition at that chain length.

Overall, the alkene compositions for the emerged B73 silk tissue amongst the two different lipid extraction methods stayed consistent with double bonds defined at the 7^{th} and 9^{th} positions representing most of alkene total composition. Overall, a broader and more abundant array of HCs (alkanes, alkenes and dienes) are displayed in the extracted SLs than if silks were extracted from powderized silk, which contains intracellular components.

Table 7 Alkene comparisons of fresh, whole to dry, powderized silks

% Specific Alkenes at Each Chain Length

	Powderized	Whole		Powderized	Whole		Powderized	Whole		Powderized	Whole
C10Δ1	100%	100%	C26Δ6	16.0%	1.8%	C30Δ13	1.7%	3.3%	C35Δ16	10.2%	1.3%
C11Δ1	100%	100%	C26Δ7	37.4%	27.0%	C30Δ14	2.6%	3.7%	C35Δ17	4.8%	7.7%
C12Δ1	100%	100%	C26Δ8	10.0%	12.9%	C30Δ15	1.5%	2.9%	C37Δ7	ND	9.2%
C13Δ1	100%	100%	C26Δ9	18.4%	39.7%	C31Δ1	ND	0.0%	C37Δ9	ND	51.3%
C14Δ1	100%	100%	C26Δ10	8.6%	11.6%	C31Δ5	0.2%	0.0%	C37Δ10	ND	2.6%
C15Δ1	100%	100%	C26Δ11	4.2%	4.8%	C31Δ6	0.2%	0.2%	C37Δ11	ND	5.1%
C16Δ1	100%	100%	C26Δ12	3.6%	1.0%	C31Δ7	25.5%	20.8%	C37Δ13	ND	8.0%
C17Δ1	100%	100%	C26Δ13	1.7%	1.3%	C31Δ8	0.9%	1.0%	C37Δ15	ND	19.2%
C18Δ1	100%	100%	C27Δ1	ND	1.4%	C31Δ9	51.5%	50.8%	C37Δ17	ND	4.6%
C19Δ1	100%	100%	C27Δ5	0.8%	2.8%	C31Δ10	3.5%	2.7%			
C20Δ1	100%	100%	C27Δ6	0.8%	1.0%	C31Δ11	1.6%	1.9%			
C21Δ1	100%	94.9%	C27Δ7	45.1%	35.8%	C31Δ12	1.7%	1.9%			
C21Δ6	ND	5.1%	C27Δ8	5.0%	5.0%	C31Δ13	2.8%	4.7%			
C22Δ1	ND	14.2%	C27Δ9	33.5%	38.7%	C31Δ14	5.1%	5.8%			
C22Δ6	ND	61.7%	C27Δ10	9.3%	9.1%	C31Δ15	7.0%	10.1%			
C22Δ7	ND	6.0%	C27Δ11	1.6%	1.9%	C32Δ7	12.0%	20.0%			
C22Δ8	ND	18.1%	C27Δ12	2.9%	3.2%	C32Δ8	6.5%	7.3%			
C23Δ1	ND	3.3%	C27Δ13	0.9%	1.2%	C32Δ9	59.9%	35.2%			
C23Δ4	ND	0.1%	C28Δ6	4.0%	2.6%	C32Δ10	7.7%	18.7%			
C23Δ5	ND	0.1%	C28Δ7	69.9%	56.9%	C32Δ11	3.3%	5.6%			
C23Δ6	6.0%	3.9%	C28Δ8	6.3%	6.4%	C32Δ12	ND	5.8%			
C23Δ7	54.7%	60.4%	C28Δ9	13.9%	21.8%	C32Δ13	ND	0.5%			
C23Δ8	7.5%	3.9%	C28Δ10	2.0%	4.5%	C32Δ14	ND	1.6%			
C23Δ9	22.5%	24.1%	C28Δ11	1.0%	2.3%	C32Δ15	5.9%	4.5%			
C23Δ10	5.1%	2.8%	C28Δ12	1.4%	1.7%	C32Δ16	4.6%	1.1%			
C23Δ11	4.2%	1.5%	C28Δ13	0.9%	2.6%	C33Δ1	ND	0.0%			
C24Δ4	ND	0.4%	C28Δ14	0.6%	1.1%	C33Δ7	20.4%	17.4%			
C24Δ5	ND	0.0%	C29Δ1	ND	0.4%	C33Δ8	0.9%	1.0%			
C24Δ6	22.3%	2.1%	C29Δ5	0.4%	0.6%	C33Δ9	37.7%	40.2%			
C24Δ7	30.7%	35.5%	C29Δ6	0.3%	0.3%	C33Δ10	3.5%	3.9%			
C24Δ8	14.7%	22.6%	C29Δ7	51.7%	43.1%	C33Δ11	5.3%	4.1%			
C24Δ9	17.4%	30.9%	C29Δ8	1.6%	1.3%	C33Δ12	5.8%	0.8%			
C24Δ10	7.0%	7.0%	C29Δ9	31.4%	37.1%	C33Δ13	5.3%	3.9%			
C24Δ11	4.7%	1.3%	C29Δ10	3.6%	3.2%	C33Δ14	1.5%	1.3%			
C24Δ12	3.2%	0.2%	C29Δ11	0.8%	1.2%	C33Δ15	11.2%	16.7%			
C25Δ1	ND	1.6%	C29Δ12	4.8%	5.5%	C33Δ16	8.4%	10.7%			
C25Δ4	ND	0.0%	C29Δ13	1.3%	2.0%	C35Δ7	11.2%	19.9%			
C25Δ5	0.3%	1.0%	C29Δ14	4.1%	5.5%	C35Δ8	ND	0.5%			
C25Δ6	0.6%	0.2%	C30Δ6	ND	0.8%	C35Δ9	33.8%	30.6%			
C25Δ7	41.2%	32.3%	C30Δ7	27.1%	24.6%	C35Δ10	ND	5.4%			
C25Δ8	4.4%	5.4%	C30Δ8	8.8%	8.3%	C35Δ11	1.8%	7.4%			
C25Δ9	44.6%	50.4%	C30Δ9	48.5%	45.1%	C35Δ12	ND	0.2%			
C25Δ10	6.7%	7.1%	C30Δ10	7.0%	7.7%	C35Δ13	10.9%	8.3%			
C25Δ11	1.3%	1.2%	C30Δ11	1.6%	2.1%	C35Δ14	ND	0.0%			
C25Δ12	1.0%	1.0%	C30Δ12	1.3%	1.6%	C35Δ15	27.4%	18.5%			

Fatty acid investigation

While whole silk extracts showed a wide array of saturated FAs (data not shown) ranging from 8 to 34 carbons in length, powderized silk showed the best array for investigating unsaturated FA precursors. This could be from the fact that homogenized silk (powderized) "releases" internal fatty acids, which may explain the large abundance in unsaturated FAs. In Fig. 13a, a C24:1Δ17 FA is shown with a double bond position between the 17^{th} and 18^{th} carbons from the carboxyl end. After fragmentation, two prominent mass values of $(A)^+$ 145 and $(B)^+$ 329 were seen, corresponding to the omega fragment and the carboxyl fragment, respectively. Also prominent is the mass ion 297, which corresponds to the loss of the methanol from the carboxyl fragment. In Fig.13b, methyl 15-tetracosenoate is displayed with a similar mass spec pattern in regards to fragmentation. In the DMDS adducts, daughter ions of $(A)^+$ 173 and $(B)^+$ 301 were generated, coming from the break between the 15^{th} and 16^{th} carbons from the carboxyl side. Again, loss of the methanol group generated a mass ion of 269 from the loss to the carboxyl fragment.

While the most abundant fatty acid was linoleic in our GC analysis, we did see other di-unsaturated fatty acids with double bonds situated at the 6^{th} and 9^{th} carbons from the omega end. For eicosa-11,14-dienoic acid (Fig. 13c), after transmethylation and treatment with dimethyl disulfide, we found daughter ions of A^+ 131 [$C_7H_{15}S$], B^+ 317 [$C_{16}H_{29}O_2S_2$], D^+ 245 [$C_{13}H_{25}O_2S$] and C^+ 203 [$C_{10}H_{19}S_2$] corresponding to cleavage

breaks between the 11th and 12th carbons as well as the 14th and 15th carbons from the ester side. This omega (6,9) fatty acid also generated 2 other prominent mass ions from the loss of the methyl thio groups that were (C^+ - 48) 155 and (B^+ - 48) 269. Finding these distinct mass ions for this cyclic thietane ring DMDS adduct confirmed the metabolite as eicosa-11,14-dienoic acid.

Although no trienes were evident in our GC analyses, we did discover a tri-unsaturated fatty acid derivative from powderized silk, octadeca-9,12,15-trienoic acid, in great abundance (Fig. 13d). While the mass spectra are difficult to decipher for tri-unsaturated fatty acid adducts, a cyclic M^+ ion was found (450) which indicated a 18-carbon length compound; this also gave rise to prominent mass ions of [M^+ - 47] 403 and [M^+ - 95] 355. Other daughter ions seen were [$C_7H_{13}S_2$] 161, [$C_{14}H_{25}O_2S_2$] 289, [$C_{10}H_{17}S_3$] 233, [$C_{11}H_{21}O_2S$] 217 which clearly showed cleavage breaks in the fragmentation for this compound between the 9th and 10th carbons as well as the 12th and 13th carbons. Also abundant were the mass ions corresponding to the loss of the methyl thio groups from 161 (113 m/z), 289 (241 m/z) and 233 (185 m/z). These mass ions provide further support that the molecule has double bonds situated at the 9th, 12th and 15th carbons from the ester side.

Figure 13

(a)

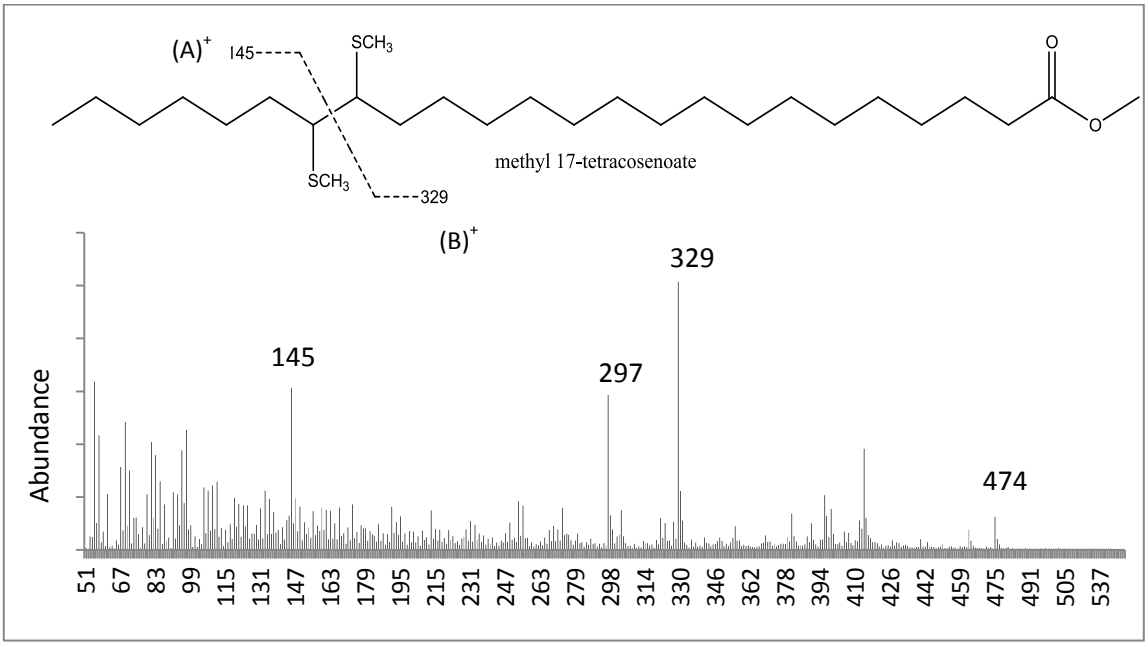
(A)+
145
SCH3
SCH3
329
methyl 17-tetracosenoate
(B)+
329
145
297
474
Abundance
51 67 83 99 115 131 147 163 179 195 215 231 247 263 279 298 314 330 346 362 378 394 410 426 442 459 475 491 505 537

(b)

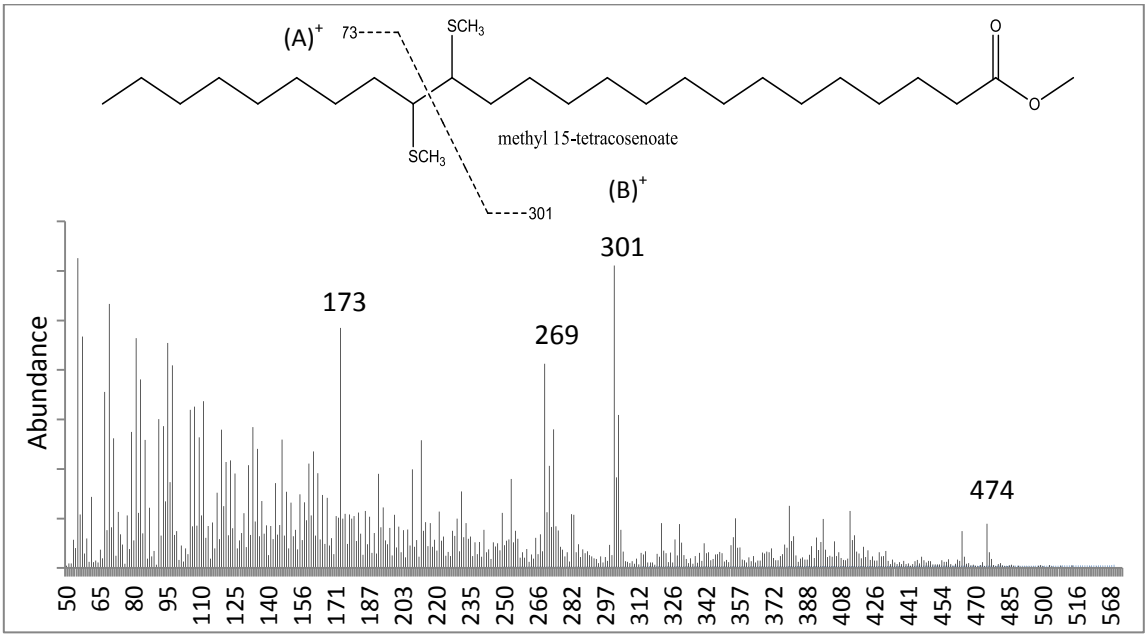
(A)+
73
SCH3
SCH3
301
methyl 15-tetracosenoate
(B)+
301
173
269
474
Abundance
50 65 80 95 110 125 140 156 171 187 203 220 235 250 266 282 297 312 326 342 357 372 388 408 426 441 454 470 485 500 516 568

(c)

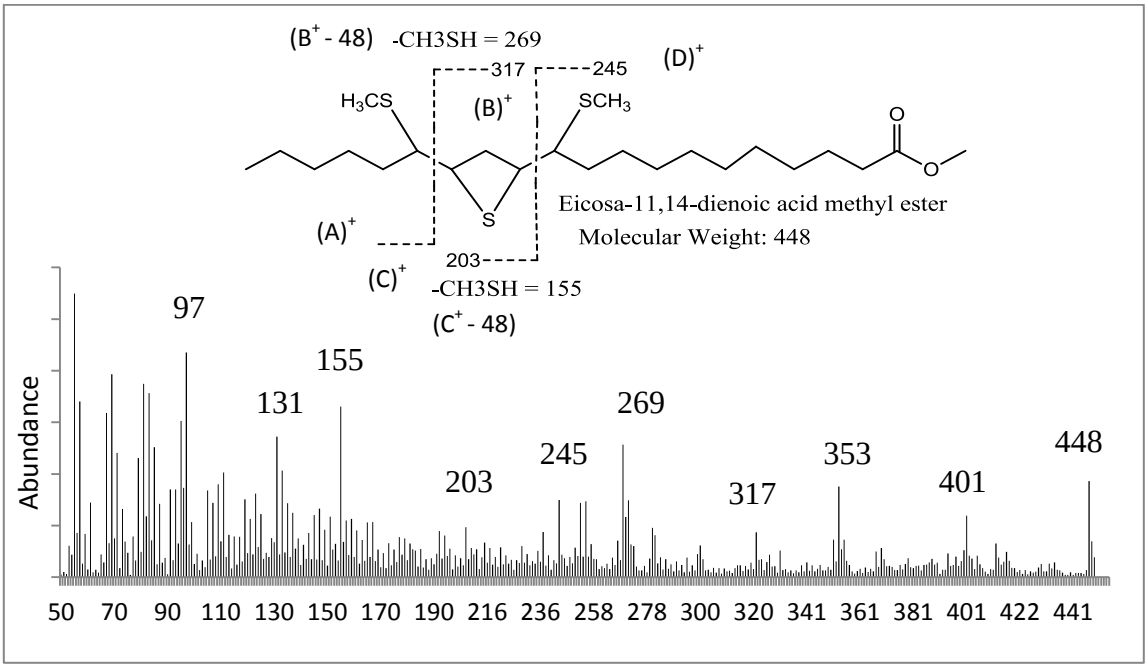
(B+ - 48) -CH3SH = 269
317
245
(D)+
H3CS
(B)+
SCH3
O
O
S
(A)+
Eicosa-11,14-dienoic acid methyl ester
Molecular Weight: 448
203
(C)+
-CH3SH = 155
(C+ - 48)
Abundance
97
155
131
269
203
245
317
353
401
448
50 70 90 110 130 150 170 190 216 236 258 278 300 320 341 361 381 401 422 441

(d)

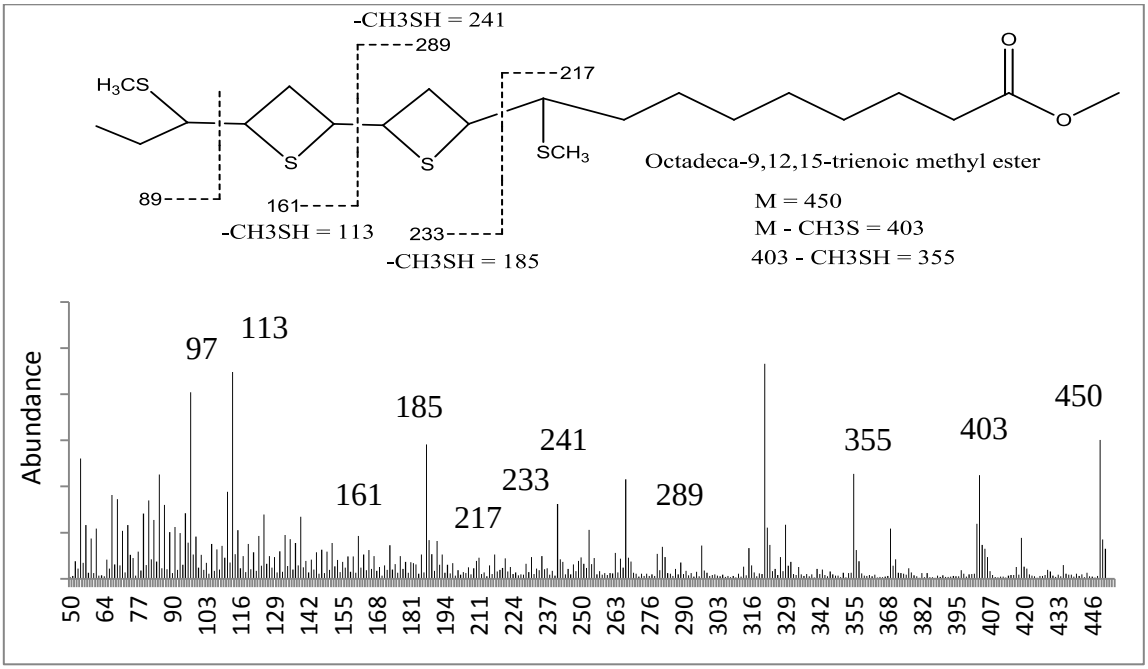
-CH3SH = 241
289
217
H3CS
O
O
S
S
SCH3
Octadeca-9,12,15-trienoic methyl ester
89
161
-CH3SH = 113
233
-CH3SH = 185
M = 450
M - CH3S = 403
403 - CH3SH = 355
Abundance
97
113
185
241
161
233
217
289
355
403
450
50 64 77 90 103 116 129 142 155 168 181 194 211 224 237 250 263 276 290 303 316 329 342 355 368 382 395 407 420 433 446

Figure 13 Transmethylation aids in recovery and identification of DMDS adducts

(a-d) To protect fatty acid groups, sample extracts were first subjected to transmethylation. After derivatization, dimethyl disulfide was added and used to look at double bond positions. For methyl 17-tetracosenoate (a), daughter ions included 145 [$C_8H_{17}S$] and 329 [$C_{19}H_{37}O_2S$] which placed the double bond between the 7^{th} and 8^{th} carbons on the omega end. Also, methyl 15-tetracosenoate (b) was examined and characterized by the resulting mass-spectral adducts of 173 [$C_{10}H_{21}S$] and 301 [$C_{17}H_{33}O_2S$]. Eicosa-11,14-dienoic acid (c), displayed daughter ions of 131 A^+ [$C_7H_{15}S$], 317 B^+ [$C_{16}H_{29}O_2S_2$], 245 D^+ [$C_{13}H_{25}O_2S$] and 203 C^+ [$C_{10}H_{19}S_2$] corresponding to cleavage breaks between the 11^{th} and 12^{th} carbons as well as the 14^{th} and 15^{th} carbons from the ester side. Also prominent were the mass ions corresponding to the loss of the methyl thio groups that were 155 (C^+ - 48) and 269 (B^+ - 48), which helped confirm the omega 6,9 fatty acid. Octadeca-9,12,15-trienoic acid, in great abundance (Fig. 4d). While the mass spectra is difficult to decipher with for tri-unsaturated fatty acid adducts, a cyclic M^+ ion was found (450) which indicated a 18-carbon length compound; this also gave rise to prominent mass ions of 403 [M^+ - 47] and 355 [M^+ - 95]. Other daughter ions seen were 161 [$C_7H_{13}S_2$], 289 [$C_{14}H_{25}O_2S_2$], 233 [$C_{10}H_{17}S_3$], 217 [$C_{11}H_{21}O_2S$] which clearly showed cleavage breaks in the fragmentation for this compound in between the 9^{th} and 10^{th} carbons as well as the 12^{th} and 13^{th}. Also abundant were the loss of the methyl thio groups from 161 (113 m/z), 289 (241 m/z) and 233 (185 m/z). For the tri-unsaturated fatty acid, octadeca-9,12,15-trienoic acid (d), a cyclic M^+ ion was found (450) which indicated a 18-carbon length compound with other identifying mass ions at 403 [M^+ - 47] and 355 [M^+ - 95]. Other daughter ions seen were 161 [$C_7H_{13}S_2$], 289 [$C_{14}H_{25}O_2S_2$], 233 [$C_{10}H_{17}S_3$] and 217 [$C_{11}H_{21}O_2S$] which clearly showed double bond positions between the 9^{th} and 10^{th} carbons as well as the 12^{th} and 13^{th}. Also in great abundance were the loss of the methyl thio groups from 161 (113 m/z), 289 (241 m/z) and 233 (185 m/z) which confirmed the tri-unsaturated compound.

To examine FAs more thoroughly, powderized silk was chosen to conduct a transmethylation experiment on FA precursors, which may be the exact precursors to the unsaturated hydrocarbons that were identified. In Table 8, powderized extracts

were transmethylated and all FAs were quantified. For 6 biological replicates (0.5 g of powderized tissue), after the lipids had been extracted from powderized silk, extracts were subjected to transmethylation. After transmethylation, the derivatized fatty acids were eluted in hexanes (0.3 ml). From the table, we can see odd-chain FAs as well as even-chain FAs that were detected. DMDS reactions were conducted to identify double bond positions for the unsaturated fatty acids. The most predominant unsaturated fatty acid identified in extracts from powderized silks were monoenoic fatty acids of even and odd chain lengths and double bonds at either the 7^{th} or 9^{th} positions from the omega-end of the fatty acids. We believe the identification of ω-7 and ω-9 unsaturated odd- and even-chain FAs proves that the Δ7 and Δ9 alkenes, found within (Table 7), are biosynthesized by these FA precursors.

Table 8 Fatty acid composition of powderized silks

Metabolite	nmol/g dry weight [a]	Metabolite	nmol/g dry weight [a]
12-carbon metabolites		**22-carbon metabolites**	
dodecanoic acid	2.30 ± 0.39	docosanoic acid	197.95 ± 6.22
13-carbon metabolites		13-docosenoic acid	10.67 ± 0.95
tridecanoic acid	0.54 ± 0.09	15-docosenoic acid	12.46 ± 0.86
14-carbon metabolites		13,16-docosadienoic acid	87.31 ± 5.37
tetradecanoic acid	29.37 ± 4.07	**23-carbon metabolites**	
15-carbon metabolites		tricosanoic acid	55.85 ± 4.06
pentadecanoic acid	23.54 ± 1.82	16-tricosenoic acid	1.23 ± 0.31
16-carbon metabolites		**24-carbon metabolites**	
hexadecanoic acid	2,658.45 ± 34.90	tetracosanoic acid	321.23 ± 15.16
9-hexadecenoic acid	192.78 ± 4.82	15-tetracosenoic acid	11.13 ± 0.55
7,10-hexadecadienoic acid	36.20 ± 1.41	17-tetracosenoic acid	21.91 ± 1.19
17-carbon metabolites		**25-carbon metabolites**	
heptadecanoic acid	78.69 ± 4.40	pentacosanoic acid	52.48 ± 3.91
a,b-heptadecadienoic acid	4.71 ± 0.84	16-pentacosenoic acid	1.13 ± 0.23
18-carbon metabolites		18-pentacosenoic acid	3.91 ± 0.58
octadecanoic acid	838.63 ± 25.07	**26-carbon metabolites**	
11-octadecenoic acid	911.58 ± 15.69	hexacosanoic acid	71.92 ± 4.25
9-octadecenoic acid	136.52 ± 10.25	17-hexacosenoic acid	8.11 ± 0.30
9,12-octadecadienoic acid	4,748.09 ± 27.87	19-hexacosenoic acid	19.23 ± 1.34
9,12,15-octadecatrienoic acid	1,339.52 ± 24.14	**27-carbon metabolites**	
19-carbon metabolites		heptacosanoic acid	8.02 ± 0.77
nonadecanoic acid	3.67 ± 0.35	18-heptacosenoic acid	0.52 ± 0.10
12-nonadecenoic acid	11.72 ± 2.15	20-heptacosenoic acid	2.33 ± 0.44
20-carbon metabolites		**28-carbon metabolites**	
eicosanoic acid	69.96 ± 3.59	octacosanoic acid	8.64 ± 0.55
11-eicosenoic acid	32.89 ± 3.06	19-octacosenoic acid	2.20 ± 0.28
13-eicosenoic acid	25.78 ± 2.20	21-octacosenoic acid	4.24 ± 0.36
11,14-eicosadienoic acid	134.58 ± 2.30	**30-carbon metabolites**	
21-carbon metabolites		triacontanoic acid	2.20 ± 0.42
heneicosanoic acid	13.36 ± 1.42	21-triacontenoic acid	0.55 ± 0.11

[a] Average value of six independent analyses ± 1 standard deviation

Aldehyde examination via transmethylation

In our dip experiments, we identified many saturated and unsaturated fatty aldehydes that formed acetals upon transmethylation derivitization; these consisted of saturated chain lengths of 9 to 34 carbons. While the double bond positions have not yet been identified for the unsaturated aldehydes, acetals were formed upon transmethylation for carbon chain lengths ranging from 26 to 32 carbons. We propose that, if identified, they would represent the ω-7 and ω-9 aldehydes, which would represent the immediate precursor to the alkenes identified. In Fig. 14, the mass spectrum is displayed for octacosanal-dimethylacetal. While the molecular ion is rarely present in these compounds, three other significant mass ions are. Cleavage between the 1^{st} and 2^{nd} carbons on the acetal side generate a significant base peak at 75 [$C_3H_7O_2$] which is characteristic for saturated and unsaturated aldehydes subjected to transmethylation. Two other daughter ions are also prevalent, which are 423 [M^+ - 31] and 390 [M^+ - 64]. These 3 mass ions confirm the presence of a methylated 28-carbon chain length saturated aldehyde.

Figure 14

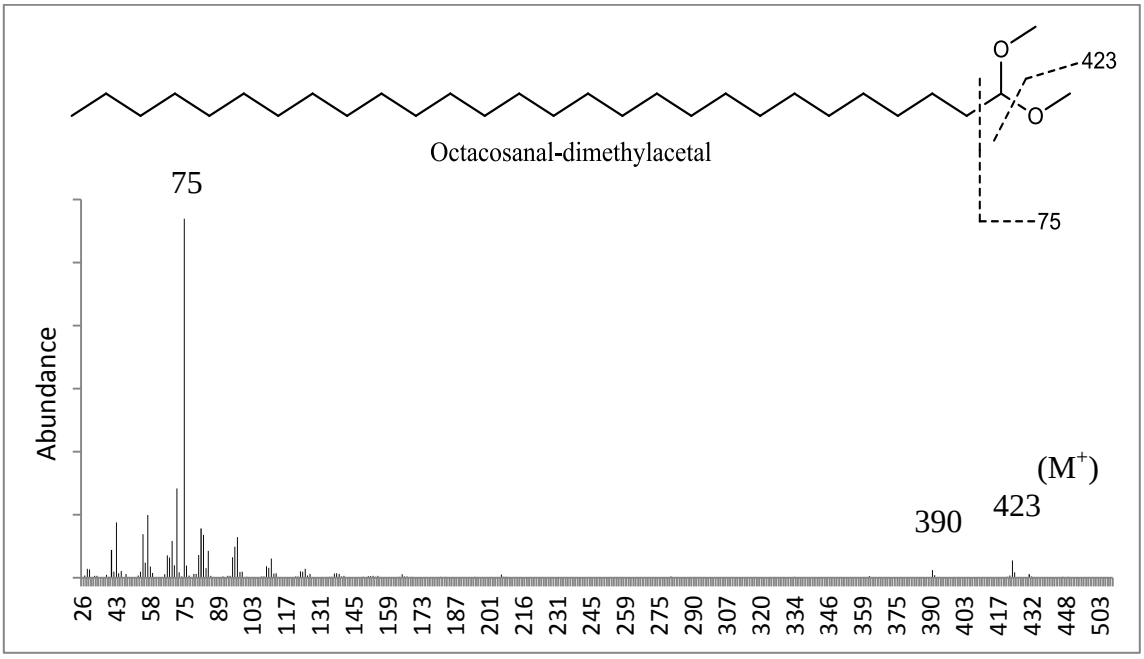

Figure 14 Detection of dimethylacetals by transmethylation

Aldehydes were also protected which transmethylation; this converted the compounds to acetal forms upon derivatization. For octacosanal (e), after methylation, fragmentation resulted in a very abundant 75 base peak [$C_3H_7O_2$] with lesser abundant daughter ions at 423 [M^+ - 31] and 390 [M^+ - 64]. These abundant mass ions confirm the acetal form of octacosanal after transmethylation.

Proposed biosynthetic pathways for production of maize silk hydrocarbons

From these sets of experiments, we have identified saturated and unsaturated sets of fatty acids, aldehydes and hydrocarbons in maize silk extracts. We propose that hydrocarbons are biosynthesized by the elongation of saturated and unsaturated fatty acid precursors, which upon reduction to corresponding aldehydes, are then

decarbonylated to generate the alkanes, alkenes and dienes that we have identified. This decarbonylation pathway is how we believe hydrocarbons are biosynthesized in maize which support previous work [2]. Many of the glossy mutants, which have been identified and characterized to be involved in the FA elongase system generating VLCFA precursors of SLs [4,27,28,29,30], provides additional evidence to our proposed pathways. Consistent with this hypothesis, we have identified the aldehydes and alkanes that would be expected based on a precursor-product relationship. Since many alkenes were detected, we cannot rule out another pathway of decarbonylation that begins with elongation of saturated FA precursors, which upon desaturation, get decarbonylated from a reduced aldehyde intermediate [2].

The most abundant saturated aldehydes that were detected ranged from 20 to 34 carbons in chain length with the most abundant alkanes ranging from 19 to 33 carbons. From transmethylation, we saw unsaturated even-chain aldehydes that ranged from 26 to 34 carbons. For each even-numbered carbon chain length starting at C26, we saw evidence of 2 unsaturated aldehydes up to 34 carbons in chain length. While the determination of unsaturated aldehydes is currently in progress, we believe that these 2 unsaturated aldehydes per chain length represent the immediate precursors to the most abundant alkenes that were detected with double bonds at the 7^{th} and 9^{th} positions. Consistent with our findings, previous work in the Nikolau group identified omega 9 unsaturated aldehydes (17-hexacosenal and 19-octacosenal) in maize silks [2]. These immediate precursors that have been identified already would be

the direct precursors upon decarbonylation that would generate our highly abundant 9-alkene series (Fig. 15).

Our discovery of odd-numbered fatty acids and odd-chain aldehdyes provide support that even-chain hydrocarbons are biosynthesized by a similar type of mechanism that involves decarbonylation. Most all the metabolites proposed in our even-hydrocarbon biosynthesis pathway have not been detected yet in maize. While even-chained hydrocarbons are not new in maize silk [1,3], they weren't initially detected in B73 [2].

Among the dienes that are present in silk surface lipids, the most abundant was a series with double bonds at the 6^{th} and 9^{th} positions. While no di-unsaturated aldehydes were detected, our group has identified in past research a di-unsaturated aldehyde, 19,22-octacosenal [2], which could represent the immediate precursor in our pathway to a 27-carbon diene with double bonds at the 6^{th} and 9^{th} positions. This 6,9-diene series was very prevalent in our GC analysis and was seen to range from 23 to 33 carbons in chain length. Our fatty acid analysis showed di-unsaturated even-chain fatty acids with double bonds situated at the omega 6 and 9 positions for chain lengths ranging from 18 to 22 carbons. These findings give evidence for the elongation of linoleic acid to fatty acid precursors up to 34 carbons in length that would generate the 6,9-diene series that we saw from our GC-MS analyses (Fig. 15), which also is consistent with previous work [2].

As with the odd-numbered hydrocarbons, we believe the even-chain hydrocarbons are biosynthesized by a similar type of mechanism that begins with odd-chain fatty acid precursors which are elongated then reduced to corresponding aldehydes before being decarbonylated to the corresponding alkanes and alkenes. Even-numbered hydrocarbons could potentially be produced via a dehydration mechanism, wherein a FA is reduced to an aldehyde, which is subsequently reduced to an alcohol and then dehydrated to the corresponding HC. However, the detection of odd-numbered fatty acids in this study suggests that even-numbered hydrocarbons are derived from odd-numbered fatty acids that are reduced to odd-numbered aldehydes and subsequently decarbonylated to the hydrocarbon. Just like with the most abundant even-chain monoenoic fatty acid precursors that were detected, odd-chain monoenoic fatty acids showed the same pattern with double bonds at the omega 7^{th} and 9^{th} positions. These results were very consistent with the alkenes that were detected which showed double bonds positioned at the 7^{th} and 9^{th} carbons. For odd and even-chained alkanes, a full spectrum of saturated FAs and aldehdyes were present in odd and even-chain lengths ranging from 8 to 34 carbons. This suggests that odd- and even-chain alkanes are generated from the elongation of saturated FA precursors which are reduced to aldehydes then decarbonylated to the corresponding alkane.

Our proposed pathways (Fig. 15 and Fig. 16) were determined by quantifying lipids on the silk cuticle as well as from powderized silk, which also contains intracellular metabolites. To see if this tissue could relate to what was seen on the

extractible lipids on the cuticle, both tissues were examined for alkene content. After seeing that the delta 7 and 9 alkenes were still the most abundant unsaturated hydrocarbons among both extracted tissues (tables 7 and 8), we could then use what was seen from the powderized composition to provide further verification and evidence for our hypothesized pathway models.

Many other alkenes were also detected for both odd and even-chained lengths ranging from 21 to 37 carbons. These alkenes contained double bonds at the 1^{st}, 4^{th} to half the length of the molecule (shown in Table 7). While many precursor monoenoic fatty acids were found for these specific positioned alkenes, we are hesitant to conclude that all of these alkenes are biosynthesized by the elongation of unsaturated fatty acid precursors. Another decarbonylation pathway could explain the biosynthesis of these hydrocarbons by means of a desaturation step occurring after fatty acid elongation for which the fatty acid is reduced to a corresponding aldehyde then decarbonylated to the specific alkene. For the monoenoic fatty acids that were evident from the DMDS analyses, this secondary pathway doesn't seem to be the case for how most of the alkenes are biosynthesized.

Given the positions of the double bonds in the alkenes detected in silks, a double bond could be introduced before, during or after elongation has finished. Since not all potential FA precursors were found for defined constituents, there could be multiple pathways which involve either desaturation-elongation or elongation-

desaturation before reduced to the aldehyde. In this study, alkenes with a double bond at the 9^{th} position, as with the silks herein, were the most dominant monoenes that were detected. The most prominent fatty acid in powderized silk tissue that was detected was linoleic acid ($C18{:}2D^{9,12}$); in plants, this is the most common di-unsaturated fatty acid. In literature, it has been found to be the product of the ER-localized FAD2-desaturase. This desaturase has been shown to enzymatically desaturate phosphatidylcholine-associated oleic acid [31]. We believe from what the fatty acid analyses show, that linoleic acid goes through FA elongation to be reduced to the corresponding aldehydes that would generate the 6,9-diene series that was detected in great abundance.

Figure 15

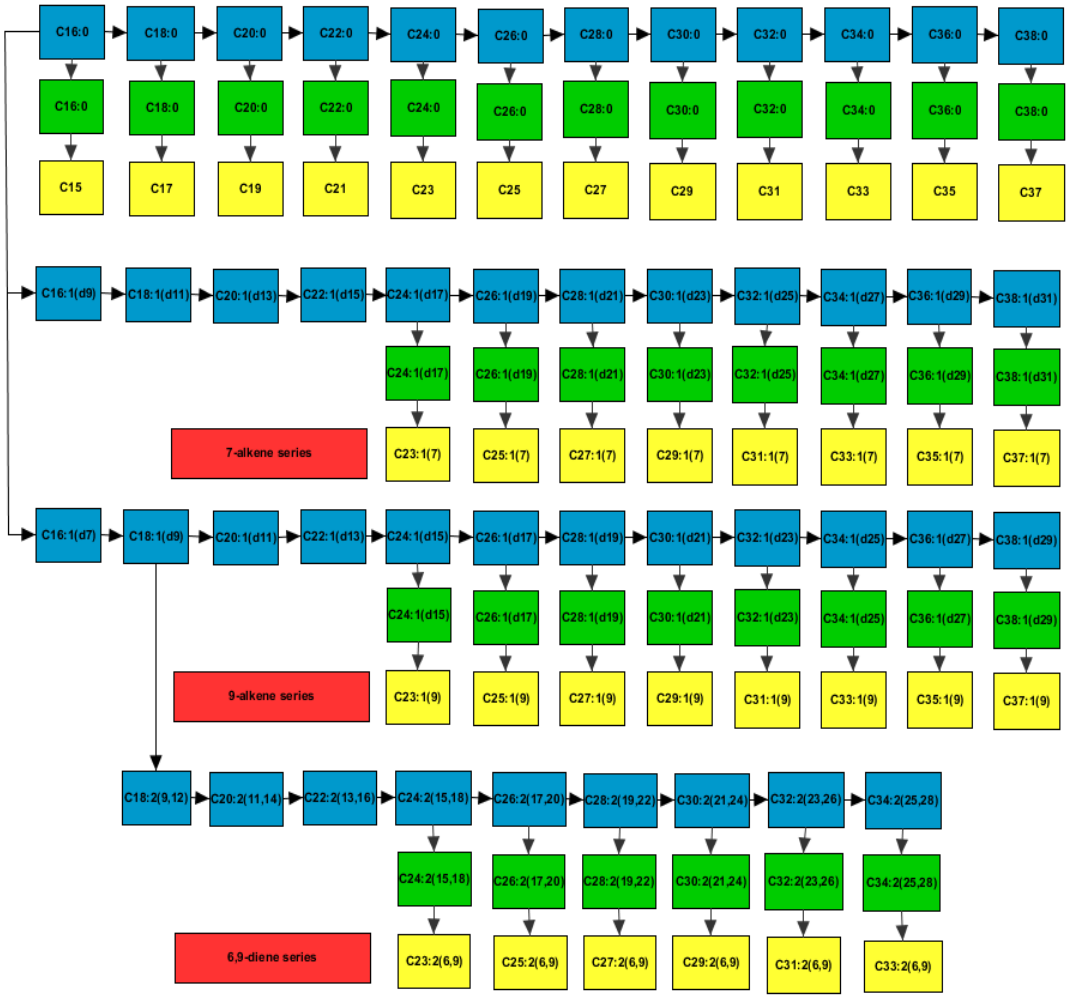

Figure 15 Putative odd-numbered hydrocarbon biosynthetic pathway

Even saturated fatty acids up to 38 carbons in chain length are generated from the elongation of hexadecanoic acid (C16:0). From these saturated fatty acid precursors, alkanes can be generated from a decarbonylation reaction through a saturated aldehyde intermediate (shown above). Through another decarbonylation pathway, the elongation of unsaturated 16-carbon fatty acids with double bonds at the 7^{th} and 9^{th} positions (C16:1Δ7 and C16:1Δ9) gives rise to the series of alkenes with double bonds situated at the 7^{th} and 9^{th} positions (shown above). Also seen by the elongation of linoleic acid, a diene series has been seen which has double bonds situated at the 6^{th} and 9^{th} positions. Seen by the figure above, blue boxes indicate fatty acids, while green and yellow boxes represent aldehydes and hydrocarbons, respectively.

Figure 16

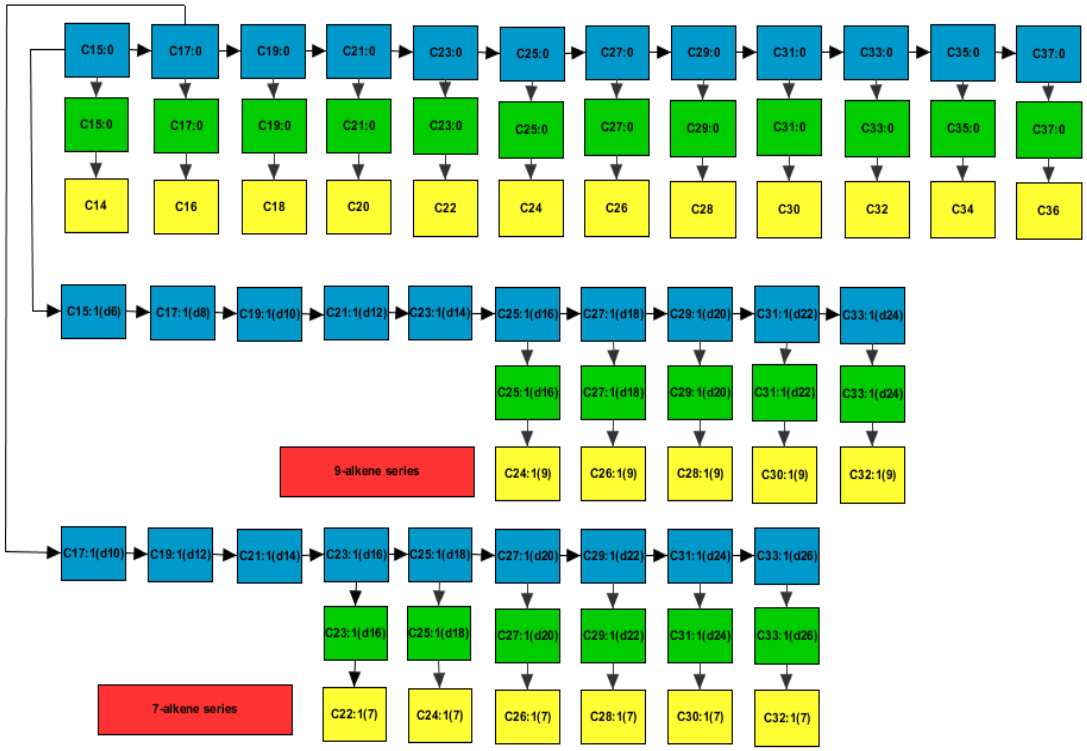

Figure 16 Putative even hydrocarbon biosynthetic pathway

Odd saturated fatty acids up to 37 carbons in chain length are generated from the elongation of pentadecanoic acid (C15:0). From these saturated fatty acid precursors, alkanes can be generated from a decarbonylation reaction through a saturated aldehyde intermediate (shown above). Through another decarbonylation pathway, the elongation of an unsaturated 15-carbon fatty acid with a double bond at the 6th position (C15:1Δ6) gives rise to an alkene series with a double bond at the 9th position (shown above). Also present was a series of alkenes with a double bond at the 7th position. From our fatty acid analysis, we believe this is initiated from the elongation of a 17-carbon fatty acid (C17:1Δ10). Blue boxes indicate fatty acids, while green and yellow boxes represent aldehydes and hydrocarbons, respectively.

Methyl-branched hydrocarbons

While the surface lipids that coat the silk contain mostly non-isoprenoid HCs, some methyl alkanes were identified in extracts from powderized but not from whole silks. Iso-alkanes are not uncommon in maize silk [1,3], but vary among genotypes for both relative abundances and positions of the methyl-branches. In the maize inbred CO272, highly abundant methyl alkanes with a branched methyl group at the 2^{nd} carbon were nearly as abundant as the odd-chain alkanes [3]. These iso-alkanes were highly abundant and eluted just before the corresponding alkanes (C27, C29 and C31).

While they are hard to identify, a combination of retention indices and mass spec analyses were used for confirmation. In Fig. 17a, 5-methyl heptadecane is shown; while unusual in most cases, the M^+ is present (254). By analyzing the mass spec fragmentation, a large daughter ion (197) is observed from the fragmentation between the 4^{th} and 5^{th} carbons [$C_{14}H_{29}$], indicating a methyl group that is attached to the 5^{th} carbon. This break occurs with the carbon attached to the methyl group and the carbon nearest the terminal end (the most unstable side of the fragment). For 4-methyl pentadecane, Fig. 17b, the M^+ ion is present (226), as well as a large abundant ion (183) that depicts a methyl group on the 4^{th} carbon from the end [$C_{13}H_{27}$]. The same holds true for 3-methyl hexadecane, Fig. 17c, which a large daughter ion is seen (211) depicting a methyl group on the 3^{rd} carbon from the end [$C_{15}H_{31}$].

Figure 17

(a)

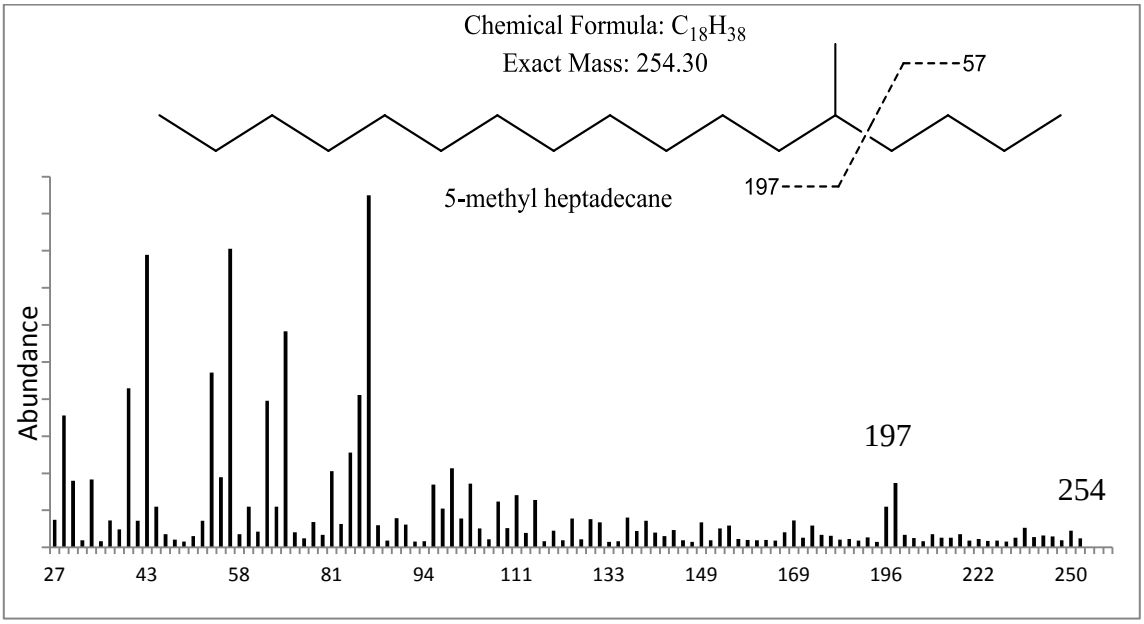
Chemical Formula: $C_{18}H_{38}$
Exact Mass: 254.30
57
197
5-methyl heptadecane
Abundance
197
254
27 43 58 81 94 111 133 149 169 196 222 250

(b)

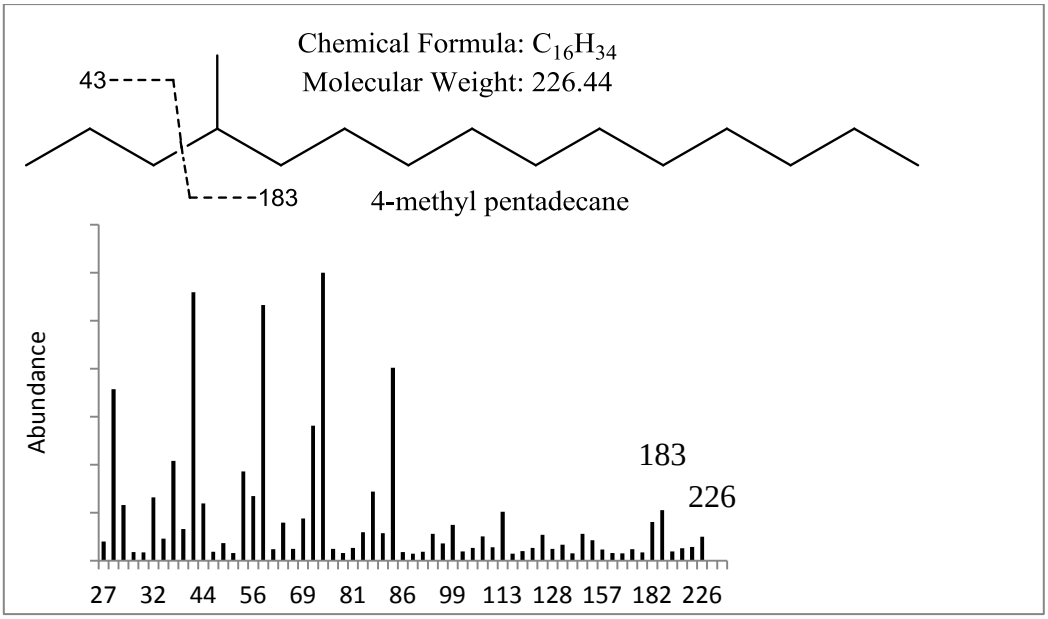
Chemical Formula: $C_{16}H_{34}$
Molecular Weight: 226.44
43
183
4-methyl pentadecane
Abundance
183
226
27 32 44 56 69 81 86 99 113 128 157 182 226

(c)

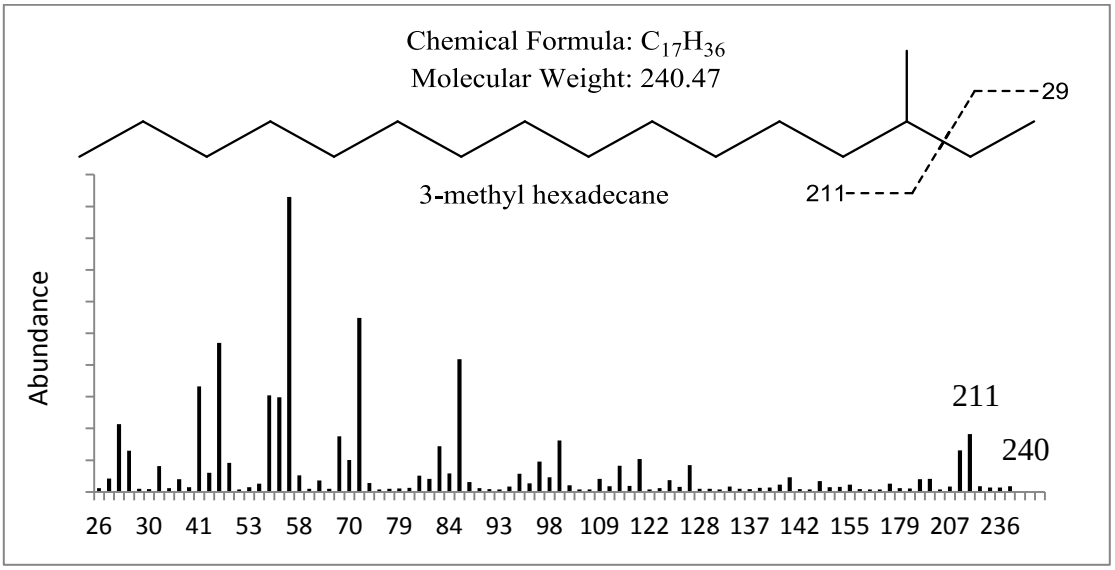

Fig. 17 Mass spectral identification of methyl branched hydrocarbons

(a-c) Mass spectral analyses of extracted silk lipids show evidence of branched chained hydrocarbons. While the M^+ ion is only evident at times, we do see an abundant daughter ion at the characteristic cleavage site at the branched position.
For 5-methyl heptadecane (a), we see a mass spectrum similar to that of octadecane, but with an abundant daughter ion at 197 [$C_{14}H_{29}$] which places the methyl group on the 5th carbon from the end. For 4-methyl pentadecane (b), we see a similar mass spec to hexadecane with a cleavage ion displayed at 183 [$C_{13}H_{27}$], which puts the methyl branch on the 4th carbon from the terminal end. Lastly, 3-methyl hexadecane (c), which shows a similar mass spec to heptadecane, with a branch on 3rd carbon from the end, displayed by the abundant ion at 211 [$C_{15}H_{31}$].

Small amounts of branched hydrocarbons were identified with chain lengths from 16 to 18 carbons (Table 9). Among the methyl alkanes detected, branched

positions were seen at the 2nd, 3rd, 4th, 5th, 6th and 7th carbons for pentadecane and hexadecane. Also detected for heptadecane was a branched group on the 2nd, 4th, 5th and 7th carbons. No unsaturated branched hydrocarbons were detected.

Table 9 Composition of saturated branched hydrocarbons

Metabolite	nmol/g dry weight [a]
16-carbon metabolites	
pentadecane, 2-methyl	4.42 ± 0.55
pentadecane, 3-methyl	5.11 ± 0.25
pentadecane, 4-methyl	1.84 ± 0.09
pentadecane, 5-methyl	2.51 ± 0.20
pentadecane, 6-methyl	1.70 ± 1.48
pentadecane, 7-methyl	8.96 ± 0.56
17-carbon metabolites	
hexadecane, 2-methyl	5.38 ± 0.19
hexadecane, 3-methyl	5.77 ± 0.74
hexadecane, 4-methyl	3.53 ± 0.24
hexadecane, 5-methyl	4.60 ± 0.52
hexadecane, 6-methyl	3.54 ± 0.35
hexadecane, 7-methyl	15.79 ± 2.01
18-carbon metabolites	
heptadecane, 2-methyl	1.32 ± 1.25
heptadecane, 4-methyl	4.72 ± 0.74
heptadecane, 5-methyl	0.70 ± 0.61
heptadecane, 7-methyl	22.76 ± 2.24

SUMMARY

Since gene function and regulation in the plant SL metabolic network is largely unknown, additional metabolomic studies are required to decipher the pathway(s) for

the synthesis of surface lipids. In this study, many hydrocarbons as well as fatty acids were analyzed and profiled to help decipher and visualize how these metabolites are biosynthesized on the surface of silk. Metabolite analyses on silks has showed a broad array of unsaturated fatty acids as well as hydrocarbons, herein, that have not yet been reported yet in maize silks.

From the metabolites identified by GC-MS, we are led to believe that hydrocarbons are biosynthesized by the elongation of fatty acid precursors that are reduced to corresponding aldehydes that are decarbonylated to generate the specific alkanes and alkenes found within which are consistent with previous findings [2]. The finding of omega 7 and 9 fatty acid precursors for both odd and even chain fatty acids from C16 to C32 indicates that odd and even-chained hydrocarbons are biosynthesized by a similar type of mechanism. Odd-numbered FAs have not been well characterized or demonstrated. While the immediate unsaturated aldehyde precursors were not found in this paper, previous research within our lab has found unsaturated aldehyde metabolites that would generate some of the specific alkenes and dienes that were detected [2]. Concurrently, isoprenoid HCs at defined chain lengths have also been identified within this Chapter which gives rise to a complex SL metabolomic network with additional reactions for the production of branched HCs.

The hypothesized alkene biosynthetic pathway mentioned within requires the action of many enzymatic reactions as well as enzymes that have not been

characterized and isolated to date. From the two hypothesized pathways mentioned, which can elongate unsaturated or saturated fatty acids before the reduction to corresponding aldehydes, fatty acid elongase(s) are needed, which to date, are largely uncharacterized and unexplored [30,32,33,34,35,36,37,38]. While evidence herein support the hypothesis of desaturation-elongation prior to reduction, the elongation-desaturation pathway cannot be ruled out for the production of some of the alkenes identified. To produce the aldehyde substrate(s) for the decarbonylation reaction mentioned within, the pathway requires the action of a fatty acyl reductase which acts on fatty acyl-CoAs.

With the rich display of non-isoprenoid HCs that are found on the surface of the silk, maize is an ideal system to study how these simple hydrocarbons are biosynthesized. Silks can be harvested easily and both metabolomic and molecular studies can be handled easily and efficiently. Moreover, the recent sequencing of the maize genome [39] combined with the extensive collection of maize *glossy* mutants which affect cuticular wax deposition [40,41] provide an opportunity to combine metabolomic analysis of maize mutants with genomic data to decipher the complex biosynthetic pathway. Future work would perhaps consist of metabolomic studies that deal with the *glossy* mutants, which in turn could define/test our proposed metabolic network. Moreover, these newly developed extraction methods could be applied to new silk sources that exhibit genetic or morphogenetic variation in surface lipid accumulation.

MATERIALS AND METHODS

Plant Material

Experimental tests were conducted using the maize (*Zea mays L.*) inbred line B73. The silks in this study were covered with a white paper bag prior to silking. Emerged silks were harvested at the point of emergence from the husk leaves, 3 days after silks first emerged.

Plants were grown in the spring of 2013 in the Plant Pathology greenhouse at Iowa State University in Ames, IA, USA. After harvesting, the ears were carried back to the lab in ice coolers where they were cut at the emergence point and placed into 50 mL conical tubes. For whole-silk experiments, silks were fresh weighed, flash-frozen with liquid nitrogen, and stored at -80˚C. Prior to metabolite extractions, silks were lyophilized, dry-weighed, then powderized using a Geno/Grinder2010. For silk surface experiments, fresh silks were transported to the lab, fresh weighed and then immediately dipped in solvent for metabolite extractions.

For the composition analysis for hydrocarbons (Fig. 2), 3 independent B73 fresh silks were collected then pooled. After combining these fresh silks, they were then split in half. Half of the silks (3 samples) were extracted based on whole silk immersions into solvent while the other half were lyophilized and ground for SL extractions.

Metabolite extraction

Powderized silks: Lipid metabolites were extracted using 90% hexanes: 10% diethyl ether. Each powderized sample was initially spiked with 5-10 μl of the internal standard, eicosane (1 mg/ml), depending on the mass of the sample (5 μl of standard for 0.04 to 0.06 g of sample and 10 μl of standard for 0.09 to 0.11 g of sample). Each sample was extracted in 2 mL of solvent, vortexed for 10 min and centrifuged at 3,250 rpm for 5 min. The extraction procedure was repeated three times and the pooled extracts were filtered, concentrated under N_2 gas and analyzed via GC-MS.

Whole silks: Each fresh silk sample was extracted in 8 mL of solvent that had been spiked with 5-10 μl of the internal standard, eicosane (1 mg/ml), according to the fresh weight. The silks were immersed into the solvent for 60 sec, and then the solvent was poured from the beaker into a clean glass tube and capped [2]. Extracts were concentrated under N_2 gas and analyzed via GC-MS.

Emerged silks were collected from 50 B73 ears at 3 days post silk emergence; fresh and dry weights were recorded, rendering an average water content estimate of ~90%. By recording the fresh weights of silks that were immersed in solvent, we could accurately estimate the dry weight by multiplying our fresh weight (in grams) by 0.1.

Fatty acid transmethylation

Metabolite extracts were derivatized via transmethylation by adding 2ml of 1N HCl in methanol. Samples were vortexed and then heated in a water bath for 80°C for 1 hr. After incubation, 2 mL of 0.9% NaCl and 1 mL of hexanes were added to the extract. Extracts were vortexed and then centrifuged for 5min to separate the two fractions. The hexane layer was recovered and moved to a separate tube. To the original tube, another 1 mL of hexanes added to allow for full recovery of lipid metabolites.

Dimethyl disulfide derivitization

All lipid extracts were treated with DMDS for confirmation of double bond positions for alkenes, dienes and fatty acids. For this reaction, 50µl of hexanes was added to the dried extract along with 200µl of DMDS and 50µl of an iodine solution (60mg of iodine in 1ml of diethyl ether). The reaction mixture was then incubated overnight (20hr) in a heat block set at 40˚C [26]. To recover the lipids, 500µl of hexanes and 500µl of sodium thiosulfate (Na_2SO_4) was added and the mixture was vortexed for 1 min and centrifuged at 3,250 rpm for 5 min. The hexane layers (top) was removed and placed into a new GC-MS vial. This process was repeated twice more to aid in the recovery of all lipids.

Analytical Instrumentation

Gas chromatography was performed with an HP-5MS cross-linked (5%) diphenyl (95%) dimethyl polysiloxane column (30m in length; 0.25-mm inner diameter) using helium as the carrier gas, and an Agilent Technologies series 6890 gas chromatograph, equipped with a model 5973 mass detector (Agilent Technologies,

http://www.home.agilent.com). After a 1ul sample injection (splitless), the initial temperature (120˚C) of the oven was raised to 260˚C, at a rate of 10˚C/min, and held for 1minute. This was followed by an increase to 300˚C, at a ramp of 5˚C/min, and held for 1 minute, then a subsequent ramp to 320˚C by 5˚C/min and held for 2minutes. The total run time for the non-derivatized samples was 30 minutes. After samples were treated with DMDS, unsaturated metabolites were confirmed on a much longer run time to allow separation of fatty acid and hydrocarbon derivatives. After a 1ul sample injection (splitless), the oven was increased from an initial temperature of 120˚C to 160˚C, at a rate of 10˚C/min, and held for 2minutes. After reaching 160˚C, the oven was then raised to 260˚C, at 5˚C/min, and held for 10minutes. Then the temperature was brought to 300˚C, at rate of 5˚C/min and held for 5 minutes. The last elevation was a climb to 320˚C, at 5˚C/min, and held for a 25 minute period. The total run time for these samples was 78 minutes.

Lipid analysis

For metabolite confirmation, the mass spectra as well as the retention times and retention indices for each compound were used. The retention indices of these metabolites were calculated based on a calibration file of straight chain hydrocarbons (C7-C40). Quantification analysis was performed with AMDIS (http://chemdata.nist.gov/mass-spc/amdis/). The NIST Mass Spectral library

(http://webbook.nist.gov/chemistry/) was used for identifying compounds by mass spec comparisons.

Acknowledgments

We thank members of the Lauter research group (David Hessel, Adam Bossard and Hannah Cox) for assistance in sample collection, Sam Condon and Wenmin Qin (Nikolau group) and Zhihong Song and Ann Perera (W.M. Keck Metabolomics Research Laboratory) for technical assistance with GC-MS, and Mark Brown (Jacqueline Shanks group) for assistance with Chemstation mass-spectral software.

REFERENCES

1. Yang G, Wiseman BR, Espelie KE (1992) Cuticular lipids from silks of seven corn genotypes and their effect on development of corn earworm larvae [Helicoverpa zea (Boddie)]. Journal of Agricultural and Food Chemistry 40: 1058-1061.

2. Perera MA, Qin W, Yandeau-Nelson M, Fan L, Dixon P, et al. (2010) Biological origins of normal-chain hydrocarbons: a pathway model based on cuticular wax analyses of maize silks. Plant Journal 64: 618-632.

3. Miller SS, Reid LM, Butler G, Winter SP, McGoldrick NJ (2003) Long chain alkanes in silk extracts of maize genotypes with varying resistance to Fusarium graminearum. J Agric Food Chem 51: 6702-6708.

4. Bianchi G, Avato P, Salamini F (1978) Glossy mutants of maize. VIII. Accumulation of fatty aldehydes in surface waxes of gl5 maize seedlings. Biochem Genet 16: 1015-1021.

5. Avato P, Bianchi G, Pogna N (1990) Chemosystematics of Surface-Lipids from Maize and Some Related Species. Phytochemistry 29: 1571-1576.

6. Jordan WR, Shouse PJ, Blum A, Miller FR, Monk RL (1984) Environmental Physiology of Sorghum. II. Epicuticular Wax Load and Cuticular Transpiration1. Crop Sci 24: 1168-1173.

7. Kosma D, Jenks M (2007) Eco-Physiological and Molecular-Genetic Determinants of Plant Cuticle Function in Drought and Salt Stress Tolerance. In: Jenks M, Hasegawa P, Jain SM, editors. Advances in Molecular Breeding Toward Drought and Salt Tolerant Crops: Springer Netherlands. pp. 91-120.

8. Long LM, Patel HP, Cory WC, Stapleton AE (2003) The maize epicuticular wax layer provides UV protection. Functional Plant Biology 30: 75-81.

9. Javelle M, Vernoud V, Rogowsky PM, Ingram GC (2011) Epidermis: the formation and functions of a fundamental plant tissue. New Phytol 189: 17-39.

10. Yang G, Isenhour DJ, Espelie KE (1991) Activity of Maize Leaf Cuticular Lipids in Resistance to Leaf-Feeding by the Fall Armyworm. The Florida Entomologist 74: 229-236.

11. Yang G, Wiseman BR, Isenhour DJ, Espelie KE (1993) Chemical and Ultrastructural Analysis of Corn Cuticular Lipids and Their Effect on Feeding by Fall Armyworm Larvae. Journal of Chemical Ecology 19: 2055-2074.

12. Bassetti P, Westgate ME (1993) Senescence and Receptivity of Maize Silks. Crop Sci 33: 275-278.

13. Kolattukudy PE (1976) Chemistry and biochemistry of natural waxes. Amsterdam ; New York: Elsevier Scientific Pub. Co. xx, 459 p. p.

14. Kolattukudy PE, Walton TJ (1972) The biochemistry of plant cuticular lipids. Prog Chem Fats Other Lipids 13: 119-175.

15. Kunst L, Samuels AL (2003) Biosynthesis and secretion of plant cuticular wax. Prog Lipid Res 42: 51-80.

16. Samuels L, Kunst L, Jetter R (2008) Sealing plant surfaces: cuticular wax formation by epidermal cells. Annu Rev Plant Biol 59: 683-707.

17. Post-Beittenmiller D (1996) Biochemistry and Molecular Biology of Wax Production in Plants. Annu Rev Plant Physiol Plant Mol Biol 47: 405-430.

18. Sukovich DJ, Seffernick JL, Richman JE, Hunt KA, Gralnick JA, et al. (2010) Structure, Function, and Insights into the Biosynthesis of a Head-to-Head Hydrocarbon in Shewanella oneidensis Strain MR-1. Applied and Environmental Microbiology 76: 3842-3849.

19. Sukovich DJ, Seffernick JL, Richman JE, Gralnick JA, Wackett LP (2010) Widespread Head-to-Head Hydrocarbon Biosynthesis in Bacteria and Role of OleA. Applied and Environmental Microbiology 76: 3850-3862.

20. Beller HR, Goh EB, Keasling JD (2010) Genes involved in long-chain alkene biosynthesis in Micrococcus luteus. Appl Environ Microbiol 76: 1212-1223.

21. Reed JR, Quilici DR, Blomquist GJ, Reitz RC (1995) Proposed mechanism for the cytochrome P450-catalyzed conversion of aldehydes to hydrocarbons in the house fly, Musca domestica. Biochemistry 34: 16221-16227.

22. Cheesbrough TM, Kolattukudy PE (1984) Alkane biosynthesis by decarbonylation of aldehydes catalyzed by a particulate preparation from Pisum sativum. Proc Natl Acad Sci U S A 81: 6613-6617.

23. Dennis MW, Kolattukudy PE (1991) Alkane biosynthesis by decarbonylation of aldehyde catalyzed by a microsomal preparation from Botryococcus braunii. Arch Biochem Biophys 287: 268-275.

24. Dennis M, Kolattukudy PE (1992) A cobalt-porphyrin enzyme converts a fatty aldehyde to a hydrocarbon and CO. Proc Natl Acad Sci U S A 89: 5306-5310.

25. Schneider-Belhaddad F, Kolattukudy P (2000) Solubilization, Partial Purification, and Characterization of a Fatty Aldehyde Decarbonylase from a Higher Plant, Pisum sativum. Archives of Biochemistry and Biophysics 377: 341-349.

26. Carlson DA, Roan CS, Yost RA, Hector J (1989) Dimethyl Disulfide Derivatives of Long-Chain Alkenes, Alkadienes, and Alkatrienes for Gas-Chromatography Mass-Spectrometry. Analytical Chemistry 61: 1564-1571.

27. Sturaro M, Hartings H, Schmelzer E, Velasco R, Salamini F, et al. (2005) Cloning and characterization of GLOSSY1, a maize gene involved in cuticle membrane and wax production. Plant Physiology 138: 478-489.

28. Aarts MG, Keijzer CJ, Stiekema WJ, Pereira A (1995) Molecular characterization of the CER1 gene of arabidopsis involved in epicuticular wax biosynthesis and pollen fertility. Plant Cell 7: 2115-2127.

29. Islam M, Du H, Ning J, Ye H, Xiong L (2009) Characterization of Glossy1-homologous genes in rice involved in leaf wax accumulation and drought resistance. Plant Molecular Biology 70: 443-456.

30. Xu X, Dietrich CR, Delledonne M, Xia Y, Wen TJ, et al. (1997) Sequence analysis of the cloned glossy8 gene of maize suggests that it may code for a beta-ketoacyl reductase required for the biosynthesis of cuticular waxes. Plant Physiology 115: 501-510.

31. Okuley J, Lightner J, Feldmann K, Yadav N, Lark E, et al. (1994) Arabidopsis FAD2 gene encodes the enzyme that is essential for polyunsaturated lipid synthesis. Plant Cell 6: 147-158.

32. James DW, Jr., Lim E, Keller J, Plooy I, Ralston E, et al. (1995) Directed tagging of the Arabidopsis FATTY ACID ELONGATION1 (FAE1) gene with the maize transposon activator. Plant Cell 7: 309-319.

33. Xu X, Dietrich CR, Lessire R, Nikolau BJ, Schnable PS (2002) The Endoplasmic reticulum-associated maize GL8 protein is a component of the acyl-coenzyme A elongase ivolved in the production of cuticular waxes. Plant Physiology 128: 924-934.

34. Han G, Gable K, Kohlwein SD, Beaudoin F, Napier JA, et al. (2002) The Saccharomyces cerevisiae YBR159w gene encodes the 3-ketoreductase of the microsomal fatty acid elongase. J Biol Chem 277: 35440-35449.

35. Gable K, Garton S, Napier JA, Dunn TM (2004) Functional characterization of the Arabidopsis thaliana orthologue of Tsc13p, the enoyl reductase of the yeast microsomal fatty acid elongating system. J Exp Bot 55: 543-545.

36. Leonard AE, Pereira SL, Sprecher H, Huang YS (2004) Elongation of long-chain fatty acids. Prog Lipid Res 43: 36-54.

37. Zheng H, Rowland O, Kunst L (2005) Disruptions of the Arabidopsis Enoyl-CoA reductase gene reveal an essential role for very-long-chain fatty acid synthesis in cell expansion during plant morphogenesis. Plant Cell 17: 1467-1481.

38. Denic V, Weissman JS (2007) A molecular caliper mechanism for determining very long-chain fatty acid length. Cell 130: 663-677.

39. Schnable PS, Ware D, Fulton RS, Stein JC, Wei F, et al. (2009) The B73 maize genome: complexity, diversity, and dynamics. Science 326: 1112-1115.

40. Schnable PS, Stinard PS, Wen TJ, Heinen S, Weber D, et al. (1994) The Genetics of Cuticular Wax Biosynthesis. Maydica 39: 279-287.

41. Dietrich CR, Cui F, Packila ML, Li J, Ashlock DA, et al. (2002) Maize Mu transposons are targeted to the 5' untranslated region of the gl8 gene and sequences flanking Mu target-site duplications exhibit nonrandom nucleotide composition throughout the genome. Genetics 160: 697-716.

CHAPTER 4. SUMMARY AND CONCLUSIONS

The plant SL metabolomic network still remains largely undiscovered. Metabolomic, molecular and genetic studies can be combined to decipher the complex network for hydrocarbon production. Maize silks are an ideal system to dissect this network not only because the silk surface lipids are rich in hydrocarbons, but also because silks are readily abundant, easy to harvest and the processing methods are straightforward.

Several decarbonylation-based pathways for the synthesis of alkanes and alkenes were previously proposed [1]. Although some proposed intermediates were identified in silk extracts within that study, many FAs and aldehydes that would potentially lead to the production of defined sets of alkenes were not detected. For example, mono-unsaturated FA precursors longer than 18 carbons in length, which would support a Desaturation-Elongation-Reduction-Decarbonylation pathway were not detected [1]. Herein, we have found putative FA precursors ranging from 16 -34 carbons in length, providing additional support for desaturation-elongation-decarbonylation pathway. While no unsaturated aldehydes were clearly detected in these experiments, they have previously been identified in B73 maize silks [1]. In the current study, we also identified even-chain hydrocarbons, which potentially could be formed via conversion of an aldehyde to a primary alcohol, which is subsequently

dehydrated to form a hydrocarbon. Alternatively, even-numbered hydrocarbons could result via a decarbonylation-based pathway that initiates with odd- instead of even-numbered fatty acids.

Our previous work on the SL metabolome has focused on profiling hydrocarbons only. However, comprehensive dissection of the SL metabolome requires the profiling of not only the hydrocarbon end-point metabolites, but also the hypothesized intermediates (e.g. fatty acids, aldehydes, etc.). Therefore, as reported in Chapter 2 we developed and implemented methods to capture intermediate- (e.g. fatty acids and aldehydes) and end-point (e.g. hydrocarbons) surface lipid metabolites in a single extraction procedure. Development of this method included the identification of the best extraction solvent, best incubation time and best GC-MS protocol to maximize efficacy and efficiency for quantification of each desired metabolite. In addition, silica was determined to function as a filter to remove all polar compounds from the lipid extract (i.e. for extracting only non-polar compounds, such as hydrocarbons). Overall, we found that a 9:1 mixture of hexanes to diethyl ether, a long incubation time, and the omission of silica performed best as judged by 1) throughput efficiency, 2) the breadth of identified metabolites, 3) the degree to which the quantifications of subsets of metabolites matched results from our previous best methods, and 4) the efficacy and efficiency of the GC-MS protocol required to differentiate the metabolites. This methodological study provided a new procedure for

extracting all classes of SL metabolites and it also provided an opportunity to refine our current extraction method that is specifically designed for hydrocarbon analysis.

An important aspect of this study was the application of the newly developed methods to whole silks vs. powderized silks (Chapter 3). Extraction of whole silks is presumed to enrich the relative composition of surface lipids compared to extraction from powderized silks, which are expected to harbor lipid metabolites from both apoplasm and symplasm of epidermal, mesophyll, and vascular tissues of the leaf. Notably, hydrocarbon content did not differ between whole and powderized silks, which suggests that hydrocarbons are located only on the silk surface and is supported by previous work [1]. In contrast, aldehyde and fatty acid content differed significantly between whole and powderized silks. From whole silks, broad arrays of saturated FAs were identified, whereas unsaturated FAs were only present in the powderized silks. The data suggested, herein, suggest that saturated FAs and aldehydes are constituents on the surface of whole silks. Lyophilized extracted silks did not contain virtually any aldehydes that were detectable by GC-analyses; while the surface of whole silks contained all the saturated FAs that lyophilized silk contained, it also contained a broader array of VLC FAs past 30 carbons in chain length. An alternative explanation could implicate differences in the way silks are processed for the two methods; however, there is little reason to expect that lyophilizing tissue results in the specific loss of unsaturated VLC HCs.

While hydrocarbons are most likely produced from the conversion of fatty acids, the exact biochemical mechanisms for their synthesis remain unknown. These metabolomic efforts require a series of large-scale parallel investigations that rely on metabolite extraction and gas chromatography mass spectrometry (GC-MS) for metabolite identification and quantification. Currently, we are using genomic data as well as biochemical metabolite data to piece together nodes in our hypothesized pathways. Discovering what enzymes catalyze these specific reactions and which ones are expressed at 3-days post silk emergence will resolve the biosynthesis pathway; from the work in this thesis, we have confirmed that elongation of unsaturated FA precursors occurs, and is likely followed by reduction to aldehydes and subsequent decarbonylation to the corresponding alkenes. Chapter 3 identifies a broad range of metabolites that are seen on the surface of the silk cuticle as well as in the ground silks. Many of the lipid metabolites that were detected in this work had not previously been found in maize silks or in the inbred B73 that was used in our experiments. Thus, we chose to examine the metabolites in both tissues (intact and powderized) to gain knowledge for constructing a metabolomic network.

The application of the new extraction method to whole silks resulted in two major findings that impact our previously proposed decarbonylation-based pathways for hydrocarbon synthesis on maize silks. First, we identified even-numbered hydrocarbons in addition to the odd-numbered hydrocarbons that have been routinely identified in the past [1,2,3]. These odd-chain metabolites consist of alkenes situated

at the 4th, 6th and 9th positions along with highly abundant odd alkanes from C21 to C33 [1]. Second, we identified a wide array of fatty acids present in the SLs of maize silks. The identification of these fatty acids is key to the pathways we propose for odd- and even- alkene and alkane biosynthesis (Chapter 3, Figure 6 and 7). Our data clearly show that FAs are desaturated prior to elongation, reduction, and decarbonylation. The pathways above are largely consistent with the hydrocarbon biosynthesis pathway reported previously for B73 silk tissue [1].

For hydrocarbons we detected alkanes consisting of chain lengths ranging from 14 to 37 carbons. For alkenes and dienes, a homologous series was detected which was seen to have double bonds situated at defined positions of the alkyl chains: alkenes with double bonds situated at the 1st, 4th-to-half-the-length of the molecule as well as dienes with double bonds situated at the 6th and 9th positions. From carbon chain lengths ranging from C23 to C37, alkenes with defined double bond positions at the 7th or 9th carbons seemed to be the most abundant unsaturated metabolites detected. A homologous series of dienes were also found with double bonds at the 6th and 9th positions for chain lengths ranging from 23 to 33 carbons.

Saturated fatty acids were found for chain lengths ranging from 8 to 34 carbons. For mono-unsaturated even and odd-chain fatty acids, we detected a wide variety, but the ω-7 and ω-9 series ranging from 16 to 32 carbons in chain length were most prevalent. Saturated aldehydes have been found ranging from 8 to 32 carbons in chain length. While unsaturated aldehydes were detected for even-chain lengths ranging from 26 to

34 carbons by transmethylation, the double bond positions were not identified in this work. No odd unsaturated aldehydes were identified by transmethylation, perhaps due to transience of odd aldehydes.

From the metabolites recovered and detected by GC-MS, we conclude that alkanes and alkenes are biosynthesized by the elongation of fatty acid precursors, which are reduced to aldehydes before being decarbonylated to their respective alkanes or alkenes. While we believe that the abundant alkenes with double bonds positioned at the 7^{th} and 9^{th} carbons are biosynthesized by the elongation of unsaturated fatty acid precursors, ω-7 and ω-9 respectively, we cannot rule out another pathway which involves decarboxylation. While our data supports one proposed pathway [1], already mentioned, GC-analyses have indicated that even-chained hydrocarbons are derived from odd-chain fatty acids based on the ω-7 and ω-9 odd chain FAs detected. Our hypothesized pathway which involves decarbonylation of an aldehyde precursor shows that fatty acid elongase(s) are needed. This pathway would also require the action of a fatty acyl reductase which acts on fatty acyl-CoAs.

FUTURE DIRECTIONS

Maize has many genetic and molecular resources that make it a model system to study and dissect the genetic network associated with SL production. Our group has selected 15 distinct isolines with highly diverse SL chemotypes to proceed with. Among

these 15 isolines, RNAseq data will be gathered as well as metabolite data from four developmental sections of the silk.

To key in on major regulators of the hydrocarbon biosynthesis pathway, we intend to conduct experiments across a diverse panel of genotypes that have already demonstrated to have a wide array of SL metabolomes. Within these investigations, we aim to extract and profile lipids along the silk developmental gradient in a "slice-and-dice" type of procedure. We anticipate implementing an RNAseq approach into this set of experiments in parallel, which brings in a genetics component.

The methods developed and optimized herein can now be applied to the further dissection of the metabolic network responsible for surface lipid production on maize silks. A long-term goal of this research is to identify and deliver optimized compositions of the silk surface lipid metabolome that can confer elevated levels of stress protection without compromising pollen receptivity. Through the breeding of select maize lines, we hope to improve grain yield through silks able to withstand harmful abiotic and biotic stresses. Not only would productivity improve, but there would be a decrease in agricultural inputs (e.g. chemical treatments, irrigation levels) which would increase environmental sustainability. This would also have important implications to other important agricultural crops (e.g. soybean, rice and cotton), which have similar surface lipid chemistries. Since simple hydrocarbons are highly representative on the silk cuticle, and are nearly identical replacements for current petroleum derived fuels, this

research has an added component towards engineering efforts to producing advanced biofuels.

LIMITATIONS AND CEAVEATS

Our proposed pathways for hydrocarbon biosynthesis involve the capturing and the recovery of aldehydes to prove our decarbonylation pathway mechanism. While we believe aldehydes are the immediate precursors to hydrocarbons, aldehydes accumulate in the SLs in very low abundance as compared to hydrocarbons. Currently, we have identified saturated even- and odd-chain aldehydes that range from 8 to 34 carbons in chain length, but have not identified unsaturated aldehydes. The recovery, isolation and detection of unsaturated aldehydes have proven to be a difficult feat. Since concentrated samples have been analyzed by GC-MS and unsaturated aldehydes weren't detected, it's possible that they aren't intermediates in the pathway, or that they are present only transiently, or that they are otherwise labile. However, we expect that by bulking many whole-silk lipid extracts together that we will be able to isolate these aldehydes by a silica column procedure using a sequential series of increasingly polar solvents. From this isolation, extracts will be heavily concentrated and then subjected to dimethyl disulfide derivatization to look at double bond positions of these unsaturated aldehydes.

There are other issues to resolve as well; many of the monoenoic fatty acids expected to act as precursors have not yet been detected. Another limitation of our proposed pathway was the detection of ω-6 and ω-9 di-unsaturated FAs greater than 22 carbons in chain length. We only detected ω-6 and ω-9 even-chain dienoic FAs from carbon chain lengths ranging from 18 to 22 carbons. In short, there is no shortage of questions to answer; thus we intend to build upon these findings and utilize our more effective methods to dissect this metabolomic network at both the genetic, developmental, and biochemical levels.

REFERENCES

1. Perera MA, Qin W, Yandeau-Nelson M, Fan L, Dixon P, et al. (2010) Biological origins of normal-chain hydrocarbons: a pathway model based on cuticular wax analyses of maize silks. Plant Journal 64: 618-632.

2. Miller SS, Reid LM, Butler G, Winter SP, McGoldrick NJ (2003) Long chain alkanes in silk extracts of maize genotypes with varying resistance to Fusarium graminearum. J Agric Food Chem 51: 6702-6708.

3. Yang G, Wiseman BR, Espelie KE (1992) Cuticular lipids from silks of seven corn genotypes and their effect on development of corn earworm larvae [Helicoverpa zea (Boddie)]. Journal of Agricultural and Food Chemistry 40: 1058-1061.